



National Library
of Canada

Bibliothèque nationale
du Canada

Canadian Theses Service

Service des thèses canadiennes

Ottawa, Canada
K1A 0N4

NOTICE

The quality of this microform is heavily dependent upon the quality of the original thesis submitted for microfilming. Every effort has been made to ensure the highest quality of reproduction possible.

If pages are missing, contact the university which granted the degree.

Some pages may have indistinct print especially if the original pages were typed with a poor typewriter ribbon or if the university sent us an inferior photocopy.

Reproduction in full or in part of this microform is governed by the Canadian Copyright Act, R.S.C. 1970, c. C-30, and subsequent amendments.

AVIS

La qualité de cette microforme dépend grandement de la qualité de la thèse soumise au microfilmage. Nous avons tout fait pour assurer une qualité supérieure de reproduction.

S'il manque des pages, veuillez communiquer avec l'université qui a conféré le grade.

La qualité d'impression de certaines pages peut laisser à désirer, surtout si les pages originales ont été dactylographiées à l'aide d'un ruban usé ou si l'université nous a fait parvenir une photocopie de qualité inférieure.

La reproduction, même partielle, de cette microforme est soumise à la Loi canadienne sur le droit d'auteur, SRC 1970, c. C-30, et ses amendements subséquents.

THE UNIVERSITY OF ALBERTA

MODELLING OF OUTBURSTS AT NO. 26 COLLIERY, GLACE BAY, NOVA SCOTIA

by

DAG HELLMUTH KULLMANN



A THESIS

SUBMITTED TO THE FACULTY OF GRADUATE STUDIES AND RESEARCH

IN PARTIAL FULFILMENT OF THE REQUIREMENTS FOR THE DEGREE

OF MASTER OF SCIENCE

IN

MINING ENGINEERING

MINING, METALLURGICAL AND PETROLEUM ENGINEERING

EDMONTON, ALBERTA

SPRING, 1989

Permission has been granted to the National Library of Canada to microfilm this thesis and to lend or sell copies of the film.

The author (copyright owner) has reserved other publication rights, and neither the thesis nor extensive extracts from it may be printed or otherwise reproduced without his/her written permission.

L'autorisation a été accordée à la Bibliothèque nationale du Canada de microfilmer cette thèse et de prêter ou de vendre des exemplaires du film.

L'auteur (titulaire du droit d'auteur) se réserve les autres droits de publication; ni la thèse ni de longs extraits de celle-ci ne doivent être imprimés ou autrement reproduits sans son autorisation écrite.

ISBN 0-315-53026-X

THE UNIVERSITY OF ALBERTA


RELEASE FORM

NAME OF AUTHOR DAG HELLMUTH KULLMANN
TITLE OF THESIS MODELLING OF OUTBURSTS AT NO. 26 COLLIERY, GLACE
 BAY, NOVA SCOTIA
DEGREE FOR WHICH THESIS WAS PRESENTED MASTER OF SCIENCE
YEAR THIS DEGREE GRANTED SPRING, 1989

Permission is hereby granted to THE UNIVERSITY OF ALBERTA LIBRARY
to reproduce single copies of this thesis and to lend or sell such copies for private,
scholarly or scientific research purposes only.

The author reserves other publication rights, and neither the thesis nor extensive
extracts from it may be printed or otherwise reproduced without the author's written
permission.

(SIGNED)



PERMANENT ADDRESS:

...C/O DEPT. of MINING, MET. & PET.
...ENGINEERING, UNIVERSITY OF ALBERTA
...EDMONTON, T6G 2G6.....

DATED Nov. 17..... 1988

THE UNIVERSITY OF ALBERTA
FACULTY OF GRADUATE STUDIES AND RESEARCH

The undersigned certify that they have read, and recommend to the Faculty of Graduate Studies and Research, for acceptance, a thesis entitled **MODELLING OF OUTBURSTS AT NO. 26 COLLIERY, GLACE BAY, NOVA SCOTIA** submitted by Dag Hellmuth Kullmann in partial fulfilment of the requirements for the degree of Master of Science in Mining Engineering.

V. Baur

Supervisor

W. H. Baur

F. O. Scott

F. O. Scott

Date.. *Nov. 17, 1988*

Dedication

To my wife Elizabeth
for her continued support and encouragement and
especially for making the difficult times bearable,

and to my parents
for their constant belief in me and my abilities
and teaching me to always strive for the best.

Abstract

Outbursts are sudden, violent failures in which rock and/or coal is ejected from the face together with large quantities of gas. Disruptions to a mining operation can be severe and in the extreme, may cause loss of life and mine closure. At No. 26 Colliery, outbursts caused delays in the driving of the main entries, a considerable loss of revenue and some areas of the mine were threatened with closure. A major fire has since closed this mine, but other mines in the Sydney Coal Field are expected to experience the same problems. The outbursts experienced at No. 26 Colliery originated from within sandstone (river) channels, just above (and sometimes in contact with) the coal seams. A better understanding of the mechanisms involved in an outburst could lead the way to controlling these failures.

The mechanism postulated within this thesis has been used to quantitatively model these outbursts. The mechanism treats an outburst as a series of instantaneous 'events', driven by tensile failures within the rock mass around a spalling cavity. Outbursts may be terminated simply by the changes in the shape of the cavity due to spalling. The two main factors affecting the occurrence of outbursts are the gas pressure and tensile strength of the rock.

The mechanism postulated here has been used to model the outbursts at No. 26 Colliery and gave compatible results for both size and shape of the resulting cavities. The model also explained the presence of different size cavities resulting from the changing width of exposed sandstone in the mine entry. Narrower penetrations of the entry into the sandstone produced smaller cavities. In addition, the model shows that if an outburst is not terminated by the change in cavity shape, it could spall indefinitely unless terminated by changing geology. A relationship between the final stable cavity shape and the field stress conditions was determined. The shape of the heading penetrating the sandstone affects the likelihood of outburst initiation.

A siltstone bed often intervenes between the sandstone channel and coal seam. If the sandstone is not penetrated by the heading, the siltstone must fail before an outburst can occur. In the field, the siltstone has only failed if its thickness has been reduced to less than

2.7m by a sandstone channel. This failure has been analysed as the 'cutter roof' failure of a surcharge loaded beam. Results from this method of analysis are compatible with field observations.

Remedial measures are essential when mining near an area prone to outbursts, such as when approaching sandstone channels. Providing active support in the form of rock bolts could prevent the failure of the siltstone bed, and thus, prevent an outburst. In the case where the sandstone channel is penetrated, degassing the sandstone by induced fracturing is recommended.

Acknowledgements

I wish to express his gratitude to Dr. Ken Barron, Professor of Mining Engineering, for giving me the opportunity to work on this project and for his, supervision, guidance and encouragement to see it through to its conclusion. His enthusiasm and confidence in the project provided great incentive when progress and desire was minimal.

A special thanks also to Professor Wayne Griffin for his supervision during the absence of Dr. Barron and for the numerous discussions of various aspects which have proven to be invaluable towards the completion of this thesis.

I also greatly appreciate the cooperation of Mr. Doug Booth especially in the development of the computer program.

The personnel of CANMET, Sydney, Nova Scotia, especially Dr. Tim Aston and Mr. Bill Gallant, and the Cape Breton Development Corporation, especially Mr. Steve Forgeron, have provided invaluable information through data and discussions without which this project would never have been conceived. Their kindness and hospitality during my short visit was also greatly appreciated.

This project was partially funded through grants from CANMET and NSERC.

Table of Contents

Chapter	Page
1. Introduction	1
1.1 The Hazards of Outbursts	1
1.2 Problem Faced by No. 26 Colliery, Glace Bay, Nova Scotia	1
1.3 Objective of this Study	2
1.4 Analysis of the Problem	2
1.5 Thesis Layout	3
2. Geology of the Sydney Basin	4
2.1 Coal Origin	4
2.2 Coal Seams	5
3. No. 26 Colliery Operation	7
3.1 Mine Geology in General	7
3.2 Mining Method	9
4. Outbursts	13
4.1 What are Outbursts?	13
4.2 Sandstone Outbursts at No. 26 Colliery	14
4.2.1 Gas Migration to Sandstone	14
4.2.2 Outburst Geology	14
4.3 Other Non-Coal Outbursts noted Elsewhere	18
4.3.1 West Germany	19
4.3.2 USSR and Poland	20
4.3.3 England	21
4.3.4 United States	21
4.4 Previously Proposed Outburst Mechanism for Coal	21
4.4.1 Discussion of Paterson's Proposed Model	23
5. Insitu Properties	24
5.1 Insitu Gas Pressure	24

5.2	Rock Properties	26
5.3	Insitu Field Stress	27
6.	Posulated Mechanism of Non-Coal Outbursts	30
6.1	Posulated Spalling Mechanism	31
6.2	Proposed Outburst Model and Assumptions	32
7.	Spalling Mechanism	35
7.1	Boundary Element Method and Program	35
7.1.1	Effect of Boundary Element Length and Field Point Density	38
7.1.2	Secondary Computer Program - SAFCON - Safety Factor Contouring ..	40
7.2	Gas Pressure	40
7.3	Failure Criterion	41
7.4	Safety Factor Contouring	41
7.5	Computer Modelling	43
7.5.1	Objectives of the Model	43
7.5.2	Sample Run of Model	44
7.5.3	Gas Pressure Required to Cause Spalling	48
7.5.4	Comparison of Model Results with Recorded Events	52
7.6	Observations of Outburst Cavities	56
7.6.1	Effect of the Heading Face	57
7.6.2	Effect of the Width of Exposed Sandstone Above the Heading	58
7.6.3	Reconsideration of Element Lengths and Field Point Density	61
7.7	Summary	63
8.	Siltstone Roof Failures	65
8.1	Cutter Roof Failure	65
8.1.1	Method of Analysis	65
8.2	Cutter Roof Failure of Siltstone	67
8.3	Summary	71
9.	Remedial Measures Against Outbursts	72

10. Conclusions	77
10.1 Recommendations For Further Work	78
References	81
Appendix A - Outburst Information	85
Appendix B - Insitu Strata Gas Pressures	104
Appendix C - Rock Properties	110
Appendix D - Insitu Stress Test	133
Appendix E - Program SAFCON	142
Appendix F - Sample Input and Output For Computer Programs	185

List of Tables

Table	Page
3.1 Effect of Sandstone Channels of Coal Production	10,11
5.2a Average Rock Properties	26
5.2b Parameters of the Hoek and Brown Failure Criterion Used in the Model	27
5.3 Insitu Stress Field	28
A.1 Details of Outbursts From No. 26 Colliery	86-95
C.1a Sample Dry Densities for Sandstone and Siltstone	110
C.1b Uniaxial and Triaxial Tests on Sandstone and Siltstone	111
C.1c Porosity Test	111
C.1d Constant Head Permeability Tests	112
C.2a Strengths and Elastic Properties of D-164 Cores	114
C.2b Porosity and Permeability of D-164 Cores	114
C.3a Strength of Harbour Seam Coal at Donkin-Morien	115
C.3b Strength of Coals From the Sydney Coal Field	116
C.4 Test Results for Carbon / Carbonate Content in Sandstone	117
C.5 Proximate Analysis on Outburst Prone Sandstone	118
C.6 Strength and Elastic Properties of Various Rock Types from Donkin-Morien	120
C.7a Classification of Borehole D-165 Cores	123
C.7b Strength of Borehole D-165 Cores	124
C.7c Gas Permeability Tests on Sample D-165-18	125
C.7d Stress Change Simulation Results	129
C.8 Rock Properties	131
D.1 Overcoring Test Locations and Comments	134
D.2 Biaxial Test Results	136
D.3a Input Parameters for Stress Tensor Calculation	137
D.3b Average Stress Tensors by Least Squares Solution	137
D.3c Principal Stress Magnitudes and Directions	138

List of Figures

Figure	Page
2.1 Structures and Harbour Seam Contours for Western Sydney Basin	5
2.2 Coal Seam Sequence of the Sydney Coalfield	6
3.1 Coal Mining Operations in the Sydney Coal Basin	8
3.1i Identified Sandstone Channels	8
3.1ii Synclines and Anticlines of the Sydney Basin	8
4.1 Mine Plan Showing Sandstone Channels and Outbursts	15
4.2 Onion-Skin Texture of the Outburst Cavity	16
4.3 Cross-section of Cavity Produced by Outbursts #36 and #37	17
4.4 Outburst Damage in Development Heading	18
4.5 Timber Cribbing to Support Cavity Back	19
5.1 Various Test Site Locations	24
7.1 Flow Chart of Model Iterative Process	36
7.2 Size Effect of Boundary Element Length	39
7.3 Field Point Results Produced by Model	42
7.4 Contouring of Shear and Tensile Failures	43
7.5 Sample Run: Iterations 1, 2, 3 and Final Cavity	46,47
7.6 Gas Pressures Required to Cause Spalling	49
7.7 Final Cavity Shapes For Various Stress Conditions	51
7.8 Comparison of Outburst Cavities with Model Results	53
7.9 Comparison of Outburst Cavities with Model Results	55
7.10 Longitudinal Section of the Cavity from Outbursts #36 and #37	56
7.11 Relationship Between the Breakthrough Width and Siltstone Bed Thickness	58
7.12 Effect of Breakthrough Width on Cavity Volume	60
7.13 Tensile Failures Around the Cavity - Infinite Spalling	61
7.14 Stress Distribution Around a Stable Cavity	62
8.1a Initial Forces Acting on the Potential Shear Planes	66

8.1b	Limit Equilibrium Forces After Shear Plane Relaxation	66
8.2	Siltstone Beam Dimensions and Stress Distribution	67
8.3	Gas Pressure Required to Fail Siltstone Beams	70
A.1	Longitudinal-Section of the Cavity from Outbursts #36 and #37	96
A.2a-n	Cross-Sections of the Cavity from Outbursts #36 and #37	97-103
B.1	Test Cavity Pressure During Packer Test	105
B.2	Methane Content in Return Airway at the Time of Outburst No. 37	106
C.2	Core Log For Borehole D-164	113
C.7a	Sandstone Failure Curve	128
C.7b	Rapid Stress Changes	128
C.8	Sandstone and Siltstone Failure envelopes	132
D.1-8	Core Deformation During Overcoring and Biaxial Tests	139,140
E.1	Flow Chart of Relationship Between SAFCON Routines	148

1. Introduction

1.1 The Hazards of Outbursts

An outburst is the violent ejection of gas and rock and/or coal into an opening from a freshly exposed face (usually from a heading) that takes place in a matter of seconds. Outbursts usually occur in coal seams but they also occur within salt and sandstone. Disruptions in the mining operations have been severe and in some instances were the reason for the closure of a mine. Loss of life can be considerable; for instance, in Japan in 1981, ninety-three men died as a result of a coal outburst.[32]

Many attempts have been made to derive a mechanism to explain the initiation and propagation of these events but no explanation has yet been given that is able to predict the occurrence or quantify the extent of the outbursts. Many models that have been suggested give a description of the influencing factors [18,29,35,41,42,47,48] but are unable to comprehensively describe the initiation and development of the event to its final stable geometry. In most outbursts, geologic disturbances (such as faults or intrusions) have played a key role in their occurrence. A great number of parameters must be quantified before the occurrence of outbursts can be accurately predicted. Until this has been accomplished, outbursts will continue to pose a severe threat to the mine workers and the mine itself.

1.2 Problem Faced By No. 26 Colliery, Glace Bay, Nova Scotia

Since the summer of 1977, thirty-seven outbursts, or events, of rock and gas occurred in the development headings of No. 26 Colliery. The last two outbursts were so severe that the mine was threatened with closure if these events continued. Shortly afterwards a fire closed the mine in April 1984. An extensive testing program had been devised to get a better understanding of the insitu conditions leading to the outbursts but was never initiated due to this closure. A neighbouring colliery, Lingan, is presently in operation and will soon (late 1989 to early 1990) be mining at a depth where No. 26 Colliery began experiencing outbursts. A better understanding of the problems of No. 26 Colliery could save time and money for the

future operations in the area.

The outbursts occur in sandstone channels overlying, and at times penetrating, the coal seam; siltstone commonly intervenes between the coal seam and sandstone beds. High pressure methane gas is present in the low porosity, nearly impermeable sandstone beds. Because of the low permeability, gas drainage by drilling boreholes into these beds has proven to be ineffective. Outbursts have occurred while driving headings in all directions at a depth of at least 700m below sea level and when the sandstone beds penetrated to within 2.7m of the top of the coal seam. The only geologic anomalies known in the region of the outbursts are the presence of these sandstone channels.

1.3 Objective of this Study

The objective of this study is to attempt to define a mechanism that could explain the outbursts that have occurred at No. 26 Colliery. A model was then developed, based on this mechanism, to back-analyse these outbursts. This model can then be used to analyze and evaluate potential remedial measures that can be taken to reduce the effects of, or eliminate, these outbursts.

1.4 Analysis of the Problem

Although little information is available from records of the events at No. 26 Colliery, a better understanding of the mechanics of these events could give some indication of the remedial measures that are required to produce a safer mining environment. There is presently no model in existence that can predict the occurrence or severity of outbursts originating either from coal or other rock. The mechanism and model presented here are able to do that, and were used to reproduce the final cavity shape of the outbursts of No. 26 Colliery with surprising accuracy. With the ability to model these outbursts, remedial measures can be evaluated for their effectiveness. This model makes several assumptions to simplify the analysis (such as two-dimensional stress evaluation) but the mechanism has proven itself in back-analysis.

1.5 Thesis Layout

Chapters 2 to 5 contain summaries of data collected and tests conducted in the mines and surrounding area of the Sydney Coal Field. Information ranges from the general geology of the coal field to a description of the outbursts and stating the insitu properties that will be used within the model. Appendices A to D contain the details of the tests conducted, the results obtained and data collected from the recorded outbursts at No. 26 Colliery.

Chapter 6 gives a general description of the postulated mechanism used in the modelling of the outbursts and the assumptions made in the model. This postulated spalling mechanism applies to cases where the sandstone abuts immediately against the coal seam or where the entry heading penetrates the overlying sandstone. Chapter 7 gives an explanation of the operation of the computer programs used to model the outbursts, results of the model, and a comparison of the model results with the actual outburst cavities. A listing and description of the programs, input and output files for each program, are given in Appendices E and F.

In those cases where siltstone intervenes between the sandstone and coal, and the entry does not penetrate the sandstone, it is assumed that the siltstone fails in a 'cutter roof' mechanism. Once such failure has taken place, the spalling of the sandstone may proceed. Chapter 8 contains a description of the method of analysis of 'cutter roof' failures. This mode of failure is used to explain the failure of a siltstone beam above the heading. Other methods of analysis are also addressed.

Using the information and understanding of the spalling mechanism derived from the model, possible remedial measures are presented and discussed in Chapter 9. Recommendations for further work are given (Chapter 10) with respect to the mining operation and the modelling of outbursts.

Tables and figures are numbered according the chapters in which they can be found; i.e. the first character represents their chapter (or appendix). Equations are handled in the same manner. References are numbered in alphabetical order and only the reference numbers are used in the text of this thesis as shown in square brackets.

2. Geology of the Sydney Basin

The Sydney Coal Basin is located off the north-east coast of Cape Breton Island with the majority of the coal seams situated offshore, as shown in Figure 2.1. The basin is saucer-shaped with beds dipping towards the deeper central part. Both the land and submarine parts of the coal field are part of a Carboniferous Basin extending almost as far as Newfoundland, covering approximately 36,300km². [23,34] Minor folding is present throughout as a result of a series of folds and faults at the southern and western portions of the basin near the land masses. Except for two major thrust faults in the south and west having significant vertical displacements, only minor faulting is present. [23] In general then, major local structures are due to the variations in subsidence as a result of differential compaction of basin strata sediments. [27]

A significant agent in the formation of the Sydney Coal Fields were meandering rivers. Distribution and accumulation of clastic material appears to have been controlled entirely by river courses and their transportation power. This is evidenced by the absence of marine fossils in the sediments, the cross bedded nature of the coarser beds, the channeling of sandstone into underlying strata, presence of rain pitted shales, and the rapid lateral variation in the composition of the strata. [27] There are also no distinct boundaries between sandstone, siltstone and shale. Mudstones and limestones are also present in the sediments that separate the coal seams. [25]

2.1 Coal Origin

Vegetation began growing in the lower portions of the basin (Glace Bay area) and migrated westward to higher ground, resulting in the thinning out of the coal seams to the west. Periods of flooding caused thin bands of clastic material to form within the coal while intermitancy of river flow caused the formation of rider seams and partings. Deposition of peat is rarely witnessed in the river channels themselves; erosion is common in the river borders and where the rivers beds have shifted. Where sandstone replaces shale in the roof of the coal seam, the course of an old river is likely being approached. [23]

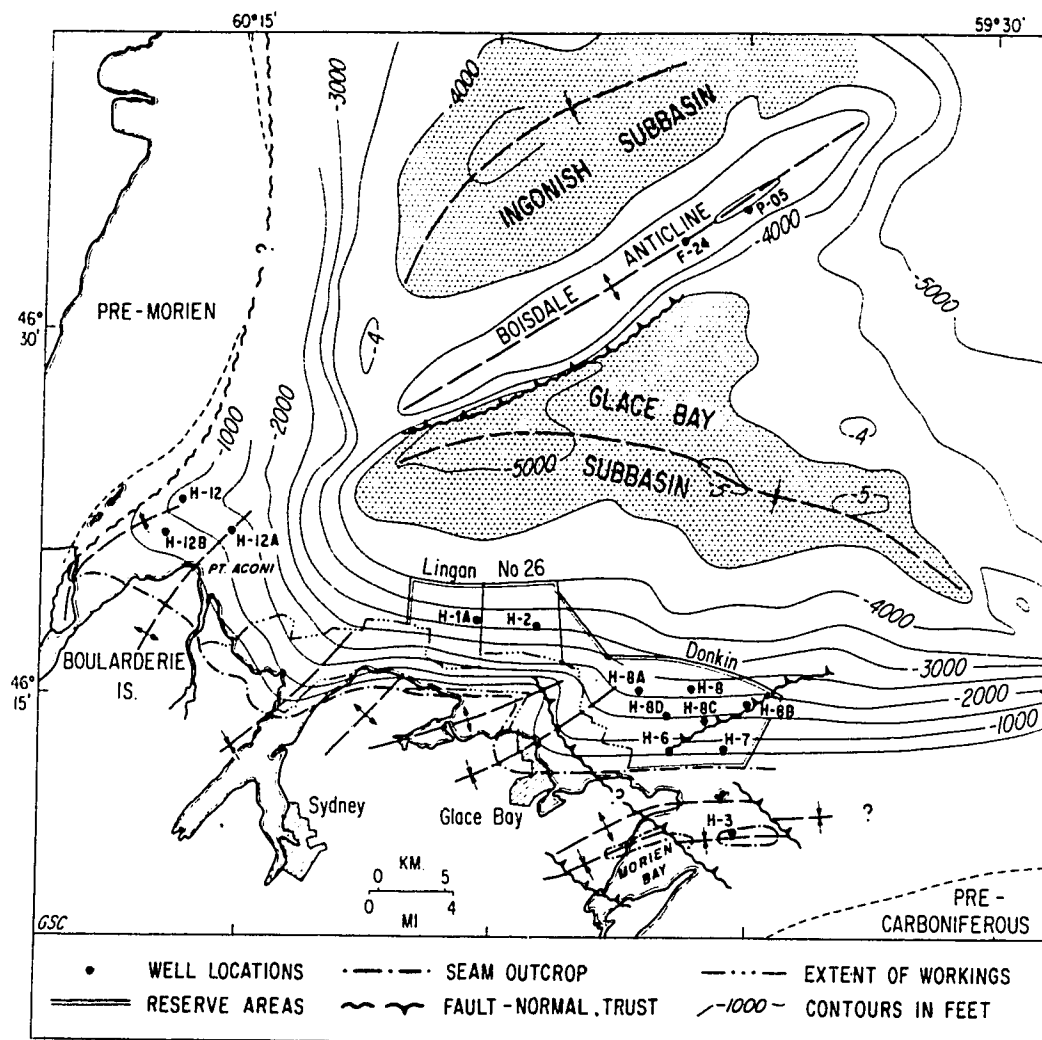


Figure 2.1 Structures and Harbour Seam Contours for Western Sydney Basin (after [23])

2.2 Coal Seams

The high volatile bituminous 'A' coal is of Middle to Late Pennsylvanian in age.[24] Coal rank increases with depth as well as from a west to east direction within the same seam. Coking characteristics also improve with the rank of the coal. This, together with the increased thickness of the coal seams, makes the Donkin area a very favourable location for an operation.[23]

Eleven major coal seams have been found in the basin ranging in thicknesses of 1.0 to 4.5m, with six of these being economically mineable. Figure 2.2 shows the sequence of these seams, thicknesses and depths between them. Presently, several of these seams are being mined: Harbour Seam at Langan, No. 26 (until 1984), Donkin-Morien, Florence and Princess Collieries; Hub Seam at Prince Colliery; Phalen Seam at the Phalen Mine (presently under construction).

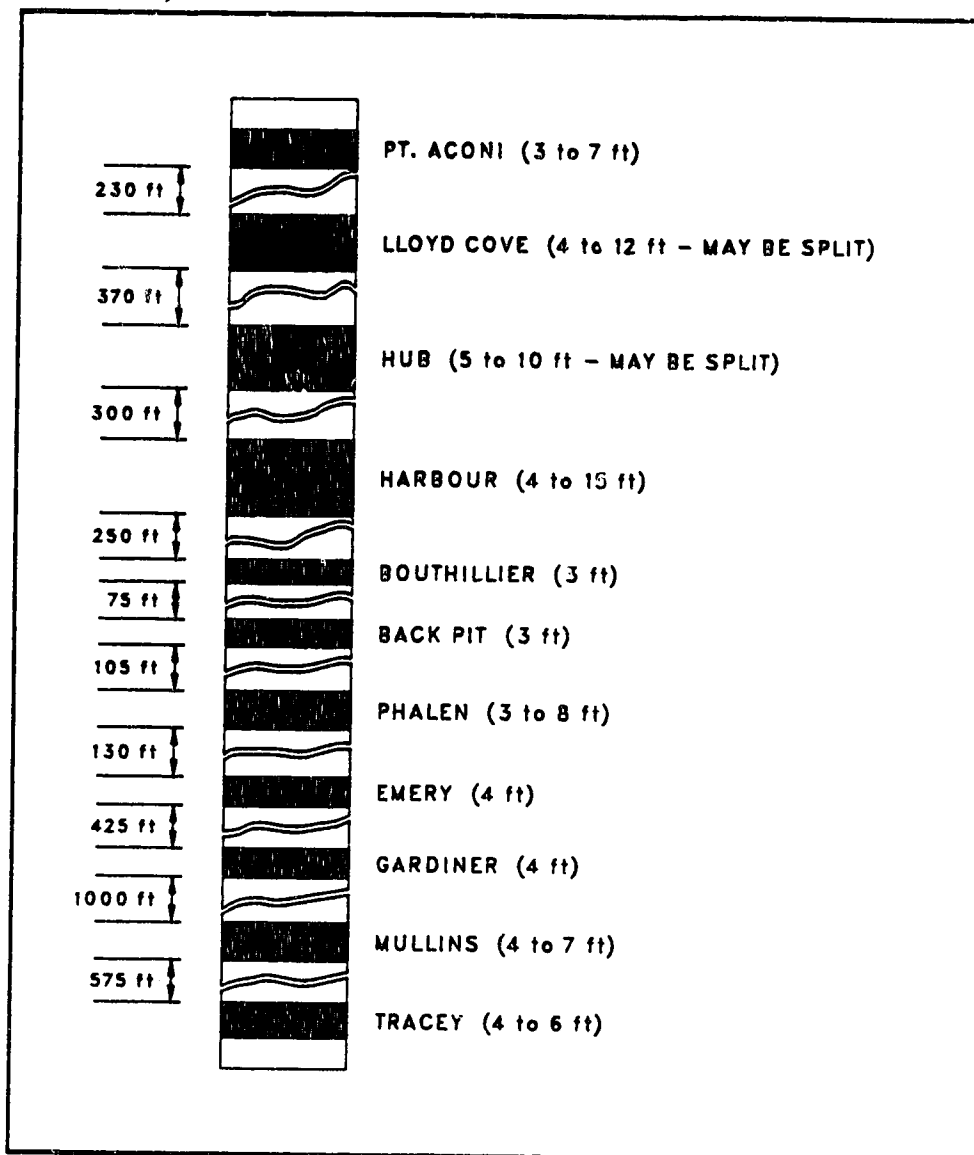


Figure 2.2 Coal Seam Sequence of the Sydney Coalfield (after [14])

3. No. 26 Colliery Operation

3.1 Mine Geology in General

The western part of the Sydney Basin was explored extensively in 1972 using seismic reflection techniques. These findings were proven accurate by an off-shore drilling program in 1977 and 1978 resulting in the Harbour Seam contours shown in Figure 2.1, page 5.[23] A meandering river was present during the deposition of the upper part of the Harbour Seam in the western part of the field. It eventually terminated the vegetation growth completely by flooding the entire region and depositing the clastic sediments of the roof rock.[25] The main channel flowed in a north-easterly direction from Boularderie Island where it eroded large amounts of peat and completely cut the seam within the channel. The resulting sandstone channel in the roof of the Harbour Seam is one of the dominant diagnostic features of the washout.[25]

The linear and roughly parallel nature of the sandstone channels suggest that the streams were braided as opposed to a system of tributary streams.[14] The various coal mining operations in the Sydney Coal Field (past and present) are shown in Figure 3.1; Overlay 3.1i shows the sandstone channels that have been associated with these operations. The presence of these braided streams may be the reason for the apparent independence of one channel from another, many of which appear as thin lenses. Near vertical exploratory drillholes next to some channels have revealed no sandstone.[13] These holes were drilled to a limestone horizon approximately 50ft above the Harbour Seam; this horizon is consistent and can be used as a division of geologic time periods. Haites [27] suggests that structural and tectonic conditions at the time of deposition account for the thickest seams being situated within synclinal areas. (These areas of folding plunge northeast and fan outward.) If this is the case, the river channels would be expected to follow the same pattern as folding. Plots of the synclines illustrated in Overlay 3.1ii, show a close correlation with the sandstone channels.

Mining in No. 26 Colliery revealed an onset of sandstone channels where the normal roof strata of siltstone, mudstone and shale were eroded out and replaced by sandstone. The

National Library
of Canada

Canadian Theses Service

Bibliothèque nationale
du Canada

Service des thèses canadiennes

NOTICE

AVIS

THE QUALITY OF THIS MICROFICHE
IS HEAVILY DEPENDENT UPON THE
QUALITY OF THE THESIS SUBMITTED
FOR MICROFILMING.

UNFORTUNATELY THE COLOURED
ILLUSTRATIONS OF THIS THESIS
CAN ONLY YIELD DIFFERENT TONES
OF GREY.

LA QUALITE DE CETTE MICROFICHE
DEPEND GRANDEMENT DE LA QUALITE DE LA
THESE SOUMISE AU MICROFILMAGE.

MALHEUREUSEMENT, LES DIFFERENTES
ILLUSTRATIONS EN COULEURS DE CETTE
THESE NE PEUVENT DONNER QUE DES
TEINTES DE GRIS.

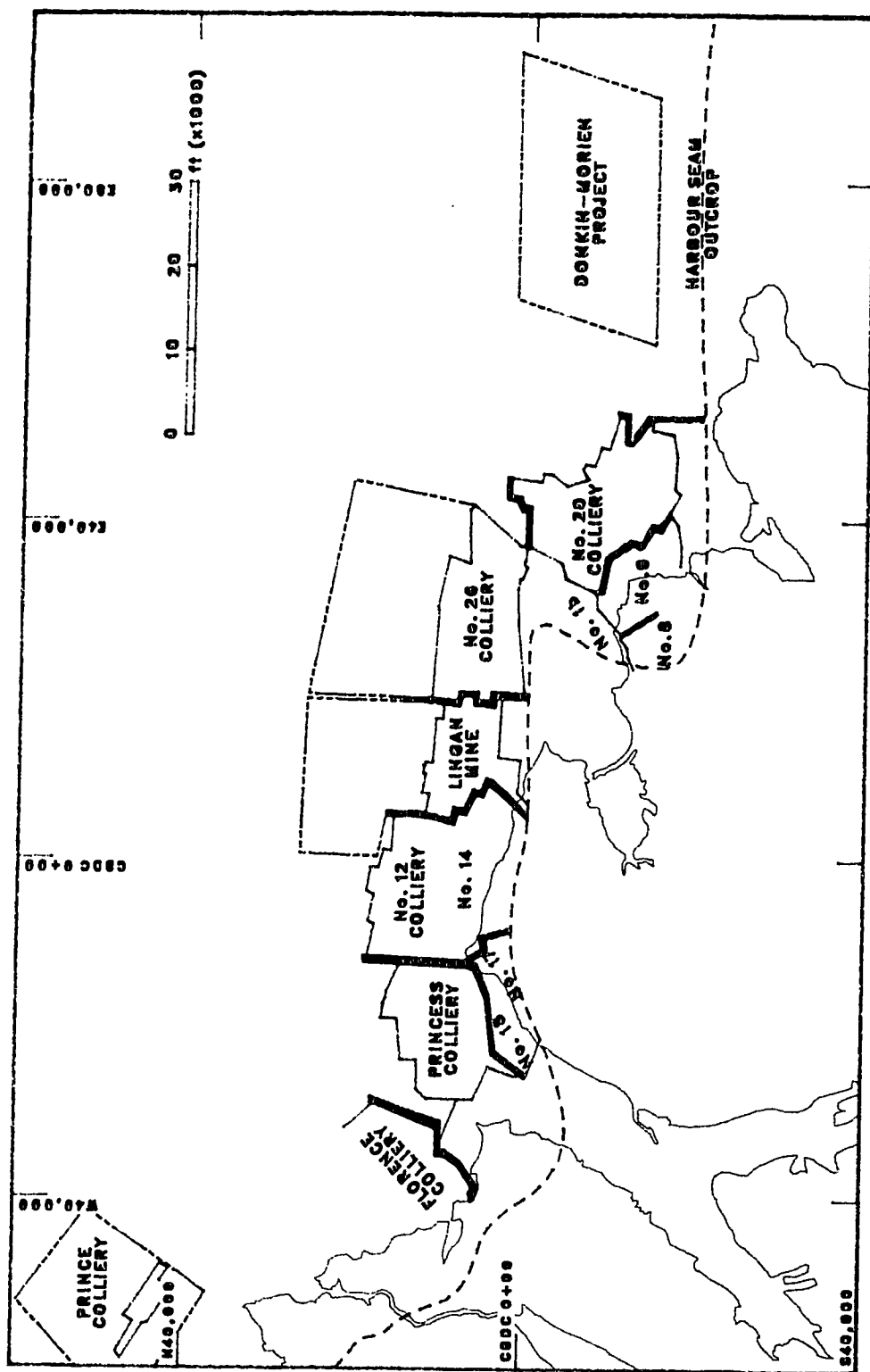
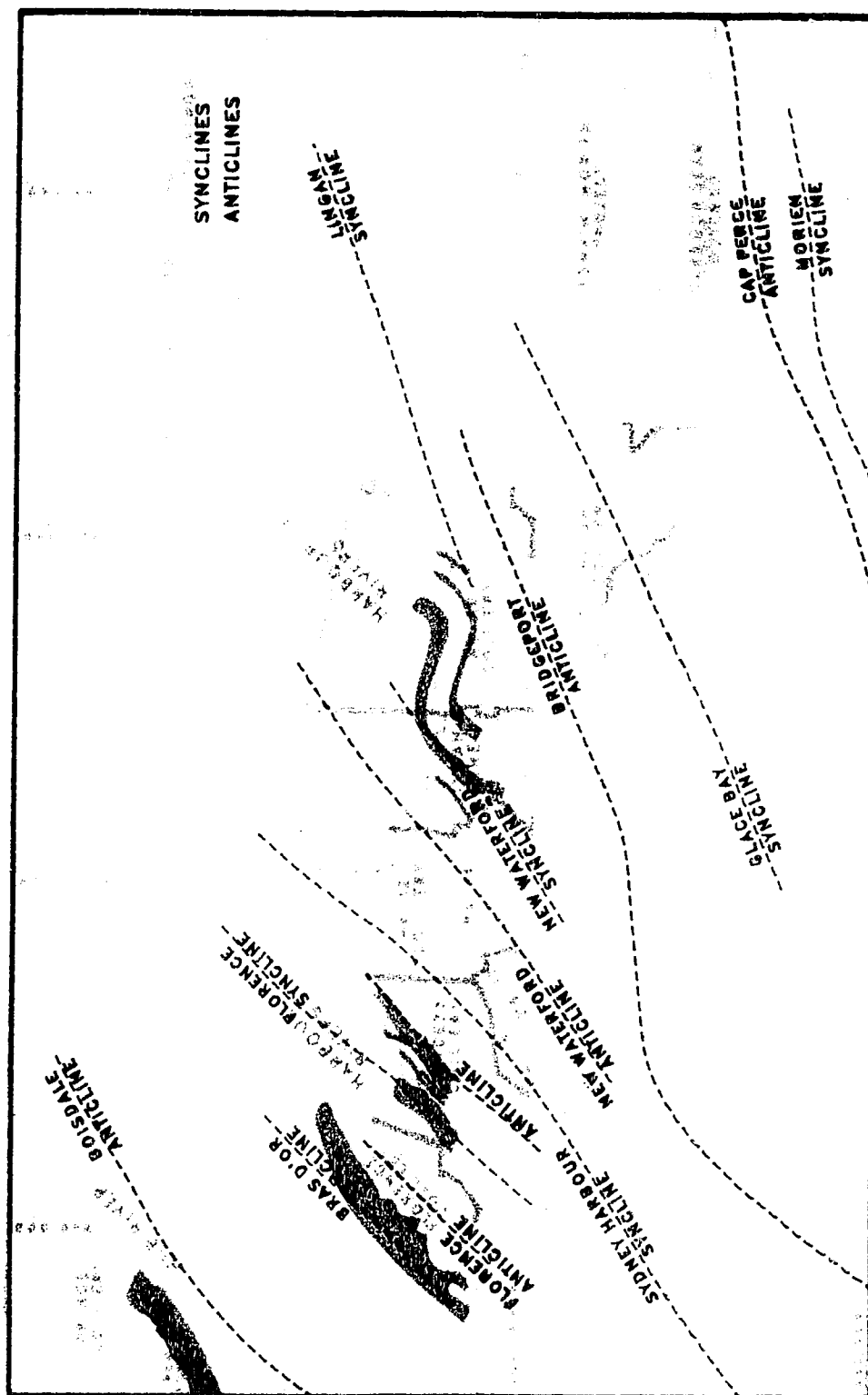


Figure 3.1 Coal Mining Operations in the Sydney Coal Basin (after [2.14.15])



largest mining region affected by sandstone channels was approximately 200ft wide with a length of 4700ft in the 12 South longwall panel.[14] Channels affect mining operations in the following manner:[14]

1. Rock between the coal seam roof and below the approaching sandstone is weak due to jointing caused by differential compaction.
2. Overlying sedimentary beds do not adhere to one another creating a plane of weakness. Roof falls can range in thicknesses from a few centimeters to over a meter.
3. Sandstone channels pinch out to a very weak rock, causing roof falls as noted above.
4. River erosion reduced the height of the coal seams.
5. Methane inflows are common in areas where the sandstone penetrates the coal seam.
6. Sparks are created when the picks of the longwall shearer strike the silicious intrusions and bands causing an extremely hazardous working environment in such a gassy seam.
7. Pyrite is associated with the intruding sandstone channels. Leaching of sulphur into the coal in areas of coal / sandstone contact created zones of high sulphur content.
8. Floor rolls are present due to the differential compaction of the more rigid and heavier sandstone. This is thought to be caused by structural synclines in which the rivers flowed.
9. Small amounts of water are commonly found along the coal / sandstone interface. This leads to slippery and generally uncomfortable working conditions.

In terms of lost revenue, Table 3.1 illustrates the effect of these channels on mine production throughout the Sydney Coal Field.

3.2 Mining Method

No. 26 Colliery, operated by the Cape Breton Development Corporation (DEVCO), is the deepest mine in the Sydney Coal Basin. Production in the Harbour Seam began in 1946 beyond the room and pillar workings of the old 1B Colliery and using those facilities to access the new mine.[35] Access to the mine was by two 205m shafts; one was used strictly for air and men and the other was a double compartment shaft used for supplies and coal. The development entries were 4.5m wide with an arched roof 3.7m high at the center. Production

Table 3.1 Effect of Sandstone Channels on Coal Production (after [14,15])

COLLIERY	MINING SECTION	PRODUCTION BEFORE HINDERANCE	PRODUCTION DURING HINDERANCE	PRODUCTION AFTER HINDERANCE	% REDUCTION DURING HINDERANCE	POTENTIAL LOSS OF REVENUE (\$40/tonne)
Lingan	2 East Longwall	665 tonnes/shift (109 shifts)	317 tonnes/shift (109 shifts)	481 tonnes/shift (109 shifts)	45%	\$1,000,000
Lingan	1 East Longwall	857 tonnes/shift (31 shifts)	636 tonnes/shift (45 shifts)	952 tonnes/shift (45 shifts)	30%	\$ 500,000
No. 26	12 South Longwall	403 tonnes/shift (612 shifts)	201 tonnes/shift (612 shifts)	415 tonnes/shift (590 shifts)	51%	\$5,000,000
No. 26	13 South Longwall (1982)	557 tonnes/shift (213 shifts)	480 tonnes/shift (213 shifts)	669 tonnes/shift (150 shifts)	22%	\$1,133,000
No. 26	13 South Longwall (1983)	636 tonnes/shift (130 shifts)	287 tonnes/shift (131 shifts)	594 tonnes/shift (131 shifts)	53%	\$1,719,000

Table 3.1 (con't) Effect of Sandstone Channels on Mining in General (after [14,15])

COLLIERY	MINING SECTION	EFFECT OF SANDSTONE CHANNELS
No. 26	10 South Longwall	Reduced height of coal seam caused premature termination of longwall
Florence	West Side	Sandstone channels reduced the coal seam to less than workable height. Workings were abandoned.
Princess	West Side	Production hampered locally (no details available)
Prince	Room and Pillar Section	Weak roof near the pinchouts of the sandstone caused roof falls that contributed to the abandonment of the room and pillar section

had advanced to about 8km from the shaft when the mine closed in April 1984 due to a fire in the main intake roadways. The advancing longwall faces were over 200m wide, 2m high, panels were 3km long and nearly 800m below sea level and were equipped with a ranging drum shearer, armoured face conveyor, and powered supports.[35] Before closure, productivity was 4 tons per man-shift resulting in a production of 900,000t/yr.[37] Mining of the 14 North District began in June 1982 and operated until the fire. Figure 4.1 (page 15) shows the layout of recent development and advance of the mine.

The longwall faces were advanced along the strike of the coal seam, and main development headings or 'deeps' were driven down dip. Headings were advanced by drilling and blasting. The only support was provided by arches spaced at 0.9m intervals with lagging installed where necessary.[10] In all cases, the floor of the roadways was coincident with the base of the coal seam.

4. Outbursts

4.1 What are Outbursts?

Conventional coal outbursts are sudden violent failures of coal and/or rock accompanied by the release of large amounts of gas, usually methane and/or carbon dioxide. Many times an outburst is indistinguishable from coal bumps (similar to rock bursts) because both liberate various amounts of coal and gas.

The most commonly accepted theory on the mechanics causing outbursts was put forward by Khodot [33]. Stresses in the ground around an excavation cause fracturing in the coal and the release of large volumes of gas. As the gas forces its way out, it takes coal with it. According to Khodot, an outburst occurs in three stages:

1. Trigger stage:

If a triaxially stressed solid within a rock mass is suddenly exposed by excavation, the solid's resistance to an internal gas pressure is significantly reduced. The inner pressure could cause fracturing of the solid at the exposed face and allow gas to escape from the original rock pores. Rock pressure causes fracturing and displacement of the coal from the face.

2. Free Gas stage:

The pressurized gas within the coal then causes the fractured coal to be ejected from the face. The effects of the ground stresses are now negligible compared to the effects of the gas.

3. Adsorbed Gas stage:

As the free gas is liberated, the confinement of the adsorbed gas is reduced thereby allowing the desorption of gas from coal. This is further enhanced by the crushing of the ejected coal, which liberates more of the gas and increases the ejecting force (energy) of the gas.

This process continues until some sort of stability is reached either by changing rock properties, gas pressures, stress field or excavation shape or a combination of these.

4.2 Sandstone Outbursts at No. 26 Colliery

The outbursts experienced at No. 26 Colliery (data given in Appendix A) differ from the conventional outbursts in that they originate from the overlying sandstone, as opposed to the coal. The sandstone contained very little carbonaceous material (as noted in Appendix C) and therefore sorbed gas accounted for only a small portion of the methane in the sandstone.[4] Low porosity ($\approx 5\%$) and very low permeability ($\approx 0.03\text{md}$) prevented quick drainage of the methane and therefore a large pressure gradient was created between the new face and the 'undisturbed' sandstone. If the rock near the face were considered to be intact then the outward pressure of the gas would cause the rock to be broken and ejected if the gas pressure exceeded the tensile strength. If the stress concentrations around an opening created shear failures, the gas would bleed off from the peripheral fracture zone.

4.2.1 Gas Migration to Sandstone [10]

Methane evolved during the diagenesis of the peat to coal. As the overburden cover increased, coal compacted to a greater degree than the overlying sandstone. Surrounding siltstone and mudstone did not have sufficient porosity or permeability to accept the methane being forced out of the compacting coal. Therefore, the methane migrated to the still unconsolidated and porous sandstone. In time, the cover increased to the extent that the sandstone compacted and trapped the methane within its pores. Compaction continued to such a degree that the trapped gas built up high pressures and had no place to escape. Anisotropies and inhomogeneities in the sandstone could have resulted in the formation of localized pockets of higher pressure gas. Water trapped within sandstones has also been known to trap gas in pockets in mines elsewhere.[6]

4.2.2 Outburst Geology

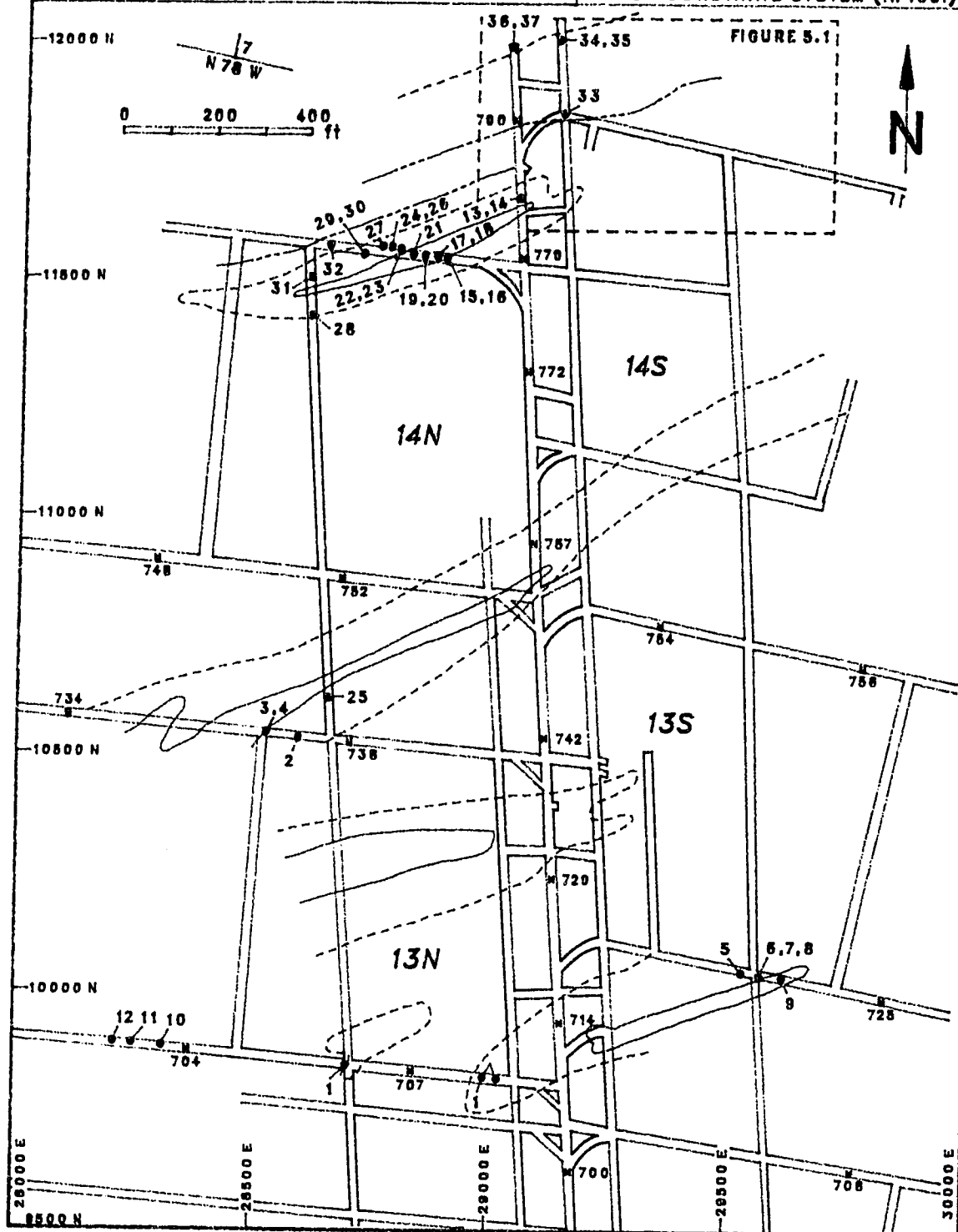
Since 1977, a total of 37 outbursts (or events) were recorded in the Harbour Seam workings of No. 26 Colliery as shown in Figure 4.1. All of these events occurred when driving single or double entries into virgin ground, relatively uninfluenced by other workings.

FIGURE 4.1 (after [2,13])

**MINE PLAN SHOWING SANDSTONE
CHANNELS AND OUTBURSTS**

- OUTBURSTS
- × DEPTH BELOW SEA LEVEL
- 13N LONGWALL PANELS
- HEIGHT OF SANDSTONE ABOVE COAL
 - 0 feet
 - - - 5 feet
 - 9 feet

MINE COORDINATE SYSTEM (In feet)



Appendix A contains all the data accumulated on these outbursts. Initially, many of these events were classified as simple roof falls due to their non-violent nature and because no increase in methane was recorded. The creation of a new face in a coal seam heading causes the release of methane from the coal. In the 'smaller' events, a minor amount of methane would also be released and could go unnoticed. However, as mining progressed to greater depths, the severity of these 'falls' increased and large methane gas emissions were detected.

All of these events exhibited ejected sandstone of a pulverized nature with an onion-skin texture around the cavity (which is typical of high pressure gas ejections from rock), as shown in Figure 4.2. This formed the basis for the reclassification of many of the earlier events as sandstone outbursts. All events occurred in areas of channel sandstone penetration to within 2.7m of the coal seam roof (and in some cases penetrating the coal seam), ie. less than 1.5m from the top of the opening, and at depths greater than 700m. All but one of the outbursts were triggered by shotfiring. Outbursts occurred independent of the direction in which the heading was driven.

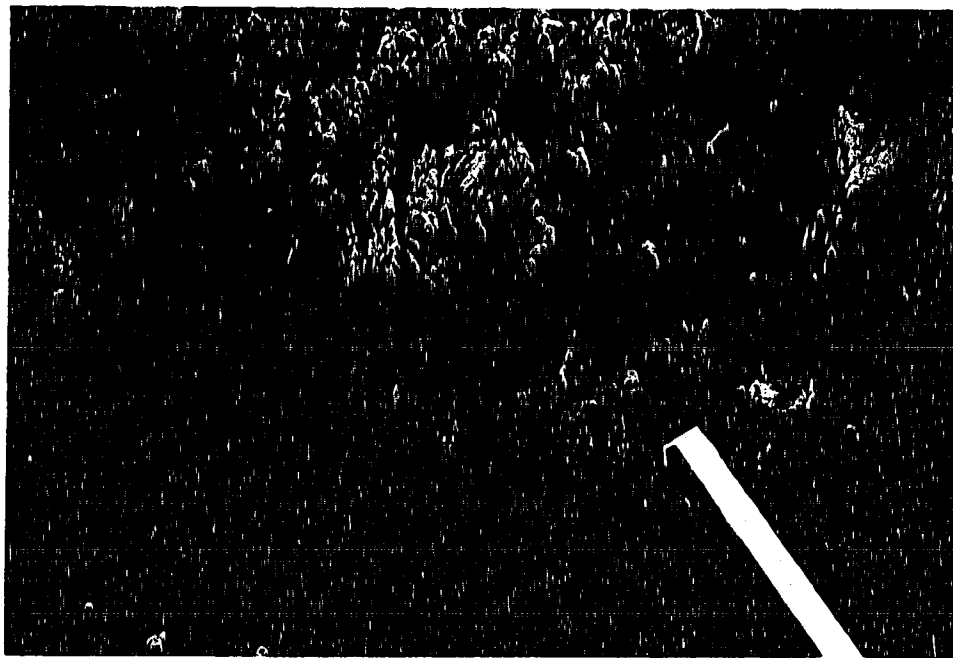


Figure 4.2 Onion-Skin Texture of the Outburst Cavity (after [16])

The second last outburst (#36 dated Nov. 23, 1983) was the largest event recorded. The size of this event was mainly due to the fall of roof material away from the face into the belt deep as a reaction to the main outburst. This 'fall' of material went back about eighty feet to the main deep / belt deep crosscut. A series of cross-sections of the resulting outburst cavity are presented in Figures A.2a to A.2n, pages 97 to 103. Figure 4.4 is a photograph of the drift one day after this outburst. Once the ejected rock had been removed, the arches were put back into place with lagging and timber cribbing used to support the cavity. An example of this is shown in Figure 4.5.



Figure 4.4 Outburst Damage in Development Heading (after [16])

4.3 Other Non-Coal Outbursts noted Elsewhere

The problems encountered in the Sydney Coalfield are not unique in mining. Cases have been noted in literature of similar events occurring in many parts of the world, and not just limited to coal mines. These include gypsum, evaporite and potash mines.[32] Methane or carbon dioxide, or both have been associated with these events.

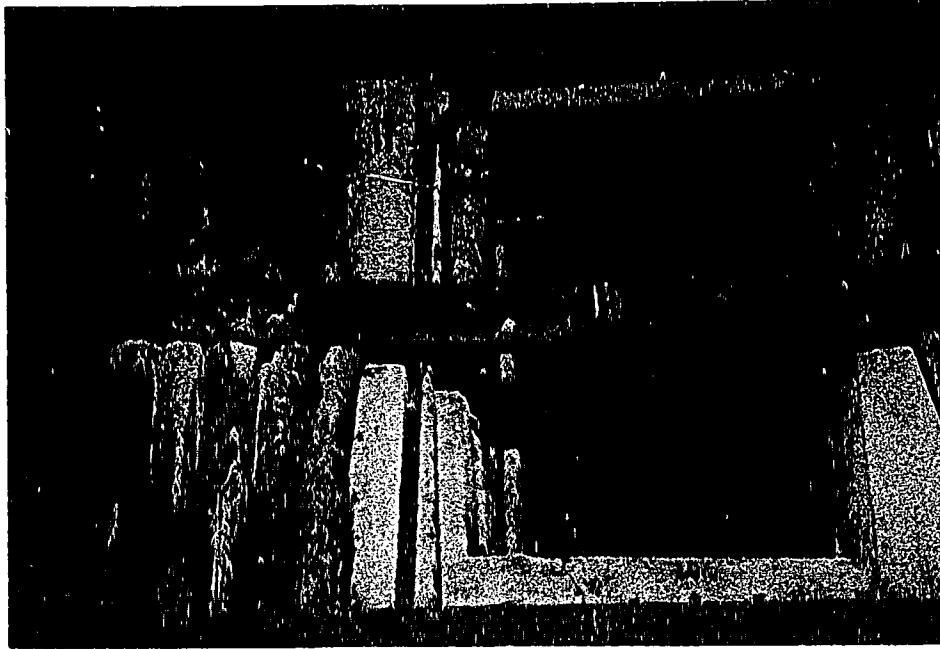


Figure 4.5 Timber Cribbing to Support Cavity Back (after [16])

4.3.1 West Germany

Ibbenbueren Colliery [32,43] has experienced many outbursts of sandstone and gas (primarily methane) that appear exceedingly similar to those that occurred at No. 26 Colliery. Anthracite seams are being mined which are overlain by a 1.6m thick argillaceous shale bed and a sandstone bed of 13-14m thick. These events are described as follows:

"Following blasting in the course of driving the headings, dome-like cavities of elliptical cross-section having a diameter of 0.5m to 3m and a height of up to several metres broke out of the roof of the headings ..." [43]

"... walls exhibited clear evidence of pressure relief exfoliation." [43]

The latter probably refers to an onion-skin texture as noted in No. 26. All bursts occurred at depths of greater than 700m (hydrostatic stress field equal to the overburden pressure) with,

up to 700m³ of rock and 6,500m³ of methane being ejected. The triggering mechanism for the majority of the outbursts was shotfiring adjacent to or into burst prone strata; to a much lesser extent, vibrations from large drilling equipment caused minor bursts. The burst-prone sandstone had a porosity of 10-14% and low strength (due to low cementing material content). Lower porosity sandstone (less than 7%) did not burst. Gas pressures have been measured in the order of 6MPa.

Core discing in the outburst prone sandstones has proven to be an adequate means of predicting potentially dangerous areas. Discs 5 to 50mm thick were produced in these zones. Boreholes, however, do not provide any relief to the gas pressure as the permeability of the rock must be quite low. Shattering of the rock is the only method of effectively relieving the gas pressure. It has been noted that even in the area of outburst cavities, the gas was drained only a few meters into the country rock.

Outbursts from the hanging wall could be avoided by driving the drifts further into the footwall and not blasting near the sandstone boundary. When driving crosscuts through the sandstone, outbursts could not be avoided. Extra precautions were taken to limit risks to the men and the outbursts were allowed to occur 'safely'. These outbursts were not as severe as the last two noted in No. 26 colliery. The actual mining area does not seem to have this problem because of 'large scale stress relief of the rock' due to roof failures in the gob.

4.3.2 USSR and Poland

The Donetz Basin in the USSR first encountered outbursts in the 1960's when mining levels reached depths greater than 700m. Almost 3500 outbursts had taken place to January 1983 and many of these originated from within sandstone beds; a total of 174 sandstone beds have been affected.[32]

The Lower Silesian coal basin in Poland suffers from coal outbursts in forty-eight mines and four of these also suffer from gas and rock bursts. Their severity appears to increase with depth.[32]

4.3.3 England

Outbursts in the East Midland Coalfield originate from the floor and roof strata bounding the coal seams. They occur in areas where the bounding beds change in thickness, causing irregular fracturing in these beds which causes sudden redistribution of the stresses around the openings.[32]

Floor outbursts in the Durham Coalfield have been associated with areas in faulted ground. It has been suggested that folding, thrust faulting, 'slip cleavage' and highly sheared coals are responsible for the release of large volumes of gas at outburst sites.[32]

4.3.4 United States

The salt mines of Louisiana experience bursts of gas and salt in five of the six mines. Bursts occur at the face or above a heading resulting in a 'generally semi-ellipsoidal cavity with axial length of up to fifty meters or more'[38]. Outbursts occur at various depths in regions where a heading approaches impure or altered salt containing trapped, high-pressure gas (primarily methane); there is a strong relationship between the shear zones and the occurrence of outbursts. Gas pressures have been estimated to be in the order of only 0.05MPa. Outbursts continue until the gas pressures are relieved or the cavity becomes so filled with loose ejected salt that spalling cannot continue.[38]

4.4 Previously Proposed Outburst Mechanism for Coal

Paterson [42] presents a model for the mechanism of outbursts in coal. The basis of this model is that an outburst is the result of the structural failure of coal due to excess stresses resulting from body forces. These body forces on the coal are equal to the pressure gradient of the gas flowing from the coal. The proposed model shows how the following factors increase the occurrence of outbursts: high rates of advance; low permeability; low strength coal or joints; greater depth.

It was stated that to model outbursts, the model must account for the gas flow, the stress field and a failure mechanism or criterion. For the flow of fluid through coal, a series

of equations were used to simulate two phase flow through a porous media. Gas flow is written in terms of permeability and porosity (both as a function of gas pressure and position), gas density (as a function of pressure) and the effect of desorption of gas from coal (as a function of gas pressure, position and time). One simplification put forward is that the sorption of gas on coal can be treated as an additional porosity.[41] Porosity and sorption are presented in the same manner (volume of gas per volume of rock) only the sorbed gas exists at a much greater volume. Therefore, the assumption is made that the degassification of sorbed gas is 'instantaneous'. This assumption has already been made by others within numerical models.

The stress distribution is determined by analysis of the effective stress equilibrium equations. For simplicity, the coal is assumed to be homogeneous, isotropic and perfectly elastic. The failure criterion chosen was a Mohr-Coulomb function with a tensile cut-off. It has been stated that an outburst is primarily a result of tensile failure. Paterson states that when the minimum (effective) principal stress exceeds the tensile strength, a crack forms and, if allowed to propagate, an outburst will occur. Different rock types may be located within the area of analysis and can be presented in terms of position around the opening. The tensile strengths of these different materials may be represented by that same function.

Paterson found that large tensile stresses occur near the face of the seam (due to a high pressure gradient near the face). If these stresses exceed the strength of the coal, tensile failure occurs, propagating cracks, resulting in an outburst.

A simplified, one-dimensional model was given. To find the maximum rate of advance, the following assumptions were made:

1. the mine opening produces no resistance to gas flow,
2. the rate of advance is uniform, and
3. the pressure gradient is given as the maximum that the rock can withstand prior to failure, thus taking into account the failure criterion.

The maximum rate of advance was then written as

$$v_{\max} = \frac{k G}{\phi \mu \left[\frac{P_i}{P_o} - 1 \right]}$$

where: k = permeability of coal
 G = gas pressure gradient
 ϕ = coal porosity
 μ = viscosity of gas
 P_i = initial or insitu gas pressure
 P_o = gas pressure at coal face (assumed atmospheric)

The effect of sorption is not included in this simplified equation.

The model has not been tested by back analysis of case histories because the number of variables is significant. A complete set of data at a given outburst site has not been measured. However, the relationship of the parameters is given and only the definition of these is required. For example, determination of the effect on permeability of changing position (different media, stress conditions, etc.) and gas pressure: this could, perhaps, be found by testing cores taken from sites within the mine and fitting some function to the results and applying this to the model.

4.4.1 Discussion of Paterson's Proposed Model

Paterson presents a mechanism that can be extremely useful, however, at present it is too general to be practical. The input parameters are so numerous, that back analysis has yet to be carried out due to the lack of available data. In general terms, it can explain the effects of influencing parameters but to be of use, several simplifications may have to be made for a given situation, thus making it site specific. Paterson evaluates the quantitative effects of different parameters on the initiation of outbursts or increased severity, but the mechanism is not an attempt at modelling outbursts. No model has yet been presented that even attempts to quantify outbursts and a considerable amount of data would have to be gathered before Paterson's model could be used in this manner. This model does, however, present an excellent basis for further work on coal outbursts.

5. Insitu Properties

Very little data is available on insitu properties in No. 26 Colliery. Most of the tests conducted have been in the vicinity of the later, and more severe, outbursts. The test results that are available are presented in Appendices B (gas pressures), C (rock properties) and D (stress field). A summary of the results will be presented in this section. Figure 5.1 shows the location of the tests that provided the most information. See also Figure 4.1 (page 15) for these locations on the general mine plan.

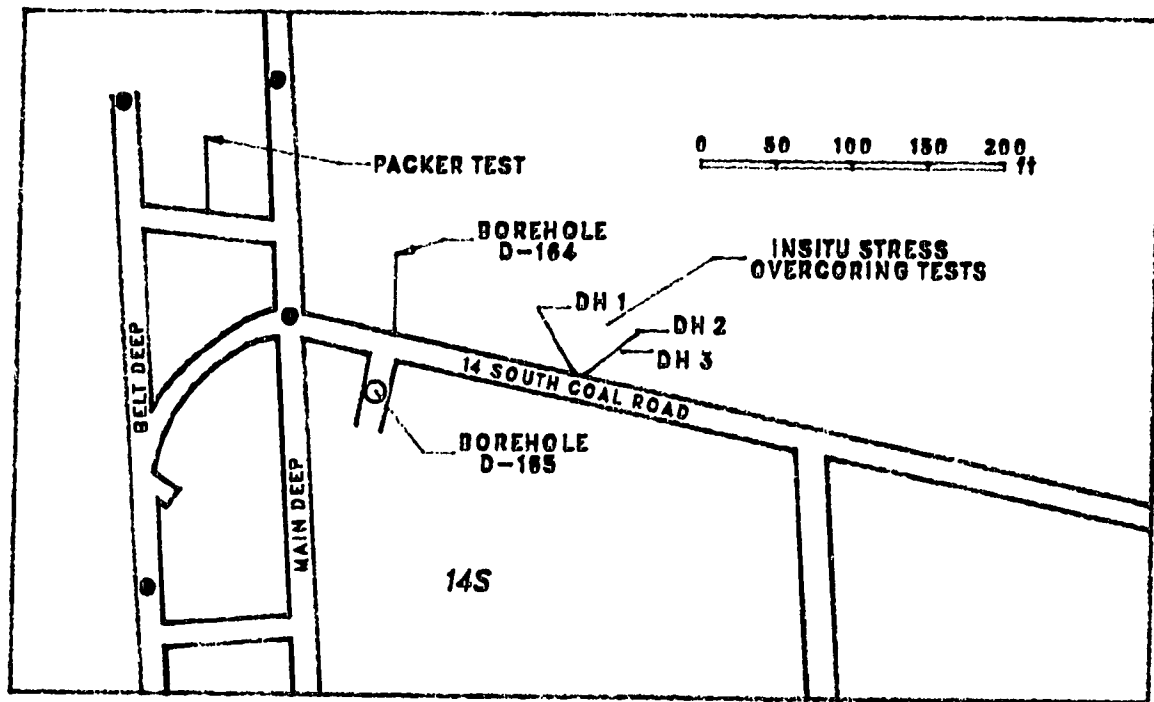


Figure 5.1 Various Test Site Locations

5.1 Insitu Gas Pressure

The insitu gas pressure was estimated by several different methods. These include a packer test in outburst prone sandstone, back calculations based on volumes of ejected sandstone and methane for the last two events, and reservoir engineering estimates.

The packer test [17] was conducted in the pillar separating the main and belt deeps in the deepest part of the mine. Several sandstone horizons were encountered during the drilling

of the test hole, which exhibited core discing. It was in one of these zones that the test was conducted. Measuring pressure build-up in the test hole failed because the rock was so impermeable that little or no gas flowed into the cavity. Pressurizing the cavity and observing the pressure dissipation lead to an eventual constant pressure of 2.76MPa for the duration of the test.

These results were not conclusive. The final pressure may only have been an equilibrium pressure between incoming gas from the strata and gas lost due to leaks in the seals, gas flow through intact rock, or loss through fractured rock around the seals. Another packer should have been placed behind the first to monitor gas flow from the test cavity. We can however conclude that the pressure of 2.76MPa was a minimum and could have been greater, depending the severity of any leakage of the packers. Analysis of the gas in the test cavity after the test indicates that there was probably no inflowing strata gas.

Back calculations using the General Gas equation (based on the ideal gas law) were done based on the data for the last two events (#36 and #37) to determine the gas pressure. [3] Recorded values for the volumes of ejected rock, a porosity of 5%, an assumed water saturation of 2% and recorded methane levels were used. Methane volumes were estimated based on increased methane readings in the return airway at the time of the burst (as shown in Figure B.2, page 106). Results indicated a pressure of 4.9MPa for event #36 and 41.8MPa for event #37. The strata gas composition has been reported to be the following:

CH ₄	75 - 80%
N ₂	≈ 10%
C ₂ H ₆	5 - 10%
other hydrocarbons and CO ₂	2 - 5%

These derived gas pressure are only as good as the input data. The survey of ejected material for event #37 was taken before the clean-up was completed and the face was still heavily fractured. Loose and broken rock still hanging up in the cavities could significantly increase the volume of material from which the liberated methane originated. Also much of

the methane could have been due to the formation of a new coal face created during shot firing. This could have produced up to 1500m³, of methane.[18]

Paterson [42] states that a natural gas reservoir formation pressure can be estimated to be 23kPa per meter of depth. At 780m deep, the depth of the last outburst, the gas pressure would be almost 18MPa. A reservoir engineering rule of thumb estimates pressures according to a hydrostatic column of water, thus giving 7.9MPa.[4] Aston and Cain [4] estimate that the most likely range would be 2.8MPa to 7.9MPa.

For an outburst to occur, the effective stresses must exceed the tensile strength of the rock. Assuming that the total stresses around an opening are in compression only, then the gas pressure must exceed the tensile strength. If the sandstone has a tensile strength of 2.4MPa (as noted later in this section) the gas pressure must be greater than that.

5.2 Rock Properties

Several reports contain data, results of tests and best estimates on rock properties from the mines of the Sydney Coal Fields. However, very few tests have been carried out, especially at No. 26 Colliery. Properties that have been tested for include density, uniaxial compressive strength, tensile strength, elastic modulus, Poisson's ratio, porosity and permeability. A summary of the rock properties used in this report are found in Table 5.2a with a listing of acquired data in Appendix C, page 110.

Table 5.2a Average Rock Properties

ROCK TYPE	STRENGTHS		ELASTIC PROPERTIES		POROSITY (%)	PERM. (md)	CARBON CONTENT
	σ_c (MPa)	σ_t (MPa)	E(GPa)	ν			
sandstone	76.3	-5.8	18.50	0.18	5.24	0.03	2.76 %
siltstone	66.4	-12.1	26.15	0.36	1.2	< 0.01	-

The most significant results come from boreholes D-164 and D-165, shown in Figure 5.1. These holes were drilled in areas adjacent to several outbursts and intersected several

sandstone beds, some of which exhibited core discing, a phenomena associated with bursting and spalling. Samples of sandstone and siltstone were extensively tested for elastic and strength properties. However, only one series of triaxial tests were conducted (on sandstone). Failure criteria were fitted to the results as best as possible with the limited information. Variations in properties for all rock types tested were considerable.

The sandstone samples used in the triaxial tests produced strengths that were low compared with other samples under uniaxial compressive tests. When a Hoek and Brown failure criterion was fitted to the triaxial results, the tensile strength was also low. However, since only one set of triaxial tests was available, its results will be used. When considering the variability of the material, it may even be desirable to use a failure envelope of low strength. An envelope was also fitted for the siltstone using only the uniaxial compressive and tensile strengths of the rock. These are summarized in Table 5.2b. These intact properties will be used for both rocks in the model studies reported later.

Table 5.2b Parameters of the Hoek and Brown Failure Criterion Used in the Model

ROCK TYPE	σ_c (MPa)	σ_t (MPa)	m	s
sandstone	48.42	-2.4	19.94	1.0
siltstone	50.50	-11.4	4.20	1.0

5.3 Insitu Stress Field

One set of overcoring tests was carried out [21] to determine the insitu stress conditions near the area of the last outbursts. The location chosen was one of uniform geologic environment and absence of geologic structures. Tests were completed in December 1983 in the 14 South Coal Road shown in Figure 5.1. Three boreholes were drilled in which nine tests were conducted. Holes 1 and 2 were drilled into the siltstone above the coal seam and hole 3 penetrated the overlying sandstone channel. The site of these tests was about 40m

cast of the D-164 borehole so material properties were expected to be similar to that of the last two outbursts.

The overcoring tests were based on the US Bureau of Mines (USBM) method.[31] Deformation gauge buttons, 120° apart, measure the deformation of a pilot hole in a plane normal to the borehole axis. Five of the tests proved successful, one each from drillholes 1 and 3 and three from hole 2. Tests failed primarily due to premature breakage of the core along bedding planes. Biaxial testing of the recovered cores was conducted to determine the elastic modulus of the tested rock. Only three of the cores could be recovered to carry out the biaxial tests. Two cores were recovered from drillhole 1 and one from drillhole 3. Once again bedding plane splitting was the cause for core failure.

The evaluation used by Golder Associates [21] assumed that the rock was linear elastic and homogeneous. This allowed the following simplifications:

1. stress determination under plane strain conditions, and
2. all data may be pooled to allow determination of three-dimensional stresses using least-squares solutions.

The test site was about 300m from the nearest longwall panel, thus the test area was considered in virgin ground with a virgin stress field.

Table 5.3 Insitu Stress Field (after [21])

STRESS	MAGNITUDE (MPa)	ORIENTATION	
		BEARING	DIP (up)
σ_x	23.31	E-W	horizontal
σ_y	24.98	N-S	horizontal
σ_z	25.27	vertical	
σ_1	26.30	due West	-25°
σ_2	23.20	N 82° W	64°
σ_3	24.05	N 9° E	-13°

Table 5.3 contains the resulting insitu stresses evaluated to principal and 'mine co-ordinate' stresses. The average vertical stress is 15% greater than the static vertical stress and the major principal stress is 17.5% greater. The ratio of the major to minor principal stresses is 1.1, nearly a hydrostatic insitu stress field.

These results are questionable when considering some of the assumption that were made during the evaluation of the test results. These concerns include the following:

1. Poisson's ratios were not determined. These have been found elsewhere to vary considerably between the siltstone and sandstone.
2. Diametral deformations were averaged when it is clear that they differ in directions normal and perpendicular to the bedding planes.
3. Tests were conducted in sandstone and siltstone and the results pooled. The test should have been conducted in the same rock bed. Stress conditions have been known to differ between various sedimentary beds.
4. It was negligent not to consider the influence of the roadway itself when assuming that the tests were being conducted in virgin ground.

This last point was considered more closely. A boundary element program was used to re-create the stress conditions that must have existed around the roadway to reproduce the results that are reported above. A more detailed description of this is given in the summary of Appendix D, page 141. The re-evaluated stress field was approximated by:

$$\sigma_1 = \sigma_x = 26.3\text{MPa}$$

$$\sigma_3 = \sigma_y = 24.0\text{MPa}$$

where x and y are the horizontal and vertical directions. These values will be used later in the model.

6. Postulated Mechanism of Non-Coal Outbursts

An outburst is the result of the failure of rock due to excessive pore fluid pressure. If the effective stress exceeds the tensile strength of the rock, tensile failure will occur. The rock is shattered at these locations and thus the gas and rock is blown out, leaving a cavity. If the gas pressure is insufficient to cause tensile failure, but the shear strength is exceeded, the rock becomes sheared. It is assumed that the structure of this sheared rock is still intact except that it has become fractured. This fracturing allows the gas in the pore space to escape, producing a pressure gradient near the face of the opening. Given time (seconds, or fractions of a second) the gas pressure in this sheared zone is alleviated allowing the gas in the intact rock to permeate out over time.

As stated by Paterson [42], an outburst model must account for the flow of gas through the rock, the stress field around the opening and the failure mechanism. In the case of No. 26 Colliery, the sandstone has a very low permeability (approximately 0.03 millidarcies); assume that this value is zero. This seems reasonable when considering that during the packer test (section 5.1, page 24, and Appendix B, page 104) no gas flowed into the borehole test cavity in five days. Because of this, gas flow through intact sandstone is assumed not to exist and the model need only consider the gas flow through sheared sandstone. This gas flow produces the pressure gradient near the face of the opening. Sorption is assumed to be insignificant and will not be considered even though a little carbonaceous material does exist in the sandstone.

The stress distribution can be defined as a static force equilibrium for which the components of the stress tensors satisfy the following system of equations:[46]

$$\begin{aligned}\frac{\partial \sigma_x}{\partial x} + \frac{\partial \tau_{xy}}{\partial y} + \frac{\partial \tau_{xz}}{\partial z} - F_x &= 0 \\ \frac{\partial \sigma_y}{\partial y} + \frac{\partial \tau_{xy}}{\partial x} + \frac{\partial \tau_{yz}}{\partial z} - F_y &= 0 \\ \frac{\partial \sigma_z}{\partial z} + \frac{\partial \tau_{xz}}{\partial x} + \frac{\partial \tau_{yz}}{\partial y} - F_z &= 0\end{aligned}\tag{6.1}$$

where σ_x and τ_{xy} are the stress tensor components and F_x are the external, or body, forces

acting at that point of the rock (force per unit volume).

In the case of a pore pressure existing within the rock structure, effective stresses replace the total stresses in the above equation and the body forces acting on the structure now represent the hydrostatic gas pressure.[46]

$$\begin{aligned}\frac{\partial \sigma'_x}{\partial x} + \frac{\partial \tau'_{xy}}{\partial y} + \frac{\partial \tau'_{xz}}{\partial z} - \frac{\partial p}{\partial x} &= 0 \\ \frac{\partial \sigma'_y}{\partial y} + \frac{\partial \tau'_{xy}}{\partial x} + \frac{\partial \tau'_{yz}}{\partial z} - \frac{\partial p}{\partial y} &= 0 \\ \frac{\partial \sigma'_z}{\partial z} + \frac{\partial \tau'_{xz}}{\partial x} + \frac{\partial \tau'_{yz}}{\partial y} - \frac{\partial p}{\partial z} &= -\rho g\end{aligned}\tag{6.2}$$

where σ'_x and τ'_{xy} are the effective stress tensor components, g is gravitational acceleration, ρ is the density of the rock and p is the insitu gas pressure. This is the case if the only body forces acting on the rock are gas pressure and gravity.

Any failure criterion can be chosen to evaluate the relationship between the strength and stress of the rock. Since the mode of failure in outbursts is one of tensile failure, a failure criterion must be chosen to represent the strength conditions when the rock experiences tensile stresses. Since such testing is not a common practice, assumptions must be made as to the behaviour of rock under these conditions. An example of this is the Mohr-Coulomb function with a tensile cut-off, as used by Paterson. The Hoek and Brown [30] failure criterion will be used in the model presented here.

6.1 Postulated Spalling Mechanism

The spalling of rock during an outburst is considered to be a series of instantaneous events. As the cavity spalls, the stresses are altered around the cavity being formed. The stress distribution will depend on several parameters:

1. nature of the rock (homogeneity, isotropy, elastic properties)
2. shape of the cavity
3. virgin stress field (horizontal to vertical stress ratio - K)
4. influence of the heading and other workings

The shape of the cavity changes due to the ejection of rock and gas in localized areas of the rock near the face of the cavity. The face of the cavity is assumed to be gas-stress relieved due to its sheared nature. Outward from the face into the rock, there is a gas pressure gradient. If the effective stress at any point becomes greater (negatively) than the tensile strength, the rock and gas is ejected, thus changing the cavity shape. Eventually, the cavity will reach its most stable shape. However, this most stable shape is not necessarily the end of the spalling; if the gas pressure is great enough, confining pressure may not build up fast enough near the face to stop the formation of tensile stresses. In such a case, spalling continues indefinitely unless there is a reduction in gas pressure, or an increase in rock strength or until the volume of ejected material in the cavity produces confining pressures great enough to prevent formation of tensile stresses.

6.2 Proposed Outburst Model and Assumptions

The model proposed here will aid in the prediction of when outbursts will occur and the extent to which spalling within the cavity will proceed. The outburst can be assumed to be an instantaneous event; the model assumes that an outburst can be modelled as a series of instantaneous events. Several assumptions have been made with regard to the mechanism of outbursts stated earlier. These are as follows:

1. rock which has failed by exceeding the tensile strength is expelled, forming a cavity and changing the opening shape;
2. rock which has failed by shear is assumed to remain in place, but its strength is reduced, the gas pressure is reduced instantaneously to zero but the elastic properties are assumed to remain the same;
3. at the boundary between sheared and intact rock, there exists an infinite pressure gradient from zero to the insitu gas pressure;
4. tensile failure destroys the sandstone structure. Gas within this zone ejects the pulverized (tensile fractured) rock taking with it any sheared rock existing at the face of the cavity wall;

5. sandstone is homogeneous and isotropic, impervious to gas flow when intact and gas pressures are hydrostatic throughout;
6. a Hoek and Brown failure criterion will be used to assess the stability of intact rock around the cavity; the Coulomb-Navier failure criterion is used in sheared rock;
7. stresses will be evaluated using a two-dimensional boundary element program under plane strain conditions (the program will be discussed later);
8. the boundary element program does not allow the evaluation of effective stresses, only total stresses. Therefore, the gas pressure cannot be entered as a body force acting on the sandstone. The simplification used will be that the hydrostatic gas pressure can be superimposed onto the final stress field and the effective principal stresses thereby determined.

The boundary element program (BEP) will be used to evaluate the stress field around the cavity. Gas pressures are then superimposed onto the field stresses for the intact sandstone only. (The BEP uses two isotropic half-planes that are bonded together. This allows the use of two materials; sandstone and siltstone or coal.) Now that the 'equivalent' effective stresses are known, the failure criterion can be applied and the stability of the cavity be assessed. The zone in which tensile failure occurs will be removed and a new cavity boundary is formed and is input for the next boundary element iteration. There will also be a zone in which shear failure occurs and this will be degassed and given a lower strength. In the next run, the sheared zone will not have the gas pressure superimposed and the stability of this zone will be evaluated under a second failure criterion. The process iterates until the cavity has reached stability (no tensile failure) or the program stopped when it becomes clear that spalling can continue indefinitely under the given conditions (ie. usually that the gas pressure selected was too large).

Two different scenarios will be modelled. The first is to get a cavity to stabilize from spalling solely by the changing of the cavity shape. The second is to observe the effect of the introduction of an upper limit to the sandstone bed. The latter condition appears to be important for the No. 26 Colliery outbursts as it seemed to have produced an upper limit to

the spalling of the cavity, as seen in the cross-sections of Figures A.2a to A.2n, pages 97 to 103.

In some places there is a bed of siltstone or mudstone between the coal seam and the sandstone that is broken through first, and only then can spalling occur. In these situations, the intervening bed was thicker than 1.68m, the height of the heading above the coal seam, and less than 2.7m (the latter is the thickest bed that has broken through, allowing an outburst to occur). The destruction of this siltstone barrier will be analyzed as a 'cutter roof' failure of a beam loaded from the top by the gas pressure from the sandstone bed. It has been stated that the bond between the siltstone and sandstone is weak and that separation along the bedding plane is common. It will be assumed that this separation is due to the pressure exerted by the gas from the sandstone. If the siltstone 'beam' fails then spalling of the sandstone is allowed to occur as noted above, if the conditions are favourable to this.

7. Spalling Mechanism

The spalling mechanism was outlined briefly in the previous section; this will be dealt with in detail here. The iterative method of modelling the spalling follows these steps:

1. Define the cross-sectional shape of the heading.
2. Determine the stress distribution around this opening.
3. Superimpose the gas pressure onto the principal stresses for the intact sandstone only.
4. Evaluate the stability based on the given failure criterion.
5. Remove any material that has failed in tension; define a new opening cross-section.

Repeat from step 2.

This process is repeated until no tensile failure occurs around the cavity or until it becomes obvious that tensile failure will continue indefinitely for the given parameters. The logic that is followed through this iterative process is shown by the flow diagram in Figure 7.1.

7.1 Boundary Element Method and Program

The boundary element method is a numerical technique used to analyse stresses in solid mechanics.[11] This technique is much easier to use than the finite difference and finite element methods because only the region of interest needs to be discretized as opposed to the entire rock mass. For example, in an underground excavation, only the opening needs to be divided into elements. Boundary conditions are also more accurately represented because the boundary element method uses an infinite plane with which to define boundary conditions.

The two-dimensional program gives results based on a linear elastic rock mass under plane strain conditions. The end effects of the heading are ignored by assuming that the two-dimensional section is infinitely long. This will provide a useful starting point in the understanding of the various parameters in modelling outbursts.

The program used is one that employs two different materials, each a semi-infinite, isotropic half-plane bonded one to the other. This allows the inclusion of either coal or siltstone as an upper or lower limit to the sandstone bed in the model. The lower material chosen to be entered into the model can only be one of these, and since siltstone is usually

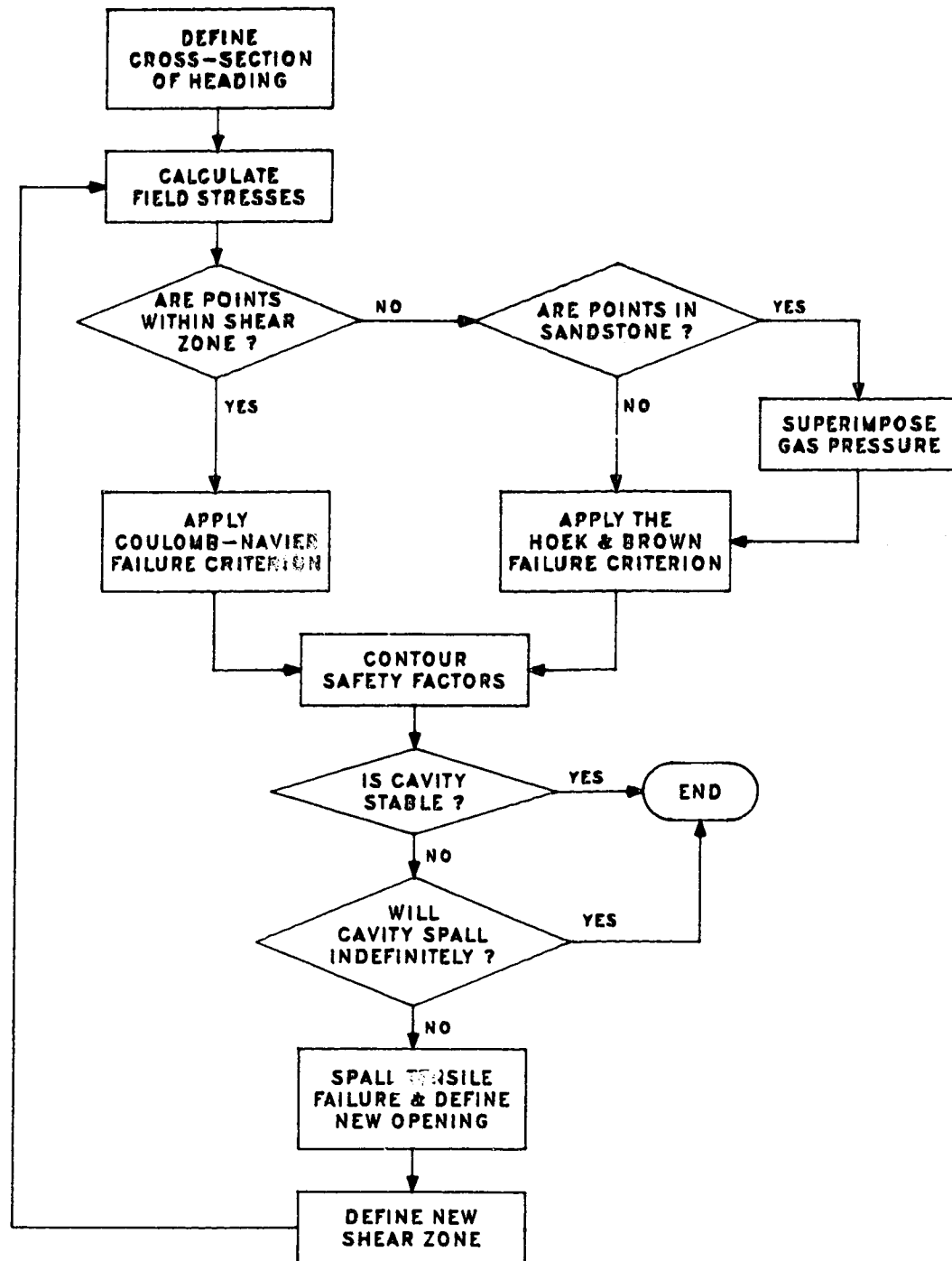


Figure 7.1 Flow Chart of Model Iterative Process

found between the sandstone and coal, the bottom material will be given siltstone properties at all times (to be consistent).

The program automatically calculates the stresses, displacements and strains on each element around the boundary. Points within the rock mass (field points) around the opening can also be selected and the above results can also be calculated for these points. A failure criterion can then be applied to the stresses to determine the stability at either a boundary or a field point. With the ability to calculate stresses at field points, the results from the boundary element program can be taken and the gas pressure can be superimposed on the field point stresses to find the 'equivalent' effective stresses. These are referred to as 'equivalent' because they are only an approximation of the effective stress tensors. Equation [6.2], page 31, can then be re-written as equation [7.1] below:

$$\begin{aligned}\frac{\partial \sigma'_x}{\partial x} + \frac{\partial \tau'_{xy}}{\partial y} + \frac{\partial \tau'_{xz}}{\partial z} &= 0 \\ \frac{\partial \sigma'_y}{\partial y} + \frac{\partial \tau'_{xy}}{\partial x} + \frac{\partial \tau'_{yz}}{\partial z} &= 0 \\ \frac{\partial \sigma'_z}{\partial z} + \frac{\partial \tau'_{xz}}{\partial x} + \frac{\partial \tau'_{yz}}{\partial y} &= -\rho g\end{aligned}\tag{7.1}$$

where $\frac{\partial p}{\partial x}$, the body forces due to the pressure gradient from equation [6.2], are assumed to be zero. Applying a failure criterion to these rock stresses, safety factors can be contoured around the opening; the safety factor being defined as a ratio of strength over stress.

The final state of stress or displacement can be defined for the boundary elements thus allowing the input of constraints on boundary conditions. The most common constraint is to allow the shear and normal stresses of the boundary elements to be relaxed to zero. Support through arching and bolting can be simulated by specifying other constraints to the boundary values.

One limitation on the program is that field points can only be evaluated at a distance of at least one element length away from the boundary. This is due to the program's inability to accurately determine stresses and strains in this region. Sensitivity to the boundary element lengths will be discussed later.

The program, **BESOL/P5005 version 1.1 (Boundary Element SOLutions)**, was written by and purchased from Crouch Research Inc. It was written to be run on an IBM personal computer, or a compatible unit, using the DOS (version 3.3) operating system. An IBM System 2 Model 60 personal computer (with MS Fortran version 4.1) was used to carry out all the computer runs. A description of the input and output files for the boundary element program is given in Appendix F.

7.1.1 Effect of Boundary Element Length and Field Point Density

The BESOL/P5005 program has a limitation of 125 elements on the number of boundary elements that can be used to define the excavation. A compromise must be made between the number of boundary and field points chosen to define a stress field around an opening and the computing time. The more boundary elements used, the closer to the boundary a field point can be to calculate stresses. The closer the field point spacing, the more accurate will be the contouring near the boundary. However, this increase in accuracy can significantly increase the computation time of a given situation. To decrease this time, a constant element length (0.25m) and field point spacing (0.3m) will be used that will give sufficiently accurate results from the first to the last iteration. (Note, as the number of iterations progress, the number of boundary elements required can increase dramatically.)

The effect of smaller boundary elements is shown in Figure 7.2. The ability to calculate field stresses closer to the boundary affects the initial iteration all around the opening and in subsequent iterations, only in the area where tensile failures occur. The latter is affected because in the areas of tensile failure, the shear zone tends to be small and the gas pressure gradient occurs close to the boundary. A short boundary element length allows the evaluation of these stresses closer to the boundary. If the pressure gradient is near the boundary, field points near this gradient will not be evaluated, and this is a critical area; if tensile failures were to occur, this would be the place. Longer elements may cause the field points in these areas to be too close to the boundary to allow evaluation. The result is possibly one or two more iterations (if any) with a similar final shape cavity. As seen in Figures 7.2,

the final cavity of the smaller elements is slightly larger but the aspect ratios of the ellipse are very similar. The cavity area produced by using larger element is approximately 13% smaller than the area derived from use of shorter elements.

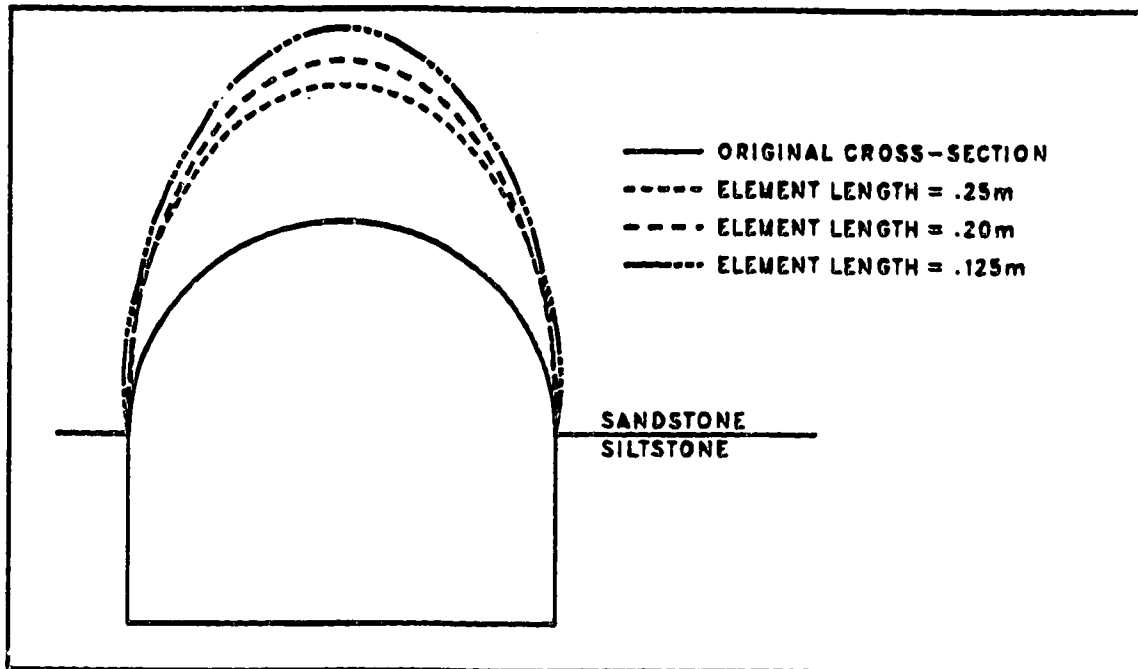


Figure 7.2 Size Effect of Boundary Element Length

Denser field points around the opening will have a similar affect on the spalling as the element lengths, except that better results are obtained for contouring around the entire cavity. The critical area is just outside the shear zone; within the shear zone, no gas pressures are applied and tensile failure cannot occur, unless field stresses are highly tensile. In the area just outside the shear zone, tensile failures can occur. Ideally, one would like to have a dense grid of field points in this area and a more widely spaced grid farther from the shear zone. This would give more accurate results where desired and reduce computation time in the less critical areas. However, the overall results would be affected very little (similar to having shorter elements) and the data manipulation required for an irregular grid would not be worth the rewards. The boundary element program accepts only a limited number of field points for input.

7.1.2 Secondary Computer Program - SAFCON - Safety Factor Contouring

A Fortran program was written that could take the results generated from the boundary element program and carry out the following functions:

- superimpose the gas pressure onto the principal stresses in the sandstone,
- apply the desired failure criterion,
- contour safety factors, and
- set up a new data file that can be entered as input to the boundary element program in the next iteration.

A listing of this program is given in Appendix E with sample input and output files listed and described in Appendix F.

Two other program packages are used within this second program. The first is a plotting library that contains Fortran subroutines (PLOT88) which can be called from any Fortran program to carry out a variety of plotting functions from lines, to contouring, to labelling. The other package (MS MOUSE) involves the use of a mouse to control a cursor on the monitor while the contoured results from PLOT88 are still on the monitor. This allows for user interaction in the definition of the new boundary and shear zone.

7.2 Gas Pressure

It will be assumed that the gas is distributed evenly within the sandstone bed and produces a homogeneous and isotropic pore pressure on the rock. The effect of sorbed gas on the carbonaceous material in the sandstone will be ignored since this, at the most, consists of only 3.5% of the rock. Gas also exists at the boundary between sandstone and siltstone or coal, resulting in an external load on these beds.

Intact sandstone is considered to be impermeable to the flow of gas. It is also assumed that in sheared rock the gas drains instantaneously, thus permitting the assumption that there is zero gas pressure in this sheared zone. This means that there is an infinite pressure gradient at the boundary between the the sheared and intact rock. Based on these assumptions, the dynamics of gas flow can be ignored and spalling can be treated as a static problem.

7.3 Failure Criterion

The failure criterion used for the intact rock is the Hoek and Brown criterion. This best represented the strength of the sandstone under triaxial conditions (refer to section 5.2, page 26, and the summary of Appendix C, page 130). Different parameters were used for the siltstone and sandstone as noted in Table 5.2b, page 27. No testing of rock was carried out successfully in which tensile stresses have been applied (except the Brazilian test). The only attempt at this failed (as noted in Appendix C and reference [20]) because to produce a radial tensile stress, a fluid must be injected into the rock specimen to produce an outward radial stress. The sandstone was too impermeable to allow this gas injection. Hence, the rock strength in the tensile region can only be assumed and will be based on the Hoek and Brown criterion which, when extrapolated to the tensile region, allows determination of the tensile strengths as noted in Table 5.2b and Figure C.8, page 132.

In the case of sheared rock, a new failure criterion was chosen. Because the rock is sheared, it can be assumed that it has lost cohesion and the only strength is provided by the internal friction of the rock. The best criterion to use is the Coulomb-Navier criterion with zero cohesion and an assumed friction angle. The sheared rock does not contain any gas pressure and thus, provided that the minor principal stress does not become less than the tensile strength, tensile failure will never occur in the sheared rock. An outburst can, therefore not be initiated from this zone.

7.4 Safety Factor Contouring

The field points (points within the rock mass around the opening) are set up in a regular grid, and the safety factors calculated at each of these points can then be contoured. The boundary elements cannot be included within the contouring because they do not fall onto a regular grid with the field points and will not be accepted by the contouring subroutine. This leaves a gap in the contoured plot where the contours must be estimated.

As the spalling proceeds (in successive iterations), there is a shear zone around the opening from the previous iteration; a tensile zone can occur behind this sheared zone. This

tensile zone is not continuous to the boundary of the cavity because of the continuous shear zone and this produces an isolated pocket. This is illustrated in Figure 7.3 at the top of the cross-section. To represent the ejection of this tensile zone, an estimate must be made as to how this rock and gas will break out through the shear zone. The contour that is estimated around the tensile failure will now become the new cross-section of the cavity. The contouring of the new shear zone is straight forward as it is continuous (as noted above about the previous iteration) and envelops the old shear zone and new tensile zone. This is illustrated in Figure 7.4.

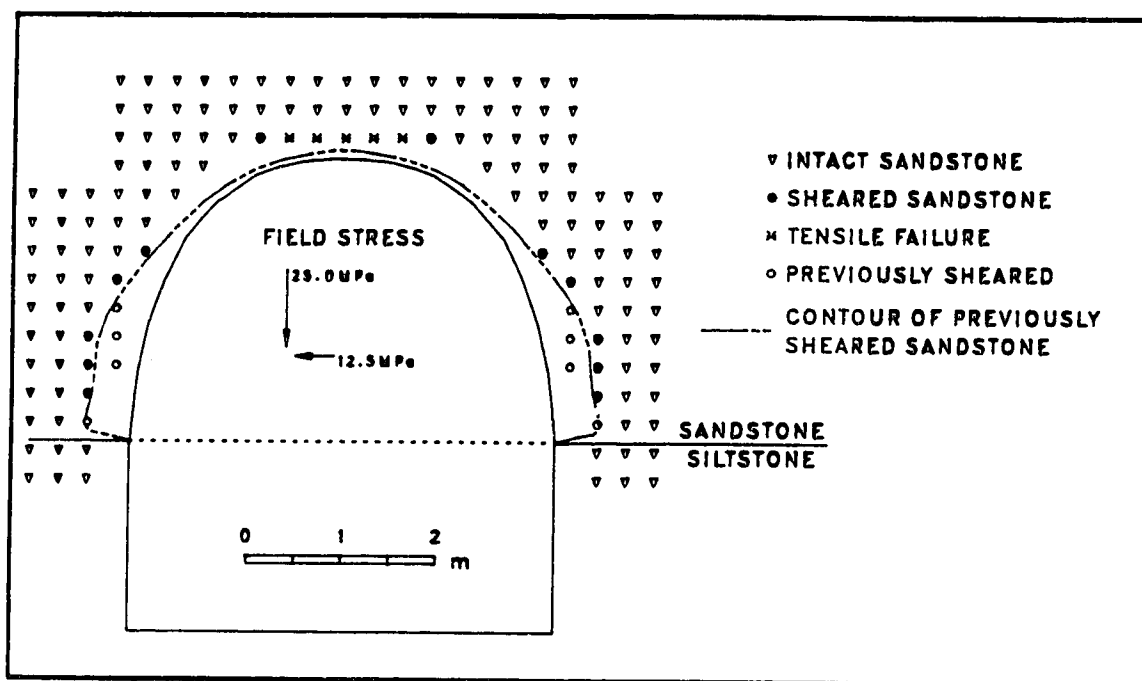


Figure 7.3 Field Point Results Produced by Model

The elastic properties of the sheared rock are assumed unchanged from that of the intact rock, only the strength is reduced. Therefore, when the stress distribution around the opening is recalculated, it is significantly influenced by the way the tensile zone is contoured; that is, by the definition of the new cavity shape. The production of small irregularities in the shape of the opening can very quickly magnify into severely irregular shapes, from which stability will never be obtained. It is highly unlikely that the natural spalling of rock will

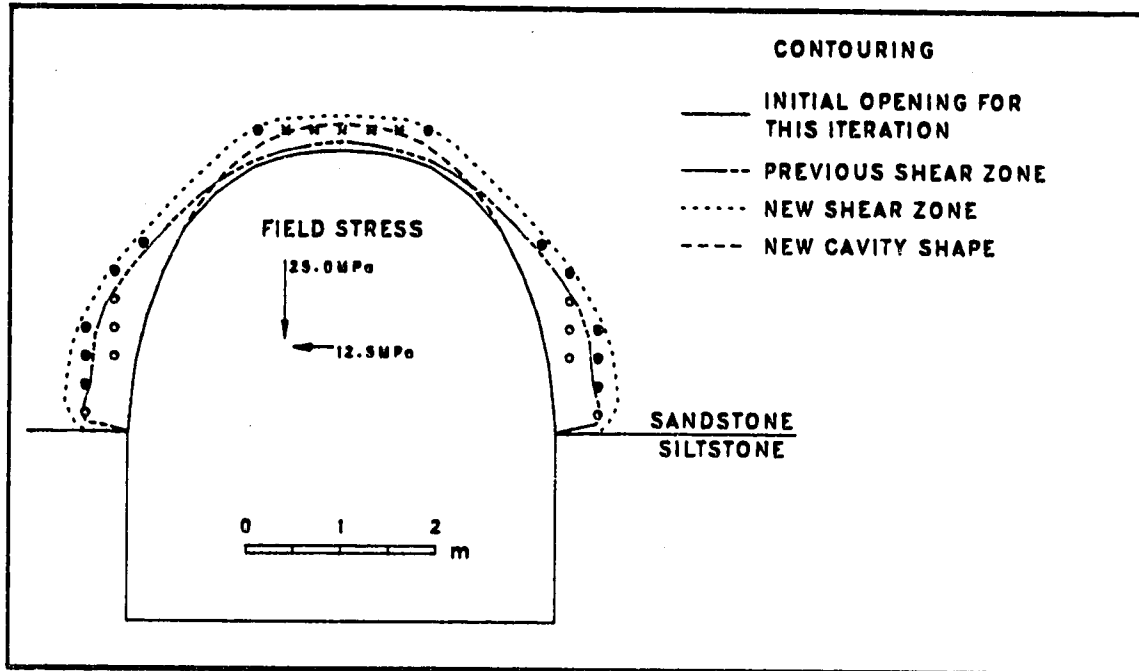


Figure 7.4 Contouring of Shear and Tensile Failures

create such conditions except when caused by the irregularities in the field properties. With the assumption that the rock properties and gas pressures are isotropic and homogeneous, the new boundary should always be smooth and regular.

7.5 Computer Modelling

7.5.1 Objectives of the Model

The objectives of the runs that were carried out were to determine the conditions that were present to cause the outbursts at No. 26 Colliery. Although the tests that were conducted give some indication of these conditions, too much is still left to speculation. The best possible estimates have been made for the rock strength and elastic properties and these values will be constant for all runs; the gas pressure will be varied and the results observed. A range of gas pressures will be found for which spalling can occur and then stop due to the changing of the cavity shape. This will be done for a series of insitu stress ratios and the final shapes of the openings can be compared. The effect of an upper limit to the sandstone bed will also

be investigated. Finally, the outburst cavities will be compared with those observed in No. 26 Colliery with regard to the general shapes and the volume of ejected material (or in this case, the cross-sectional area of the cavity). Possible remedial measures can also be discussed based on the findings of the model runs.

7.5.2 Sample Run of Model

This section contains a sample run to illustrate the operation of the programs. The first step is to define the cross-sectional shape of the heading. The boundary of this opening is then discretized into boundary elements of approximately equal lengths. Areas within the rock mass around the opening are then selected for which a grid (or several grids) of field points are located; stresses can be calculated and safety factors evaluated at the grid points, then contoured. A large area is not required since the only region of interest is near the boundary. The boundary elements and field points are then arranged in a data file together with insitu stress conditions, rock properties and other parameters required as input by the boundary element program. The output from this program contains a listing of the input data, details of the boundary elements (locations of their midpoints for which stresses are calculated, element lengths and boundary conditions specified) and the displacements, strains and stresses calculated for the midpoints of the boundary elements and field points. Sample files are given and explained in Appendix F.

With the boundary element run being completed, the program SAFCON is run to evaluate the safety factors and contour these results. This program is fully documented and listed in Appendix E. A brief description of its operation will be given here as follows:

1. BESOL/P5005 program input data is read in and the relevant information stored.
2. BESOL/P5005 program output file is scanned for the relevant output data; stresses at the boundary elements and field points.
3. Another file is set up, after each iteration, containing the coordinates of the closed polygon representing the sheared zone contour. (For the first iteration, this file will not exist. An assumption must be made regarding this sheared zone;

this will be discussed in the next section. For subsequent iterations, the data from this file is read in and stored.)

4. The location of each point (field and boundary) is evaluated to determine if a gas pressure will be superimposed onto the field stresses (if the rock is intact sandstone) and the appropriate failure criterion applied.
5. The field points are then all entered into one two-dimensional array which will be entered into the contouring subroutine.
6. With the contoured plot on the monitor, a cursor, controlled by a mouse, is used to enter the coordinates of the tensile and shear failure contours.
7. The plots are set up symmetrical about the y-axis, located vertically down the center of the heading. When the coordinates are entered for the contours, only the right side is entered and the other side will be defined as a mirror image.
8. The shear zone contour (coordinates) is then written into a file. The tensile zone contour points are then discretized into equally spaced boundary elements. The boundary element program input parameters and the new boundary elements are then written into a new input file for the boundary element program.
9. This process is repeated until there are no more tensile failures around the opening or it becomes evident that stability will never be reached under the given conditions.

Figure 7.5a shows the safety factor contours for the first iteration with the original cross-section of the heading. Note the line of symmetry: only one side of the cavity needs to be contoured and the other side is made a mirror image. The tensile zone contour must be smooth around the failed point to prevent magnification of irregularities. Field points within the siltstone, just below the interface of the two materials, are monitored at each iteration to detect failures. Unless areas within the siltstone actually show failure due to stress concentrations, shear and tensile failure contours will not be drawn through it. The shear zone contour does not need to be entered with great precision because it does not affect the stress distribution. These failure contours are shown in Figure 7.5b where the new boundary is the

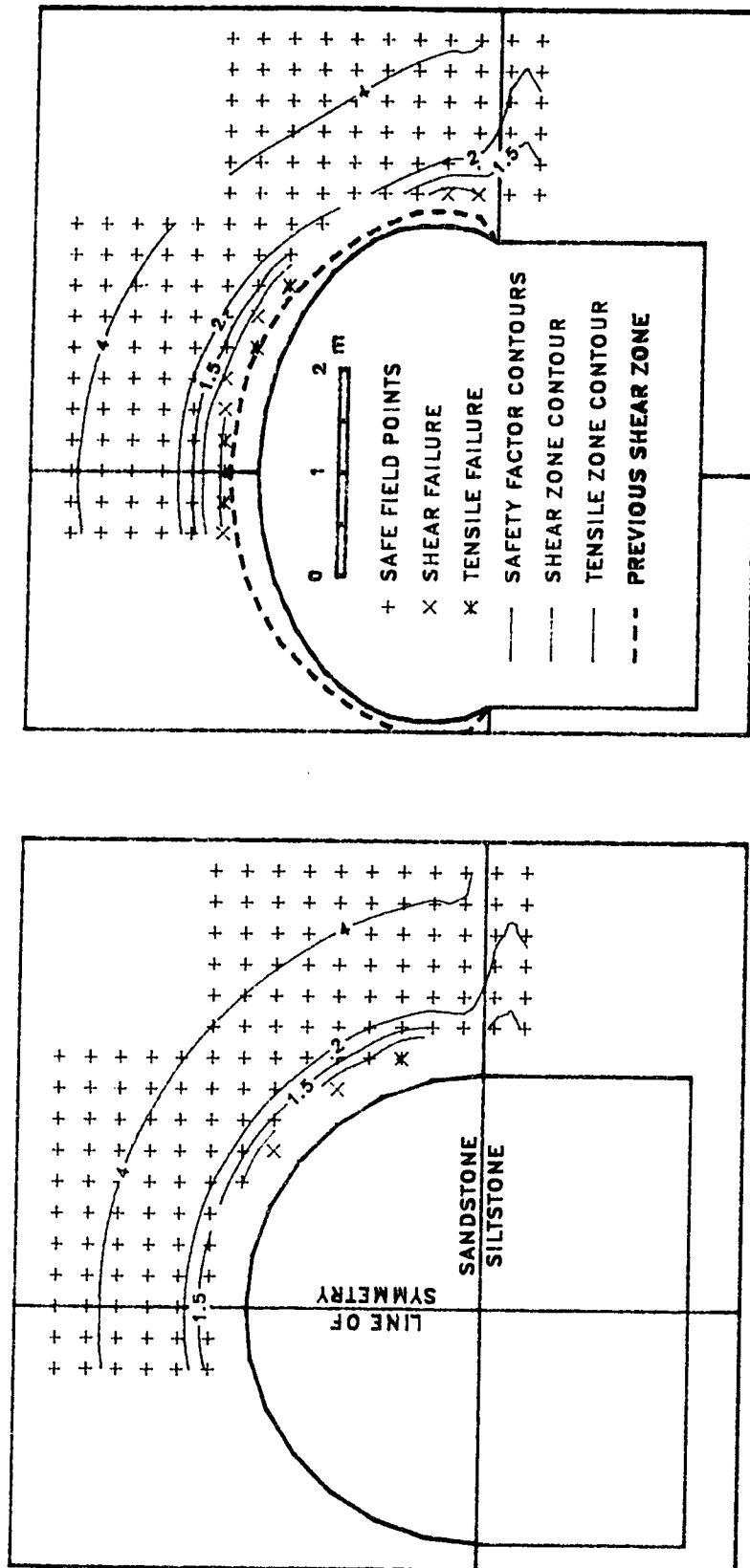


Figure 7.5b Sample Run: Iteration #2

Figure 7.5a Sample Run: Iteration #1

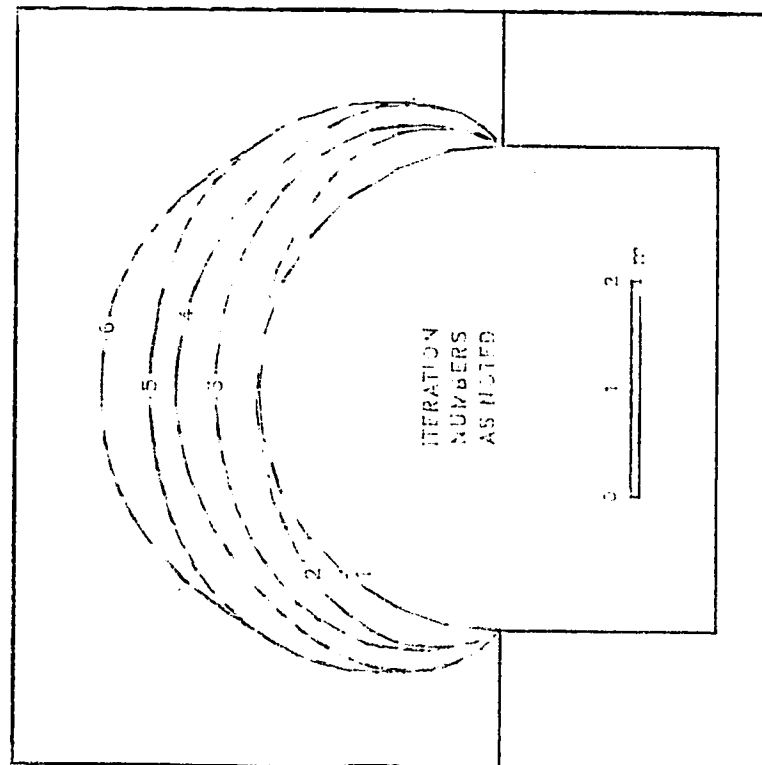


Figure 7.5d Sample Run: Final Steble Cavity

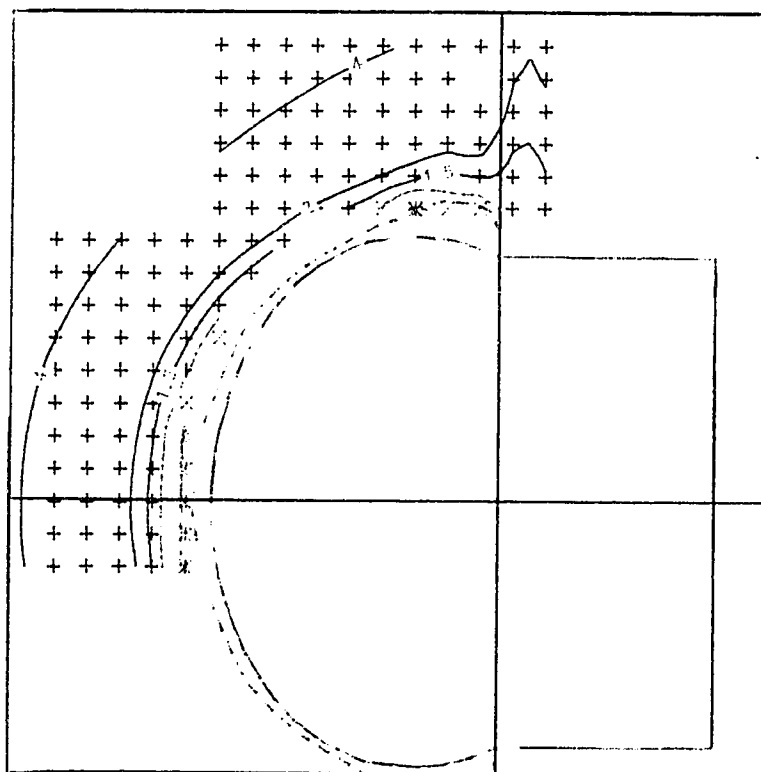


Figure 7.5c Sample Run: Iteration #3

tensile zone contour from the first iteration. The contour of the previously sheared rock in Figure 7.5b is the contour produced from the first iteration. This is repeated for the next contoured plot with Figure 7.5c showing the new opening after the second iteration. The complete set of 'intermediate' boundaries is shown in Figure 7.5d from the initial heading excavation to the final stable cavity.

7.5.3 Gas Pressures Required to Cause Spalling

A series of runs were conducted over a range of insitu stress ratios between 0.5 to 1.5 (horizontal to vertical) in an attempt to bracket a range of gas pressures that would cause spalling. The first set of runs were done to find the minimum gas pressure required to create any tensile failure. An assumption must now be made regarding the presence of a shear zone at the boundary. The program cannot calculate stresses for field points less than one boundary element length from the boundary. Without this, the safety factors cannot be evaluated near the boundary. It is known from practice that in the driving of a heading, some fracturing will occur around the opening, especially in a drill and blast operation as in No. 26 Colliery. It will be assumed that the fractured zone extends to a distance of one element length into the rock mass around the opening. The results from this series of tests must be accepted with this assumption in mind and results could vary considerably depending on what assumptions are made. If it is assumed that the rock is intact at the boundary, the gas pressure must be equal to the tensile strength of the rock to initiate tensile fracture. (In subsequent iterations, the shear zones are defined and this problem is not encountered.)

The next series of runs were conducted to determine the maximum gas pressure present that allows spalling to develop but eventually attain a stable shape. This set of runs requires several iterations at each stress ratio chosen, varying the gas pressure and, therefore, this maximum gas pressure is not dependent on the assumption of the initial definition of the shear zone as noted above. For each stress ratio, a complete set of iterations would have to be done for any given gas pressure. Depending on the result, a new pressure would be selected (accuracy to one decimal place) and run. This would be continued until a gas pressure was

found that would create a stable final cavity but applying a pressure slightly greater, the cavity would spall indefinitely. The cavity will spall indefinitely when a tensile failure zone completely surrounds the cavity (sandstone half only). This indicates that stress redistribution around the cavity will not prevent tensile stresses from forming. When the model has reached such a condition, the user terminates the computer runs for that set of input parameters.

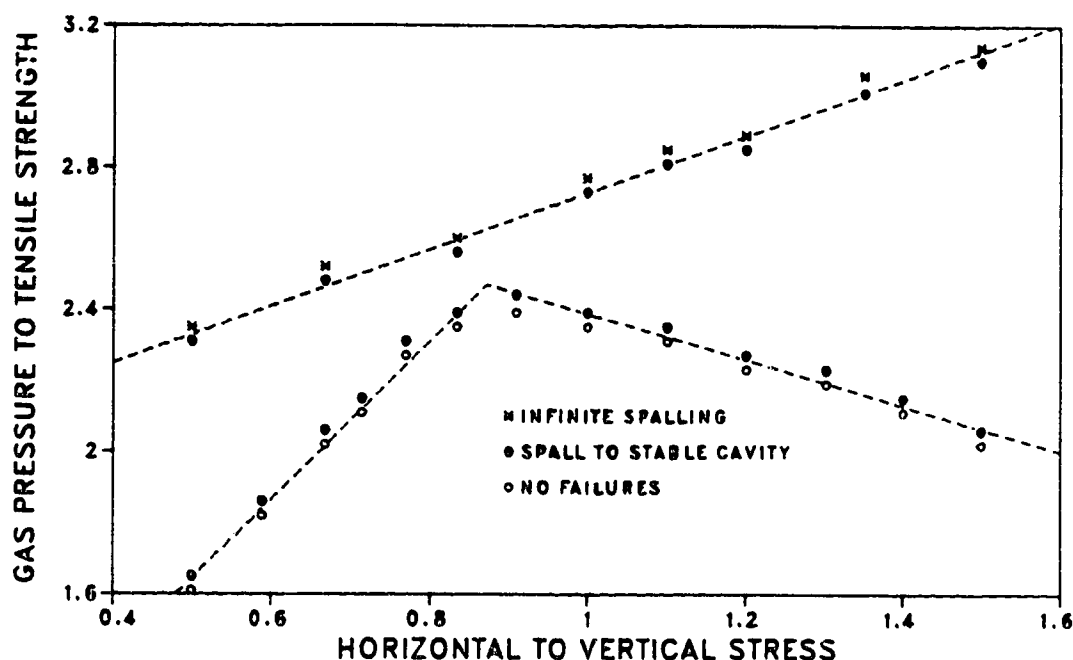


Figure 7.6 Gas Pressures Required to Cause Spalling

Figure 7.6 shows the range of gas pressures that would cause spalling and produce a stable final cavity over a range of insitu stress ratios between 0.5 to 1.5 (horizontal to vertical). The gas pressure (P_g) to tensile strength ratio was plotted versus the stress ratio to get a dimensionless graph that could be used to evaluate the effect of various stress fields, rock strengths and gas pressures. In running the various stress conditions, the vertical stress was kept constant at 25MPa and the horizontal stress was varied to produce the desired stress ratios. The relationship of these variables seems linear for the upper bound and bi-linear for the lower bound of gas pressures. The lower limit is dependent on the shape of the original opening as related to the stress field whereas the upper bound may not be. Relative dimensions of exposed sandstone, however, may have an influence on the final cavity

dimensions. The results presented in Figure 7.6 apply to the one initial cross-section at various field stresses; a plot such as this could be derived for a variety of initial cross-sections.

The final stable shapes of the cavities for the latter set of runs are shown in Figures 7.7. It can be seen that each cavity (looking at the area above the sandstone / siltstone interface only) has an elliptical shape with the long axis in the direction of the greater insitu stress. It is known that the most stable shape in a given stress field is an ellipse oriented in just such a manner. Also, the greater the deviation of the stress field from hydrostatic, the greater the aspect ratio of the most stable ellipse. Ideally, the aspect ratio of the most stable opening would be equal to the insitu stress ratio with the long axis in the direction of the greater stress, for a completely isotropic, homogeneous medium. Deviation from this arises from the effects of having two different materials as shown in the model cross-sections. In these runs, there are the effects of the having two different materials and having a lower material that will not spall remaining at a constant rectangular shape. The definition of the tensile zone is achieved by manual contouring. There is no defined point on the boundary where the ejecting rock breaks through the shear zone at the boundary. Repeating the same set of iterations several times would probably produce several slightly different final cavity shapes.

In a hydrostatic stress field, the most stable opening is circular and would require the greatest gas pressure to initiate spalling and once spalling has started, it should continue indefinitely. The heading cross-section used in these runs has a semi-circular back that cuts through the sandstone but the stress field, for which this opening is most stable, has a stress ratio of approximately 0.87 (for the lower bound gas pressure). This stress ratio also has the narrowest range of gas pressures for which spalling can occur and still produce a stable final cavity. The largest cavity for the upper bound gas pressure, however, was produced from the hydrostatic stress field. Possibly, as the cavity becomes larger due to spalling, the effects of the rectangular shape of the opening in the lower material becomes less significant. The extreme stress state of 1 to 2 also produced a larger cavity than the rest.

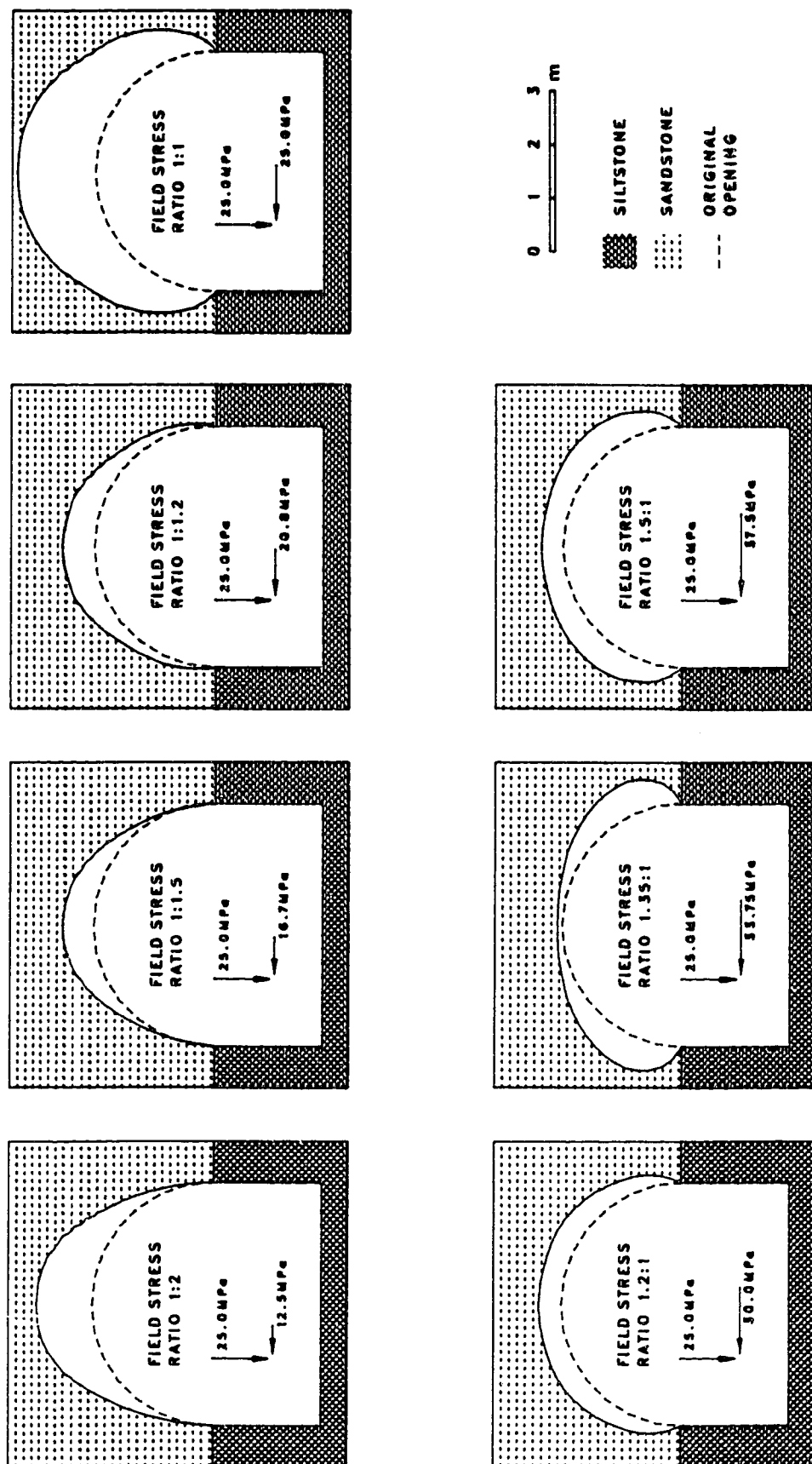
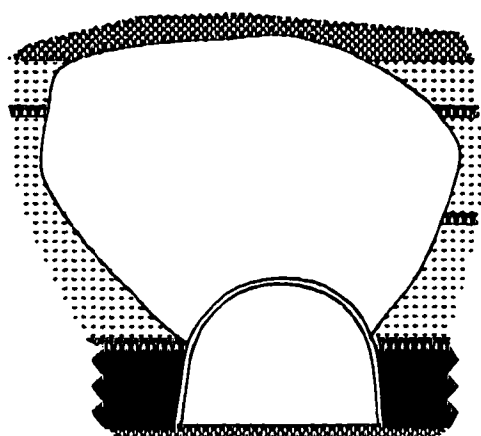


Figure 7.7 Final Cavity Shapes for Various Stress Conditions

7.5.4 Comparison of Model Results with Recorded Events

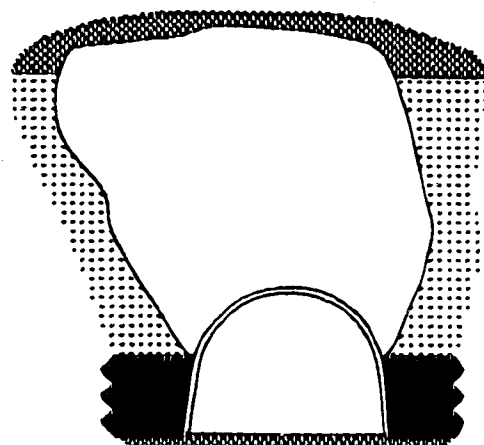
As seen in the cross-sections of Figure A.2, page 97, the upper limit of the sandstone bed appears to be a limit to the vertical spalling of the cavity. For this reason, there must be such a limit to the sandstone bed accounted for in the model. The boundary element program allows for only two different materials (one interface) and this is used to define the lower limit to the sandstone. An upper limit is artificially produced by the secondary program, SAFCON, in that any point above a specified height has no gas pressure applied to it and siltstone strength properties will be applied. The stress field calculated by the boundary element program is based on one continuous material with constant elastic properties through this 'artificial' interface. This will give only an estimate of the state of stress within this upper region but this should give correct results in terms of the presence of tensile failures since no gas pressures are being applied and shear failures do not affect the cavity shape.

The first cross-sections that will be modelled are those of Figures A.2l to A.2n, page 102-103. Siltstone properties will once again be used for the lower material since in two of the three sections, siltstone is present directly below the sandstone. The insitu stress field determined earlier has a horizontal stress (26.3MPa) to vertical stress (24MPa) ratio of approximately 1.1. Gas pressures within the range given in Figure 7.6 for this stress ratio would not produce the required size of cavity to model the appendix figures noted above. Greater gas pressures must be applied with hope that the influence of the 'upper limit' to the sandstone bed would not only stop spalling vertically, but also horizontally. From the linear upper bound in Figure 7.6, the upper limit to spalling to a stable shape is $-P_g/\sigma_t$ is equal to 2.81; if σ_t is 2.42MPa, $-P_g$ must be greater than 6.8MPa. Then the upper limit to the sandstone bed is allowed to terminate the spalling. (A gas pressure of 7.1MPa was arbitrarily chosen.) The resulting cavity is shown in Figure 7.8. The model predicted a cavity that has a very similar shape to the actual outburst and with a cross-sectional area that is close to the actual ones ranging from 8% to 16% less than the actual cross-sections. In considering the variability of the sandstone, it is not surprising that there is quite a variation (with respect to irregularities) in the sections, but all have the same general shape as the model result.



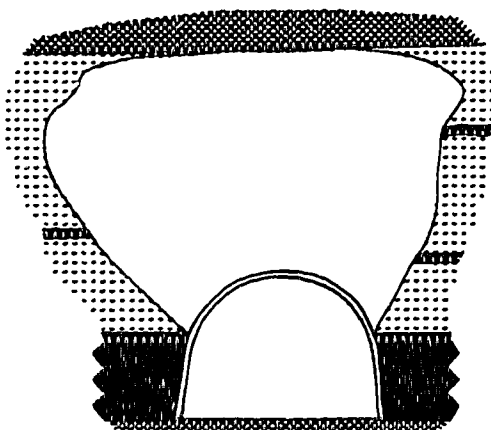
SECTION 12

66.5 feet from cross-cut
Cavity Area = 542 sq.ft.
(after [2,13])



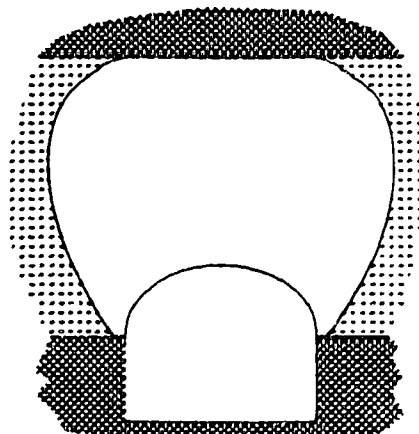
SECTION 13

74 feet from cross-cut
Cavity Area = 518 sq.ft.
(after [2,13])



SECTION 14

78 feet from cross-cut
Cavity Area = 490 sq.ft.
(after [2,13])



Final Cavity Shape
Produced by Model

Cavity Area = 452 sq.ft.

 SANDSTONE
 SILTSTONE
 COAL

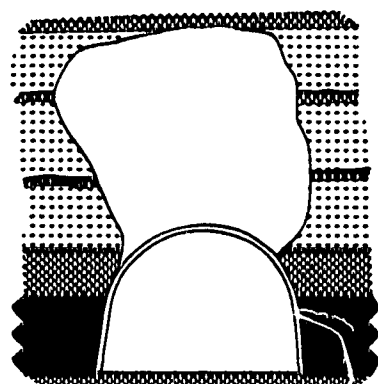
0 5 10 15 20 ft

Figure 7.8 Comparison of Outburst Cavities with Model Results

The next step was to attempt to model two other cross-sections from this outburst; sections 8 and 9 (Figures A.2h and A.2i, page 100-101). The range of gas pressures, required to cause spalling, noted in Figure 7.6 may not apply for these sections since the intervening siltstone bed is considerably thicker than in the previous cases resulting in a narrower opening of the sandstone bed to the heading. Assuming an isotropic gas pressure with the sandstone, the gas pressure here must be 7.1MPa, as before. The distance from one set of cross-sections to the other is 25 feet at the extremes. The model result for these sections is found in Figure 7.9 along with the two sections being modelled. The sections are only five feet apart and yet there is a considerable difference in the areas and shapes. The model cavity gave results that are somewhere between the two with respect to shape and area. The area of the model result is 32% greater than section 8 and 23% less than section 9 (excluding the area of the fall).

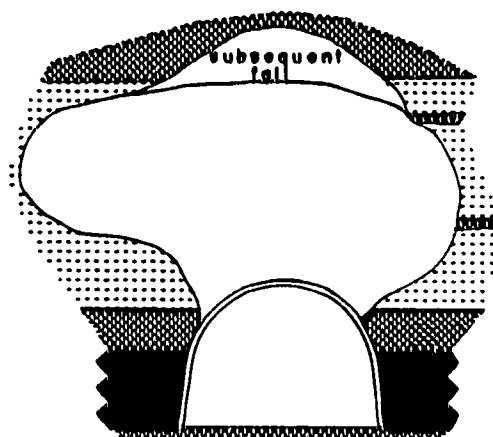
The accuracy to which the field sections were produced is highly questionable. Variability in the material and the presence of the bands of siltstone within the sandstone bed give considerable differences in the cavity sections. The siltstone bands are very irregular as seen in the sections; in some cases, they are consistent both sides of the cavity, sometimes they are offset indicating that they are discontinuous, or, completely non-existent. These bands could play a significant role in limiting the lateral spalling of the sandstone as noted in section 8, Figure 7.9. These bands could also limit spalling vertically if the span of exposed siltstone was small enough that the thin band could support the gas pressures loading it from above.

An attempt was made to model the cavity in Figure A.2c, page 98, but this failed. This cavity was much smaller than the ones previously modelled and the model could not produce a stable cavity, as noted in Figure A.2c. The model would only terminate spalling if an upper limit to the sandstone bed was considered. In this case (model), the size of the cavity is controlled by the thickness of the sandstone bed, but, in the actual case, it was not. Other factors must be responsible for this discrepancy.






SECTION 8

53 feet from cross-cut
Cavity Area = 253 sq.ft.
(after [2,13])

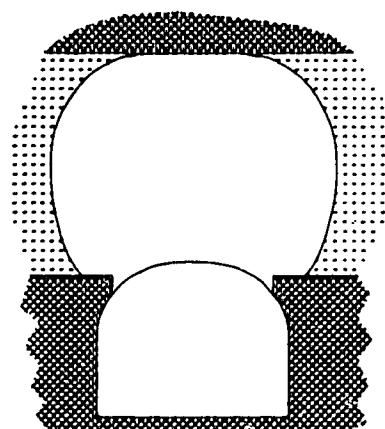


SECTION 9

58 feet from cross-cut
Cavity Area = 485 sq.ft.
(after [2,13])

 SANDSTONE
 SILTSTONE
 COAL

0 5 10 15 20 ft



Final Cavity Shape
Produced by Model

Cavity Area = 335 sq.ft.

Figure 7.9 Comparison of Outburst Cavities with Model Results

7.6 Observations of Outburst Cavities

When looking at the various cross-sections of Figure A.2, a question arises with respect to the changing volumes of the cavities. In the sections near the face, the cavity size was limited by the upper limit of the sandstone bed. However, in the first few sections, the cavities were comparatively small and did not spall to the upper limit of the sandstone bed. This is shown in the longitudinal section of the cavity in Figure 7.10. Only one of these cavities could even be considered to have the spalling limited by the thin siltstone bands - section 6, Figure A.2f. Since the length of the entire cavity was only eighty feet long, the material properties are not expected to change to the degree that would account for the differences in cavity size. For every section beyond approximately 50 feet from the cross-cut, the cavity spalled continuously to the upper limit. In every section less than 50 feet, the cavity became stable, apparently independent of an upper limit. There are changing factors, not yet considered, that could explain the effects observed in these sections. The first is one that cannot be assessed with the model; the effect of the heading face, ie. the three-dimensional problem. The second factor can be investigated with this model; the effect of a narrowing breakthrough width of the intervening siltstone bed to the sandstone.

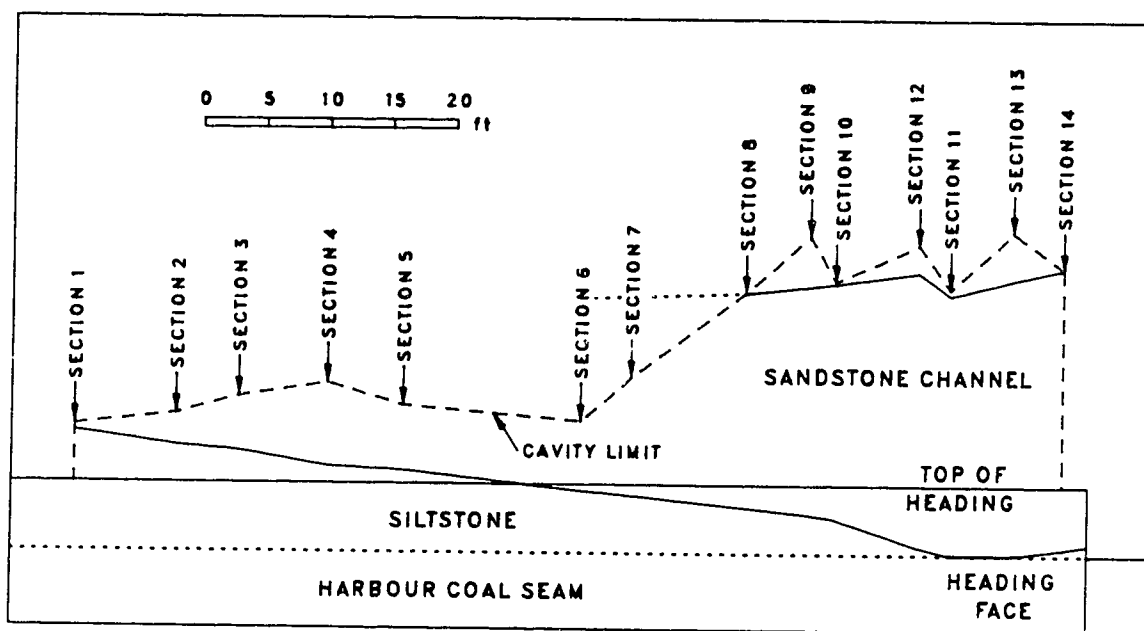


Figure 7.10 Longitudinal Section of the Cavity from Outburst #36 and #37

7.6.1 Effect of the Heading Face

The effect of the heading cannot be assessed with this model, however, a few comments can be made regarding the possible influence on the spalling action. The presence of a heading face in virgin ground produces a stress concentration around that face, greater than that given by the two-dimensional analysis. Stress concentrations are extreme at the face and become less farther from the face. The large cavities near the face of the heading *could*, in part, be due to these stresses. The farther one gets from the face, the less influence these stress concentrations will have on the 'two-dimensional' stress field. The change from a large cavity to a significantly smaller one could be partially due to the effect of the heading face.

The two-dimensional case is assumed by the model, and the absence of the 'face effect' is a simplification made by the model in producing the cross-sections of Figures 7.8 and 7.9. To model the observed sections in these figures, a gas pressure had to be chosen that would cause the cavity to spall to the upper limit of the sandstone bed, and then the cavity would stabilize due to this limit. The gas pressure chosen is partly affected by the field stress (as well as the rock properties) such that:

$$\sigma_3' = \sigma_3 - P_g < \sigma_t$$

Without a program that can model three-dimensionally, the effect of the face on the distribution of the principal stresses cannot be evaluated. (The major principal stress is important when considering the presence of the shear zone.) The initial stress field (around the opening, prior to spalling) is not the same for the various sections of Figure A.2. The model is not able to account for this variation and therefore, when modelling these sections, the results may differ significantly. When modelling the sections close to the face, a gas pressure was chosen that would produce a cavity of approximate size. Using the same gas pressure when modelling sections farther from the face could give results that do not correspond to the actual cavities. The simplification made with regard to the three-dimensional effects of the heading face no longer apply farther from the face, producing an inconsistency in modelling resulting from inconsistent assumptions.

7.6.2 Effect of the Width of Exposed Sandstone Above the Heading

The farther one gets from the face not only does the stress field change but also the thickness of the intervening siltstone bed; it is non-existent or very thin close to the face and thicker further from the heading face. In the cases of an intervening siltstone bed between the coal seam and sandstone, where the heading does not penetrate the sandstone, the siltstone must first break out before spalling can occur. From the sections of Figures A.2, the angle at which the siltstone breaks out varies from 12° to 25° (from the vertical). The variation in this angle does not seem to be related to the thickness of this bed. In the analysis of the effect of the width at which the sandstone is exposed, it is assumed that the angle is constant at 20°. Thus, by varying the thickness of the siltstone, the effect of the breakthrough width can be observed, as shown in Figure 7.11. All the input parameters will remain the same as in the previous analyses.

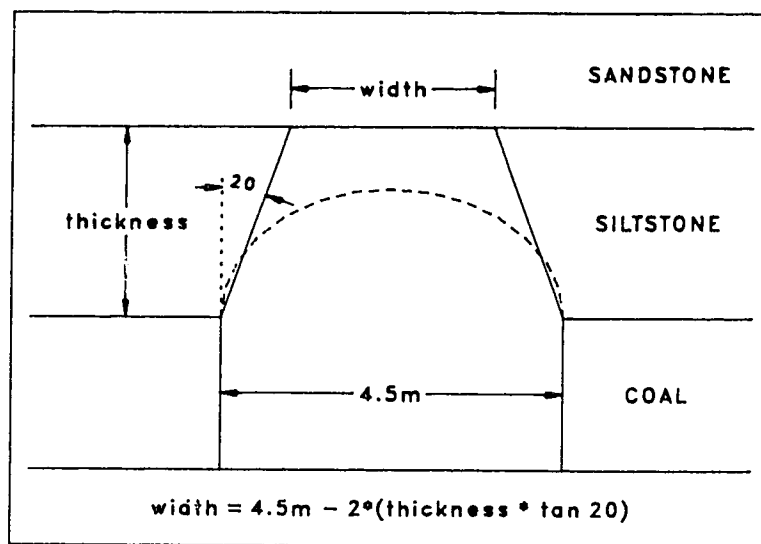


Figure 7.11 Relationship Between the Breakthrough Width and Siltstone Bed Thickness

An attempt has already been made to model the cavity from Figure A.2c and the result was infinite spalling. The breakthrough width ($\approx 10.5\text{ft}$ or 3.2m) here was already reduced from the cross-sections of Figures 7.8 and 7.9. Since the cavity would not stabilize due to a change in the shape alone, sections of narrower widths will be modelled. Relating the

thickness of the siltstone to the breakthrough width as noted above, a width of 3.2m is equivalent to a thickness of approximately 1.8m. The effect of different widths will be observed by varying the thickness from 2m to 3.5m. (Field results show that no outbursts have occurred when the siltstone was thicker than 2.7m, however, for the purposes of observing the effect of the width of exposure, thicknesses of up to 3.5m will be evaluated.)

The object of this exercise is to attempt to relate the narrower spans of exposed sandstone to the smaller cavities observed in the field. The results from the model will be compared to the sections of Figure A.2a to A.2f, page 97-99, by plotting the cavity volumes versus the breakthrough width of the siltstone. For the model runs, the thickness of the siltstone beds will be incremented at 0.5m intervals for each run. The first run at 2m thick and a span of $\approx 3\text{m}$ (10ft) spalled indefinitely, similar to the modelling attempt noted above. (Infinite spalling will be represented as a cavity of infinite size.) The next three runs (thicknesses of 2.5m to 3.5m) all produced a stable cavity of relatively small size (less than 5ft^2). These results are shown in Figure 7.12.

The relationship between the breakthrough width and the volume of ejected sandstone can be considered as a step function from the plot of Figure 7.12. The spalling of a cavity can be infinite if the gas pressure applied is great enough. However, it has been shown that as the width of the exposed sandstone becomes smaller, stable cavities are produced due to the stress redistribution resulting from the changing shape caused by spalling. The resulting stable cavity volumes will vary with the applied gas pressure. The lower the applied gas pressure, the wider can be the span of exposed sandstone for which the cavity can still spall to a stable shape.

The width at which cavities will spall indefinitely, for the situation given above, is between 8.8ft and 10ft (siltstone thickness of 2.0m to 2.5m). There must be a definite width at which the cavity either stabilizes or spall infinitely, for a given set of conditions. (In the field where the geology is variable, this definite width may be more of a range and the width of this range will depend on the variability of the parameters controlling the spalling.) When the effective minor principal stress is equal all around the cavity, the cavity has reached the 'most stable' shape. If tensile stresses are still being produced, the cavity will never reach

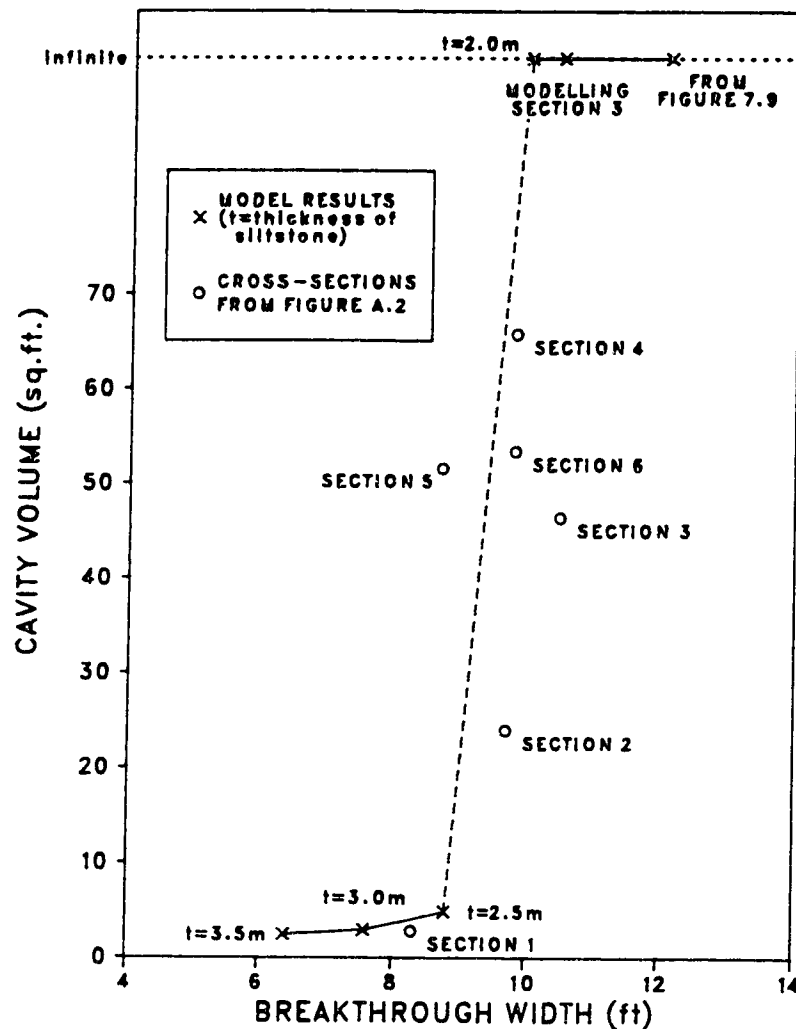


Figure 7.12 Effect of Breakthrough Width on Cavity Volume

stability. If tensile stresses occur at only some areas around the cavity, then a stress redistribution due to spalling could still produce a stable shape. When the stresses at the shear zone equal the tensile strength all around the cavity, the 'critical' breakthrough width is found; a greater width would cause infinite spalling and a smaller width would lead to a stable cavity. (This also occurred when the gas pressures were adjusted to find the upper bounding gas pressures to produce Figure 7.6, as discussed in Section 7.5.3.) Figure 7.13 shows the output for the model run of the 2.0m thick siltstone bed. Tensile failures are occurring all around the cavity at the shear zone and the 'most stable' shape has almost been reached. However, this cavity will spall indefinitely because tensile strength is exceeded at this most

stable shape. Figure 7.14 shows the output for the modelling of a 2.5m thick siltstone bed. There are no tensile failures around the cavity and the effective minor principal stresses are relatively equal on the boundary of sheared and intact rock. At some breakthrough width (or siltstone bed thickness) between these two cases, the critical width exists. (Limitations of the boundary element program prevent any further refinement of this analysis.) Element length and field point density have become critical factors in the assessment of stability for these smaller cavities.

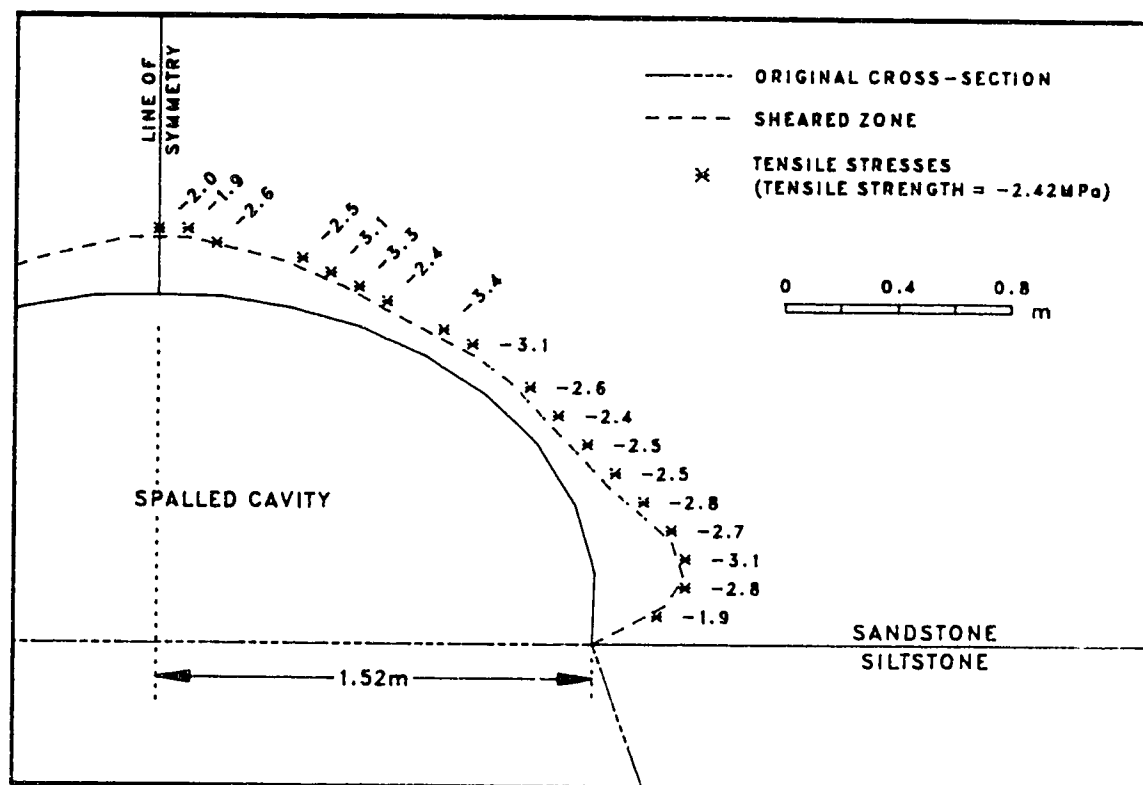


Figure 7.13 Tensile Failures Around the Cavity - Infinite Spalling

7.6.3 Reconsideration of Element Lengths and Field Point Density

When modelling cavities of much smaller size, especially near the step function to infinite spalling, the choice of element length and field point density becomes critical. In the case of such small cavities (related to those of Figures 7.8 and 7.9), the shear zone is quite small and thus to evaluate field points close to the sheared / intact rock boundary, the

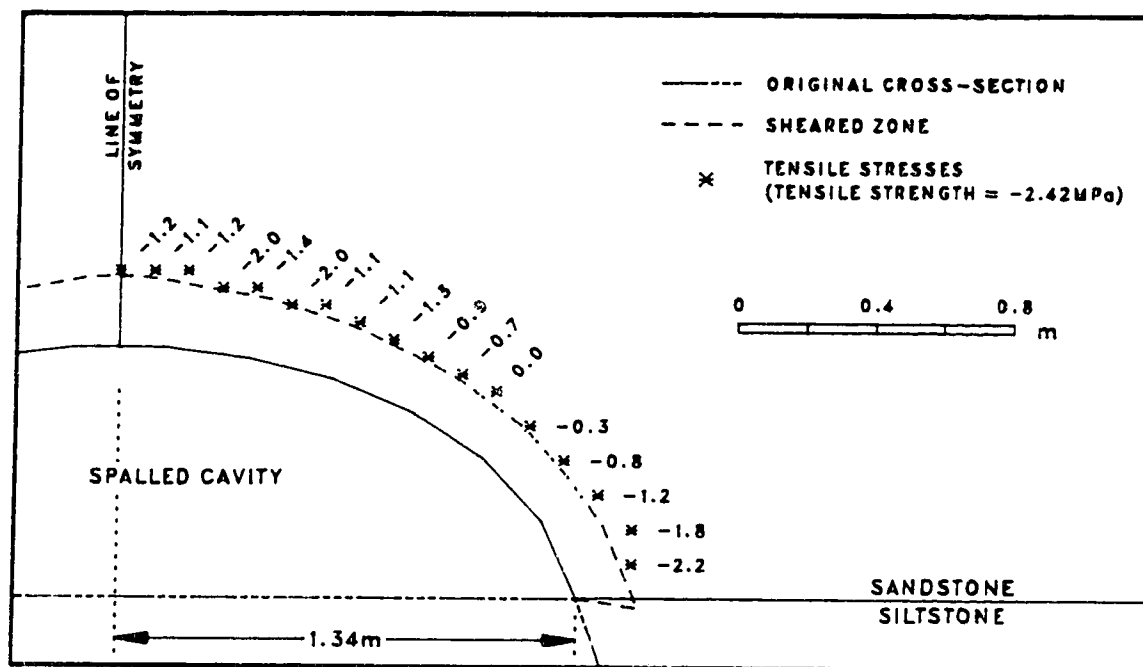


Figure 7.14 Stress Distribution Around a Stable Cavity

elements must be small enough. Also, in order to have sufficient field points close to the boundary, the field point density must be increased to prevent gaps between the boundary and the closest field point resulting in uncertainty regarding the presence of possible tensile failures. Boundary element lengths were reduced to as much as one-quarter and the field point density tripled from that of the original runs.

The element lengths were much less important in the earlier modelling runs that produced large cavities because the large shear zones associated with them meant that the field points could still be evaluated near the sheared / intact boundary. The field point spacing in these cases was also sufficient relative to the size of the cavity. The closer one gets to modelling near the step to infinite spalling the more critical these factors will be.

7.7 Summary

The mechanism and model presented here are able to explain the spalling process of an outburst in sandstone. With the use of this model, a range of gas pressures can be found for which spalling will take place and eventually become stable due solely to the change in the shape of the resulting cavity. This range of gas pressures is dependent on the rock strength, the initial shape of the heading and the field stress conditions. Different field stress ratios will produce cavities of different shapes. This final shape is ellipsoidal with long axis in the direction of greatest field stress.

The size of a cavity varies with the gas pressure and the width of the sandstone exposed to the heading. If sufficient gas pressure is applied, the cavity could spall indefinitely, or eventually be terminated by changes of geologic conditions. The same applies for an increased width of sandstone to the heading. There is a range of these values for which a stable cavity will result due to the change in the cavity shape alone. When these limits are exceeded, the cavity will spall indefinitely, thus creating a step function between these variables and the final size of the cavity. This discontinuity in the relationship, exists when the effective minor principal stress at the boundary of sheared and intact rock, is equal to the tensile strength all around the cavity. At this point, the model is exceedingly sensitive to the input parameters.

Field results show that the spalling of an outburst cavity is, at times, limited by the upper limit of the sandstone bed in which the outburst originated. The model predicts that, for the given geology, the gas pressure required to produce a cavity must exceed the maximum pressure for which a stable cavity can be reached by changing shape alone. Therefore, it is assumed that this cavity could spall indefinitely under constant conditions. However, the sandstone bed is limited in thickness and this provides a limit to the spalling of the cavity.

The model presented here evaluates stresses in two dimensions only. The model must therefore make an assumption about end effects when modelling cavities close to the face of a heading. The stress conditions vary with the distance from the face. Therefore, results from modelling close to the face cannot be compared with those from further away; the

assumptions made in both cases will not be consistent.

This model provides one possible explanation of the mechanisms involved during an outburst. The model can now be used to better assess the effects of various remedial measures that could be taken to help alleviate the hazards of mining in such conditions.

8. Siltstone Roof Failures

A siltstone bed often intervenes between the coal seam and the sandstone channels prone to outbursts. In the situation where the development headings do not penetrate the sandstone channel directly, the siltstone acts as a barrier to the sandstone and must fail prior to the initiation of an outburst. The failure of this siltstone 'beam' appears to be along a shear plane at angles between 12° and 25° to the vertical. This angle does not appear to be dependent on thickness.

There are several different methods that could be used to analyse the mode of 'beam' failure. These range from simple beam theory [45] to Voussoir (linear) arch theory [12,50,51,52] and 'cutter roof' failure [6]. The observed failures appear to resemble what is commonly referred to in the eastern United States as 'cutter' roof failure. This mode of failure will therefore be examined in more detail.

8.1 Cutter Roof Failure

Cutter roof failure is a common mode of failure in North American coal mines. The failure involves the propagation of fractures near the upper corners of a mine entry, at very steep angles. If the fractures intersect a weak bedding plane or, the fractures intersect, the resulting block may collapse. A limit equilibrium approach proposed by Brady and Brown [30] was later modified by Barron [6] for the evaluation of this mode of failure. The following section gives a brief description of the analysis given by Brady and Brown. (The derivation of the final equations can be found in the reference and will not be repeated here.)

8.1.1 Method of Analysis

Brady and Brown [8] have developed a technique of stress relaxation to evaluate the limit equilibrium forces acting on a prism (or wedge), whose shape is defined by planes of weakness (joints, shear, bedding). Barron [6] used this method to evaluate the stability of a truncated wedge. Figure 8.1a shows a free body diagram of the initial forces acting on the shear planes of the wedge. The relationship between the normal and shear forces is assumed

by Brady and Brown to be given by:

$$S = N \tan \phi \quad [8.1]$$

ie. it is assumed that shear resistance is supplied through friction only, and cohesion is zero.

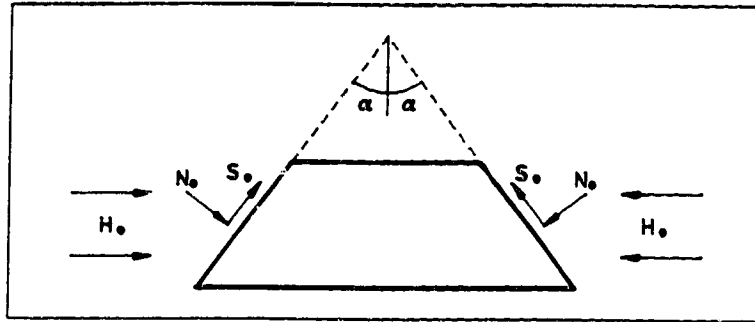


Figure 8.1a Initial Forces Acting on the Potential Shear Planes

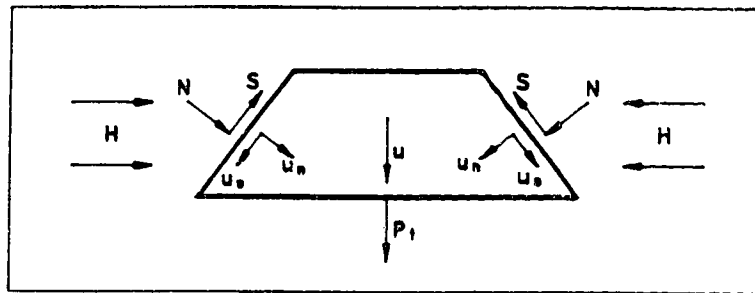


Figure 8.1b Limit Equilibrium Forces After Shear Plane Relaxation

Initially, the fractures at the ends of the wedge have a shear and normal stiffnesses so high that the presence of the fractures can be ignored. The horizontal stresses acting on this wedge can be determined by evaluating the stress distribution around the opening. The initial horizontal force (H_0) acting on the potential shear planes of the wedge is shown in Figure 8.1a. Relaxation is introduced by considering the displacement of the wedge caused by deformation of the shear plane. (Deformation of the wedge itself is ignored because fracture stiffnesses are much less than the elastic modulus of the rock.) Brady and Brown showed that the forces acting on the shear plane, after relaxation (resolved in the vertical direction), are defined by:

$$P_t = \frac{2 H_0 \sin \alpha \sin (\phi - \alpha)}{\sin \phi} \quad [8.2]$$

At limit equilibrium, Figure 8.1b, the forces on the shear plane resolved in the vertical direction, P_t , are compared to the net applied external force P . The value P equals the sum of all the external forces acting on the wedge (tensile strength across the bedding plane, surcharge loading on top of the wedge and any applied support) and the weight of the wedge. The wedge stability (safety factor, F) can then be expressed as a ratio of the resistive to external forces:

$$F = \frac{P_t}{P} \quad [8.3]$$

This analysis outlined here will be used to evaluate the safety of the overlying siltstone bed as one possible method of failure.

8.2 Cutter Roof Failure of Siltstone

Figure 7.11, page 58, shows the geometry of the heading; a simplification will be made with regard to the shape of the wedge as noted in Figure 8.2. The shear planes are assumed to originate at the siltstone / coal interface. Since a zone of fractured rock exists around the opening, a simplified wedge geometry will be used.

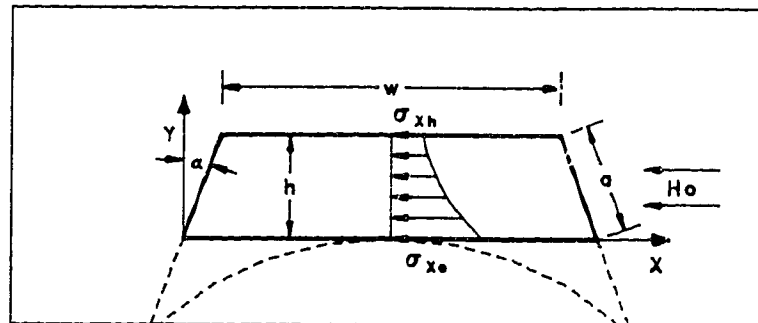


Figure 8.2 Siltstone Beam Dimensions and Stress Distribution

The boundary element program used in the outburst model can be used to evaluate the initial horizontal stresses around the opening. The stresses were evaluated at the center of the beam to simplify the stress determination, as shown in Figure 8.2. The horizontal force is

obtained by integrating the horizontal stresses (σ_x), evaluated at given points, over that area, and is given by:

$$H_o = \int_0^h f(\sigma_x) A_v dy \quad [8.4]$$

where H_o is the initial horizontal force acting on the wedge, h is the height of the wedge and $A_v (= h \cdot \text{unit depth})$ is the area over which the stresses were evaluated. Equation [8.4] can be simplified using the trapazoidal rule:

$$H_o = \frac{(f_1 + f_2) \Delta y_1}{2} + \frac{(f_2 + f_3) \Delta y_2}{2} + \dots + \frac{(f_{n-1} + f_n) \Delta y_{n-1}}{2} \quad [8.5]$$

where f_i are the field point stresses derived from the boundary element program and Δy_i are the distances between successive field points. This force H_o is assumed to be equal to the horizontal force at the shear planes prior to relaxation.

The derivation of the limit equilibrium equations given by Brady and Brown, is based on a normal / shear force relationship dependent only on the friction angle, ϕ . The spalling model presented earlier assumes that the siltstone is intact and it is assumed that, initially, no shear plane exists. Hence, the normal / shear force relationship must be modified to include cohesive strength.

The strength of siltstone used previously was given by the Hoek and Brown criterion and the same criterion should be used for the shear strength. Hoek and Brown [30] developed the following relationship between the normal and shear stresses:

$$\frac{\tau}{\sigma_c} = A \left[\frac{\sigma}{\sigma_c} - \frac{\sigma_t}{\sigma_c} \right]^B \quad [8.6]$$

where σ_c and σ_t are uniaxial compressive and tensile strengths respectively and A and B are constants determined empirically as outlined in Appendix 5 of Hoek and Brown [30]. For this siltstone, $A = 0.683$ and $B = 0.613$. Let the normal force $N = a \sigma$ and the shear force $S =$

a τ , where 'a' is the area of the shear plane. Substituting these expressions into equation [8.6] and rearranging, gives:

$$S = a A \sigma_c^{1-B} \left[\frac{N}{a} - \sigma_t \right]^B \quad [8.7]$$

Brady and Brown [8] give the expression for the relaxed normal force acting on the shear plane in terms of the initial horizontal force as follows: (see reference for derivation)

$$N = H_o \left[\frac{\sin \alpha}{\tan \phi} \right] \quad [8.8]$$

Substituting equations [8.7] and [8.8] into [8.1] and rearranging gives the following expression:

$$\phi = \tan^{-1} \left[\left[\left[\frac{H_o \sin \alpha}{a A \sigma_c^{1-B}} \right]^{1/B} + \sigma_t \right] \frac{a}{H_o \sin \alpha} \right]^{-1} \quad [8.9]$$

where ϕ is dependent on the normal stress. If this expression is substituted in equation [8.2], the value of P_t is given in terms of the Hoek and Brown strength criterion and represents an intact material, with cohesion.

Now that the expression for P_t is defined in terms that can be easily determined, the external forces can be evaluated. Assuming no tensile strength between the siltstone and sandstone and that no support force is applied, the weight of the wedge and gas pressure must be determined. The weight can easily be derived from the wedge geometry, however, it is insignificant compared to the effects of the gas pressure and will be ignored. Therefore,

$$P = P_g w = P_g (2 * (2.25 - (1.68 + h) \tan \alpha)) \quad [8.10]$$

where P_g is the gas pressure, w is the exposed width of sandstone, h is the height of the siltstone above the heading (thickness of wedge), the height of the arch above the coal seam is 1.68m and 2.25m is half the width of the heading. Combining equations [8.10], [8.9] and

[8.2] into [8.3], the factor of safety for shear failure can be found for any given thickness of siltstone and sandstone gas pressure.

To best illustrate this relationship, a series of calculations were done varying the thickness of the siltstone bed and the angle at which the siltstone sheared. In each case, a gas pressure was found that would produce a state of limit equilibrium, $F=1.0$. Figure 8.3 shows the relationship of these variables. For the last two outbursts at No. 26 Colliery, producing the cavity illustrated by sections of Figure A.2, the gas pressure was assumed to be 7.1MPa and the siltstone first failed at a thickness of 2.8m, the angle of the shear plane should have been at approximately 13° from Figure 8.3. From Figure A.2a, the actual angle of failure was about 15° .

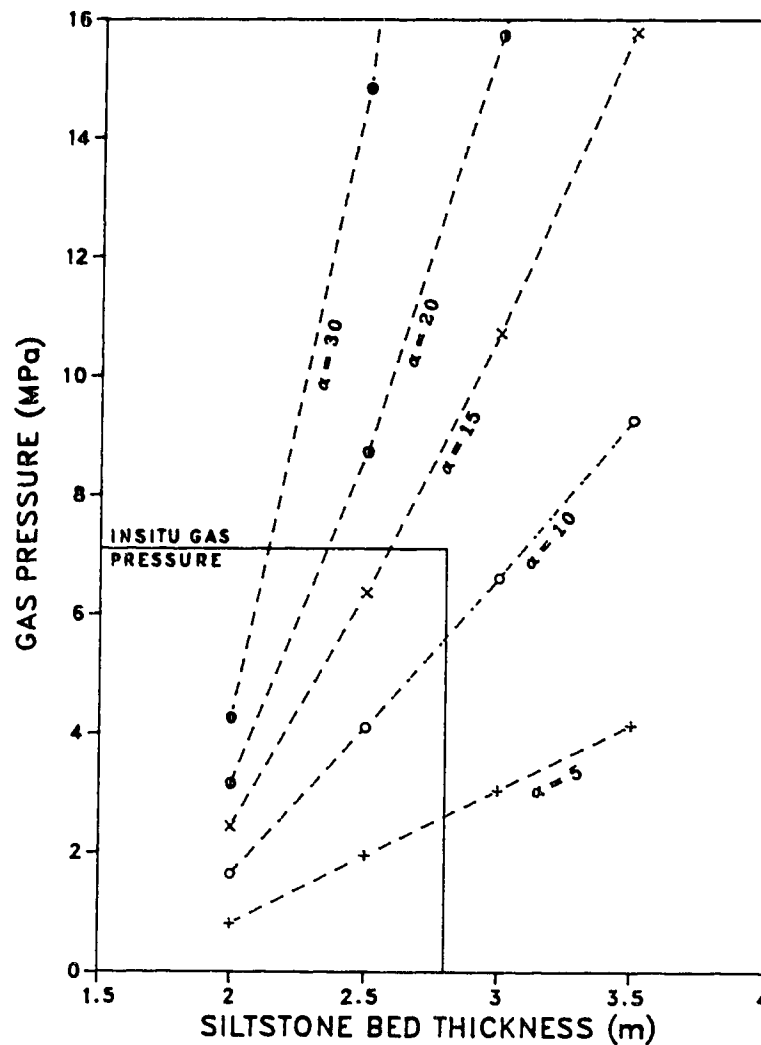


Figure 8.3 Gas Pressures Required to Fail Siltstone Beams

The results from Figure 8.3 show that a still thicker siltstone bed could fail at steeper angles for a gas pressure of 7.1MPa. In fact, steeper angles would produce a less stable situation. Field results show that the siltstone fails at angles between 12° and 25°. The method of analysis presented here, does assume a much simplified wedge geometry. The assumption made for the wedge being rectangular (as shown in Figure 8.2) ignores the rock beneath the ends of the wedge. This material could be influencing the angle at which the shear planes form. Further work could be done to evaluate this possibility.

8.3 Summary

The 'cutter' roof failure method of analysis gives adequate results in an attempt to explain the failure of the siltstone bed under surcharge gas pressure prior to the initiation of the outburst. This limit equilibrium solution allows the evaluation of external forces required to reinforce the siltstone against shear failure and thus prevent an outburst. This analysis could be incorporated directly into a spalling model to evaluate the possibility of an outburst occurring. Such an analysis would be required in three-dimensions to evaluate the extent to which a siltstone bed would fail back from the face.

Other methods of evaluation could be conducted on the stability of the siltstone bed. Simple beam theory and Voussoir arch analyses were tried, but the results did not fit the field observations. Cutter roof failure provides one possible explanation for the siltstone failures.

9. Remedial Measures Against Outbursts

At the time of mine closure, steel arches with lagging were the only support being used in the headings. Support by arches is passive; no supporting force is provided unless the ground puts a force on the arch. When driving a heading, the face of that heading provides the majority of the ground support for some distance behind the face. The arches gradually take more load the further they are from the heading face. Figure 4.4 (page 18) shows the damage caused by an outburst; it is seen from the way the arches have been pushed over that they could not have been supporting much load, if any. Studies were being done to attempt to alleviate the outburst problem and roof support was one aspect of this work. The closure of the mine in April 1984 prevented implementation and evaluation of any possible remedial measures. The severity of the final two outbursts caused a delay in the driving of the main deeps; remedial measures would have been essential for this operation to continue. In all areas that are prone to outbursts remedial measures should be considered that would, at least, minimize the effect of an outburst. The only known remedial measure attempted was by degassing of the sandstone from holes drilled in it to allow the methane to escape. The rock, however, was so impermeable that this method was not at all effective.

Two different geologic conditions must be considered when investigating different support methods; where the sandstone is in contact with the coal seam and where a siltstone bed intervenes between the two. The most effective support methods could be quite different for these two situations.

First consider the case of supporting the siltstone bed between the coal and sandstone. It has been stated earlier that no outbursts had occurred when the intervening siltstone bed was thicker than 2.7m. However, this statement may be misleading; it should be stated in terms of the height between the sandstone / siltstone interface and the top of the heading, which in this case would be 1.0m (the heading is 1.7m higher than the thickness of the coal seam). The roadways were being driven such that the bottom was coincident with the bottom of the coal seam. If the roadway was lowered, the thickness of the siltstone above the top of the heading would be increased. For the main deeps, where the major outbursts occurred,

these headings could also be driven below the coal seam for extra safety. In this case at least, the main entries should be safe. Exploratory holes could still be drilled upwards from these main deeps to monitor the position of sandstone channels. Longwall entries would then have to be angled upwards from the main deeps to the coal seam.

The siltstone above the heading appeared to fail by shear at the top corners of the opening (see previous chapter). If these potential shear plane could be sufficiently strengthened the siltstone would remain in place and the sandstone would not be exposed and could not spall out. Support, in such a case, would best be provided by the installation of rock bolts through that potential shear planes. Bolting along the top of the heading would also be required in the case of a thinner siltstone bed to prevent this bed from shattering under the stress increase. Large end bearing plates would make the stress distribution from the bolts more uniform and help support the fractured rock. Arches could still be installed, as before, for long term support. Bolting would be most important close to the face where the arches provided little or no support. Wire mesh between the bolts would help prevent ravelling before the lagging is installed.

Sandstone does not adhere very well to siltstone. If there were a separation at the sandstone / siltstone interface free gas could be present putting a surcharge load on the siltstone beam. Drilling holes to this interface would allow the gas to escape, thus reducing the stresses on the siltstone bed. The likelihood of the presence of free gas is unknown but the effectiveness of degassing the interface could be considerable. The sandstone has a low elastic modulus compared to that of the siltstone. If the gas at the interface was removed, the sandstone would deform and probably begin loading the siltstone, but the final stresses on the siltstone would be less than if a surcharge gas pressure were present at the interface.

In the case of a heading being driven through the sandstone channel, support would be much more difficult to provide. Lowering the roadway may reduce the severity of an outburst because of the narrower width over which the sandstone is exposed. The effect of a narrower width of exposed sandstone was analysed in Section 7.6.2, page 58.

In the case of the headings driven to access the the longwall panels, the headings must be in the coal seam (the top of the heading could still expose the sandstone). Where the sandstone is exposed by the heading, the most effective remedial measure would be degassing the sandstone. If successful, the sandstone would no longer be a problem and support provided by the arches would, once again, be sufficient. However, because drilling degassing boreholes was ineffective, fracturing would have to be induced.

The most common method of inducing fracturing is by hydro-fracturing; ie. the use of high pressure water injected into a borehole drilled into the sandstone to produce fractures.[1] The sandstone has a low porosity and very low permeability; the fracturing created by this technique is not very extensive and would probably not be sufficient to relieve gas pressures to any great degree. It is likely that increased water injection would propagate existing fractures but probably not create new ones. Sand mixed with the water would have to be used to retain the permeability of the cracks once the water is removed, otherwise the cracks would close up. A hydrostatic field stress is the worst condition for hydro-fracturing because the crack could form in any direction. The stress field at No. 26 Colliery is almost hydrostatic. The most effective place for the crack to be induced is near the bottom of the sandstone bed; this is the area that would be exposed during development. However, a fracture in the area could easily deviate to the sandstone / siltstone (or coal) interface, the crack would then follow the interface (since the sandstone does not adhere well to the other rock) and nothing of significance would be accomplished. If the fracture deviated into the coal seam, a considerable amount of water could be lost into the more porous and permeable coal. Mining this coal would then become much more difficult. Hydro-fracturing may be attempted, but it appears unlikely that this technique would be successful in degassing the sandstone.

Another method for inducing fractures into the sandstone would be to drill into it, well head of the face (10m - 20m perhaps), and fire a small blast. The blast would have to be large enough that the fractures created would degas a sufficiently large zone of sandstone and yet not create too much damage. Several smaller charges, over the area that would later be

exposed by the heading, would be preferable to one or two larger ones. The gas would then be allowed to escape through the boreholes and degas this zone. Given sufficient time, this zone should have given off all the gas it is able to. The loose and fractured sandstone could then be grouted so that the heading could be driven safely under it without additional support. The zone of grouted sandstone should be large enough that the area in which tensile failures could have occurred is relieved of the gas. The model presented here could be used to evaluate the extent of this required degassing zone. The grouting could be extensive such that, when undermined by the heading, no additional support is required, or alternatively, lighter grouting might be used requiring additional support later. (Arches and lagging would always be required for long-term support and safety.) Cost would be an important factor of this method.

In the drill and blast method of driving a heading, the blast will produce a new, unsupported face of rock. Outbursts usually occur in this area, just after the blast. Support could be installed prior to the blasting of that round. Long steel reinforcing bars could be put in across the top of the heading, horizontally or angled upwards slightly, such that the exposed end could be supported by (attached to) the steel arches, ie. forepoling. The other end must be deep enough to remain firmly in place after the next blast. After the blast, these bars would be supported at both ends and the newly exposed roof would be supported. These bars could either just be driven in, or grouted into the drillholes. The deep end of the bar might also be mechanically anchored. This procedure could be continued as long as the threat of an outburst exists.

Boring the headings, instead of blasting, could be quite successful because radial support is applied continuously by the machine as soon as the rock is exposed. Rock bolts and mesh could be installed while the machine is still supporting the opening and once the machine has passed, arches set up. (This method would also eliminate the added stresses from the shock front produced by blasting.) DEVCO presently have boring machines operating in mines in the area.

Outbursts appear only to occur in the vicinity of the sandstone channels. Geologists at DEVCO are presently working on mapping the locations of these channels in an attempt to identify areas that could pose a mining problem. Eventually, the mine layout might be changed in some way to minimize the effects of the sandstone channels. This could only be done if the channels were accurately mapped, so this on-going work by DEVCO geologists is extremely important.

Several different remedial measures have been presented and discussed. However, until these methods are actually attempted, their effectiveness can only be speculated upon. As an overall principle, the installation of support as close to the face as possible is necessary, and the installation of active rather than passive support would be preferable.

One interesting point to note is that no outbursts have been recorded at the longwall faces. This could be due either to large scale stress and gas pressure relief due to gob failures or the active support provided by the longwall shields, or a combination of these.

10. Conclusions

The mechanism and model presented in this thesis provide an explanation that accounts for the occurrence of outbursts from sandstone channels in No. 26 Colliery. The outburst model has not only been able to reproduce (with reasonable accuracy) the actual outburst cavities, but has also brought forth other aspects about outbursts.

Field reports show that the outbursts occurred in sandstone channels that approached to within 2.7 meters of the coal seam. The severity of outbursts increased with increased mining depth and were independent of the direction of mining. All reported 'events' occurred at the face of a development heading.

Insufficient data is available on the field conditions present at the time of the outbursts, therefore several assumptions had to be made. Additional testing is required in order to model other outbursts with greater confidence in the results.

The two main factors that affect the initiation and continued spalling of an outburst cavity are the gas pressure and the tensile strength of the rock in which the gas is present. The effective minor principal stress must exceed the tensile strength of the rock to create tensile failures within the rock mass. Outbursts are thought to be a product of these tensile failures. Other factors include the triaxial strength of the rock, which defines the extent of the sheared, degassed zone around the outburst cavity.

The postulated spalling mechanism presented here assumes an outburst to be a series of instantaneous, static events. With each iteration in this series of events, the shape of the cavity changes, and this may eventually lead to a stable cavity. In this manner, the final cavity shape may become stable through a change in cavity shape alone, without geologic influence. If a cavity will not stabilize due to shape change, geologic factors must be considered in order to predict the final cavity shape and size.

A computer model was developed, based on the postulated spalling mechanism, to model the outbursts at No. 26 Colliery. The model results fit the field observations reasonably well for cavity size and shape. Changing cavity shapes at different distances from the heading face can be explained by the model in terms of the width of exposed sandstone above the

heading. The model, however, cannot evaluate the more complex, three-dimensional effects, for cavities near the face.

The model is able to show how a cavity can spall to a stable shape in one situation and, how with a slight change in field conditions, a cavity could spall infinitely. There exists a set of conditions where a cavity will spall to a stable shape, but a small change in conditions could cause it to spall infinitely. It is at this point that the model is most sensitive to the element length used in the boundary element program.

The failure of a siltstone bed intervening between the coal seam and sandstone channels can be explained as a surcharge loaded beam evaluated as a 'cutter roof' failure. The results from cutter roof failure analyses are compatible with the observed field results. Other theories such as simple beam and Voussoir arch do not provide compatible results. A stability analysis of the siltstone bed could be incorporated directly into the spalling model to investigate the possibility of an outburst event occurring.

Prior to the closure of the mine, no additional support (over and above steel arches and lagging) was provided in areas prone to outbursts. Since arches provide only passive support, additional remedial measures must be taken to support the roof near the face of the heading. In the case of an intervening siltstone bed, reinforcing this bed through the application of rock bolts would be advised. In the case of the heading penetrating the sandstone channel, the most effective remedial measure would be degassing the sandstone channel by inducing fracturing, or lowering the heading to a sufficient depth below the sandstone channel, leaving a siltstone or coal roof.

10.1 Recommendations For Further Work

The recommendations listed below will be separated into those dealing with the mining operation and work to be done with respect to the modelling of outbursts.

In the modelling of the outbursts at No. 26 Colliery, a great many assumptions have to be made with respect to the field conditions at the time of an outburst. Very little testing of rock properties has been done, and the results are highly variable. The work done on

determining the field stress was very poor and the results are quite questionable. The most significant factor in these outbursts is the gas pressure within the sandstone, and only one test was conducted to find this gas pressure. Further testing to better define these insitu properties is essential in the prediction and control of future outbursts. The variability of these properties must also be considered, especially between different sandstone channels.

The work presently being done in mapping the sandstone channels is very important. As other mines begin to approach conditions that were present at the No. 26 Colliery outbursts, knowledge of the locations of these channels becomes essential. If areas of potential danger can be identified early enough, remedial measures such as lowering the main deeps or altering the mine layout and/or mining sequence can be considered.

If (and when) outbursts are encountered, various remedial measures should already have been considered and a program prepared to implement and evaluate these measures. Active support at the heading face should be considered first. Degassing of the sandstone channel by inducing fracturing (either by blasting or hydro-fracturing) might later be considered. Boring the headings, as opposed to blasting, could also be an effective remedial measure.

With respect to the existing model, the effectiveness of support, such as rock bolts, could be evaluated. However, the ability to evaluate support around the heading is limited in the boundary element program used in the model. Some of the limitations of the boundary element program noted in this report can be overcome by the use of the finite element method. This method could also directly evaluate the effects and stability of a siltstone bed intervening between the coal seam and sandstone channel.

The outburst (spalling) model presently requires user intervention in the contouring of the tensile and shear zones around the outburst cavity. The model could be changed to make it completely user independent. This would eliminate the subjectivity in defining the contour close to the boundary. This would be one advantage to using the finite element method.

Modelling outbursts in three dimensions could be the next step in applying the mechanism proposed here. This would be very important in the evaluation of cavity size and

outburst severity. Limitations of a two-dimensional analysis have been encountered when comparing field observations with model results close to the heading face.

It is therefore recommended that an attempt be made to develop a three-dimensional finite element model for a single heading, using the basic principles of the spalling mechanism presented here.

References

1. Associated Mining Consultants Ltd., "Hydrofracturing for Prevention of Rock / Gas Outbursts", DSS File No. 23SQ.23440-4-9092, Department of Supply and Services, Canada, May 1985
2. Aston, T.R.C., Research Scientist, CANMET, Sydney, Nova Scotia, Personal Communications and Unpublished Data, 1987-1988
3. Aston, T.R.C., "Theoretical Insitu Strata Reservoir and Pore Pressure Calculations for Material from No. 26 Colliery, N.S.", Division Report ERP/CRL 85-15(TR), CANMET, Energy, Mines and Resources Canada, March 1985
4. Aston, T. and Cain, P., "Gas and Rock Outbursts at No. 26 Colliery, Sydney Coalfield, Nova Scotia - A Case History", Proceedings of the 21st International Conference on Safety in Mine Research Institutes, Sydney, Australia, Oct. 1985
5. Aston, T.R.C., O'Leary, L.S., Young, D.A., "Coal Strength Parameters Derived for the Donkin-Morien Harbour Seam, Sydney Coalfield, N.S.", Division Report ERP/CRL 85-65(TR), CANMET, Energy, Mines and Resources Canada, June 1985
6. Barron, Ken, Professor of Mining Engineering, University of Alberta, Edmonton, Alberta, Personal Communications and Unpublished Data, 1987-1988
7. Becker, R.M. and Hooker, V.E., "Some Anisotropic Considerations in Rock Stress Determinations", U.S. Bureau of Mines Report of Investigations 6965, U.S. Department of the Interior, 1967
8. Brady, B.H.G. and Brown, E.T., "Rock Mechanics for Underground Mining", George Allan & Unwin, London, U.K., 1985
9. Cain, P., "Carbon / Carbonate Analysis of Rock / Gas Prone Sandstones From the Sydney Coalfield", Division Report ERP/CRL 86-117(IR), Oct. 1986
10. Cain, Peter, "Outbursts at Number 26 Colliery", Division Report ERP/CRL 84-1(CF), CANMET, Energy, Mines and Resources Canada, Jan. 1984
11. Crouch, S.L. and Starfield, A.M., "Boundary Element Methods in Solid Mechanics", George Allen & Unwin Ltd., London, UK, 1983
12. Evans, W.H., "The Strength of Undermined Strata", AIME Transactions, Vol. 50, 1941, pp. 475-532
13. Forgeron, Steve, Chief Geologist, Cape Breton Development Corporation, Sydney, Nova Scotia, Personal Communications and Unpublished Data, 1987-1988
14. Forgeron, S., "Some Effects of Paleo Sandstone River Channels on Coal Mining Operations, Sydney Coalfield Nova Scotia", Paper presented at the G.A.C. Annual Meeting, Halifax, 1980
15. Forgeron, S., MacKenzie, G., MacPherson, K., "The Effects of Geological Features on Coal Mining, Sydney Coalfield, Nova Scotia", Can. Inst. of Min. Metal. Bulletin, Vol. 79, No. 891, July 1986

16. Gallant, W.D., Technologist, CANMET, Sydney, Nova Scotia, Personal Communications and Unpublished Data, 1987-1988
17. Gallant, W.D. and Aston, T.R.C., "Measurements of Insitu Strata Gas Pressure at No. 26 Colliery, Sydney Coalfield, N.S.", Division Report ERP/CRL 85-10(TR), CANMET, Energy, Mines and Resources Canada, Jan. 1985
18. Golder Associates, "Development of an Outburst Model for the Sydney Coalfield, Cape Breton, Nova Scotia", Report No. 861-1290, March 1987
19. Golder Associates, "Measurement and Analysis of Rock Deformation and Support System Response in the Drill and Blast and Bored Access Drivages at the Donkin-Morien Project", Vol. 1 and 2, Report No. 831-6014, June 1985
20. Golder Associates, "Development and Use of Triaxial Rock Testing Procedures for Samples of the Sydney Coalfield, Phase two", Report No. 841-1287, March 1985
21. Golder Associates, "Insitu Stress Determination in No. 26 Colliery, Cape Breton, Nova Scotia", Report No. 831-1296, February 1984
22. Gorski, B., "Laboratory Test Results of Rock Cores from No. 26 Colliery, Sydney Coalfield", Division Report ERP/MRL 84-25(TR), CANMET, Energy, Mines and Resources Canada, March 1984
23. Hacquebard, P.A., "Geologic Development and Economic Evaluation of the Sydney Coal Basin, N.S.", Part A, Geological Survey of Canada, Paper 83-1A, 1983
24. Hacquebard, P.A., "A Geological Appraisal of the Coal Resources of Nova Scotia", CIM Bull., Vol. 72, No. 802, 1979, pp.76-87
25. Hacquebard, P.A. and Donaldson, J.R., "Carboniferous Coal Deposition Associated with Flood-Plain and Limnic Environments in Nova Scotia", Geol. Soc. of America, Special Paper 114, 1969, pp. 143-191
26. Haites, T.B., "Conjectural Shape and Extent of the Sydney Coalfield", Trans. CIM, Vol. 55, 1952, pp. 202-212
27. Haites, T.B., "Some Geological Aspects of the Sydney Coalfield with Reference to Their Influence on the Mining Operations:", Trans. CIM, Vol. 54, 1951, pp. 215-225
28. Hassani, F.P., Scoble, M.J., Whittaker, B.N., "Applications of the Point Load Index to Strength Determination of Rock and Proposals for a New Size Correction Chart", Proceedings of the 21st Annual Symposium on Rock Mechanics, University of Missouri, 1980
29. Hiramatsu, Y., Saito, T., Oda, N., "Studies of the Mechanism of Gas and Coal Bursts in Japanese Coal Mines", Proceedings of the 5th International Congress on Rock Mechanics, Melbourne Australia, 1983
30. Hoek, E. and Brown, E.T., "Underground Excavations in Rock", Institute of Mining and Metallurgy, London, 1980
31. Hooker, R.M. and Bickel, D.L., "Overcoring Equipment and Techniques Used in Rock Stress Determinations", U.S. Bureau of Mines Information Circular 8618, U.S. Department of the Interior, 1974

32. Jackson, L.J., "Outbursts in Coal Mines", Report No. ICTIS/TR25, IEA Coal Research, London UK, May 1984
33. Khodot, V.V., "Research on the Problem of Coal and Gas Outbursts", Symposium on Coal and Gas Outbursts, Nimes, France, 1964
34. King, L.H. and MacLean, B., "Geology of the Scotia Shelf", Geological Survey of Canada, Paper 74-31, 1976
35. Konda, B.W., "Methane Emission in Longwall Districts with Special Reference to 14 North District of No. 26 Colliery", Division Report ERP/CRL 85-44(IR), CANMET, Energy, Mines and Resources Canada, April 1985
36. Litwiniszyn, J., "A model for the Initiation of Coal-Gas Outbursts", International Journal of Rock Mechanics and Mining Sciences and Geomechanic Abstracts, Vol.22, No. 1, 1985, pp. 39-46
37. MacLean, A.R., "The Cape Breton Development Corporation", Coal in Canada, Editor: Patching, T.H., CIM Special Volume 31, Montreal, 1985
38. Mahtab, M.A., "Geomechanical Aspects of the Gas Outbursts in Louisiana Salt Mines", Bulletin of the Association of Engineering Geologists, Vol. 19, No. 4, 1982
39. Obert, L. and Stephenson, D.E., "Stress Conditions Under Which Core Discing Occurs", Transactions of the Society of Mining Engineers, Sept. 1965
40. Panek, L.A., "Calculation of the Average Ground Stress Components From Measurements of the Diametral Deformation of a Borehole", U.S. Bureau of Mines Report of Investigations 6732, U.S. Department of the Interior, 1966
41. Paterson, L., "The Mechanism of Outbursts in Coal and the Prevention of Outbursts by Gas Drainage", preprints, Second International Symposium of Rockbursts and Seismicity in Mines, Minneapolis, June 1988
42. Paterson, L., "A Model for Outbursts in Coal", International Journal of Rock Mechanics and Mining Sciences and Geomechanic Abstracts, Vol. 23, No. 4, 1986
43. Paul, Konrad, "Methane Bursts Involving the Ejection of Rock Material", Symposium on Methane Bursts Involving the Ejection of Coal or Rock, Luxembourg, (German trans.), July 1983
44. "Pit Slope Manual, Supplement 3-1, Laboratory Classification Tests", MLR CANMET Report 77-25, Energy Mines and Resources, Canada, 1977
45. Roark, R.J. and Young, W.C., "Formulas for Stresses and Strains", 5th Edition, McGraw-Hill, New York, 1975
46. Serafim, J.L., "Influence of Interstitial Water on the Behaviour of Rock Masses", Rock Mechanics in Engineering Practice, Editors: Stagg, K.G. and Zienkiewicz, O.C., John Wiley & Sons, London, 1979, pp. 55-97
47. Shepherd, J., Rixon, L.K., Griffiths, L., "Outbursts and Geological Structures in Coal Mines: A Review", International Journal of Rock Mechanics and Mining Sciences and Geomechanic Abstracts, Vol. 18, No. 4, 1981

48. Singh, J.G., "A mechanism of Outbursts of Coal and Gas", Mining Science and Technology, 1, 1984, pp.269-273
49. Smith, R.V., "Practical Natural Gas Engineering", PennWell Publishing Co., Tulsa, Oklahoma, 1983, pp. 1-33
50. Sterling, R.L., "Roof Design for Underground Openings in Near-Surface Bedded Rock Formations", Ph.D. Thesis, University of Minnesota, June 1977
51. Wright, F.D., "Arching Action in Cracked Roof Beams", Proceedings of the 5th International Strata Control Conference, London, 1972
52. Wright, F.D. and Mirza, M.B., "Stress Distribution Around a Vertical Crack in a Mine Roof Beam", Trans. AIME, Vol. 226, 1963, pp. 174-179

Appendix A - Outburst Information [2,13]

Table A.1 contains all the information regarding the thirty seven outbursts that have taken place. Twenty three of these events were accompanied with excessive amounts of methane with the remaining 14 having no noticeable methane elevation (these included the small docile incidents that were initially classified as roof falls). The following points summarize the data presented in Table A.1:

- all but one of the bursts were associated with shotfiring (outburst #24)
- the severity of outbursts increased with depth
- all five sandstone channels were subject to outbursts
- all outbursts occurred when the sandstone river channels approached to within 2.7m of the coal seam
- outbursts occurred independent of the direction of driving headings

Figure A.1 is a longitudinal section of the cavity produced by outbursts #36 and #37. Figures A.2a-q shows cross-sections of this cavity and the surrounding geology.

Table A.1 Details of Outbursts From No. 26 Colliery [2,13]

EVENT NO.	DATE	LOCATION	DIRECTION OF DRIVE	TRIGGER MECHANISM	ARCHES DOWN OR DAMAGED	ROCK TYPE EJECTED	BURST ACCOMPANIED BY GAS
1	Summer, 77	13 North Material Level	West	?	?	Sandstone	?
2	Jan. 5, 78	13 North Coal Road	West	Shooting at face	2 damaged	Sandstone	?
3	Jan. 23, 78	13 North Coal Road	West	Shot in coal and stone	0	Sandstone	No gas reported
4	Jan. 25, 78	13 North Coal Road	West	Shot in coal and stone	0	Sandstone	No gas reported
5	Aug. 30, 78	13 South Material Level	East	Shot in coal and stone	2 damaged	Sandstone	No gas reported
6	Sept. 1, 78	13 South Material Level	East	Shot in stone	1 damaged	Sandstone	No gas reported
7	Sept. 5, 78	13 South Material Level	East	Shot in coal and stone	1 damaged	Sandstone	No gas reported
8	Sept. 6, 78	13 South Material Level	East	Shot in coal and stone	0	Sandstone	3.5 - 5% after shooting

Table A.1 Details of Outbursts From No. 26 Colliery [2.13]

EVENT NO.	VOLUME OF GAS (m ³)	POSITION OF BURST	DIMENSIONS OF CAVITY (m) L x W x H	ESTIMATED VOLUME OF CAVITY (m ³)	SANDSTONE HEIGHT ABOVE COAL (m)	ADVANCE SINCE LAST FALL (m)	DEPTH BELOW SEA LEVEL
1	?	?	?	?	1.8	?	703
2	-	above face	0.9 x 4.3 x 1.2	5	0.61	?	737
3	-	above face	1.8 x 4.26 x 3.05	24	0	?	735
4	-	above face	1.8 x 4.26 x 3.05	24	0	1.82	735
5	-	at face	4.26 x 4.57 x 1.22	23	2.13	?	724
6	-	at face	2.74 x 4.57 x 1.22	15	1.52	4.57	724
7	-	at face	2.74 x 4.57 x 1.22	15	0.31	2.13	724
8	?	above face	0.91 x 4.57 x 1.22	5	0	0.91	724

Table A.1 Details of Outbursts From No. 26 Colliery [2,13]

EVENT NO.	DATE	LOCATION	DIRECTION OF DRIVE	TRIGGER MECHANISM	ARCHES DOWN OR DAMAGED	ROCK TYPE EJECTED	BURST ACCOMPANIED BY GAS
9	Sept. 21, 78	13 South Material Level	East	Shot in coal and stone	0	Sandstone	No gas reported
10	Jan. 24, 79	13 North Material Level	West	Not recorded	0	Sandstone*	-
11	Jan. 30, 79	13 North Material Level	West	Not recorded	0	Sandstone	-
12	Feb. 8, 9, 10, 79	13 North Material Level	West	Not recorded	0	Sandstone	No gas reported
13	Oct. 23, 80	Main Deep	North	Shot in coal and stone	4	Sandstone	20 min to clear
14	Oct. 30, 80	Main Deep	North	Shot in stone	12	Sandstone	5% after shooting, 0.5% after shift
15	Mar. 5, 81	14 North Coal Road	West	Shot in coal	0	Sandstone and coal	3%, 5 min to clear
16	Mar. 9, 81	14 North Coal Road	West	Shot in coal and stone	0	Sandstone	4% after shooting

* Sandstone exhibiting cleavage character but no serious roof control problem

Table A.1 Details of Outbursts From No. 26 Colliery [2.13]

EVENT NO.	VOLUME OF GAS (m ³)	POSITION OF BURST	DIMENSIONS OF CAVITY (m) L x W x H	ESTIMATED VOLUME OF CAVITY (m ³)	SANDSTONE HEIGHT ABOVE COAL (m)	ADVANCE SINCE LAST FALL (m)	DEPTH BELOW SEA LEVEL
9	-	above face	0.91 x 4.57 x 1.22	5	0	14.93	724
10	-	-	-	-	1.83	-	703
11	-	-	-	-	1.22	-	703
12	-	-	6.09 x 4.26 x 1.83 6.09 x 4.26 x 1.52 6.09 x 4.26 x 3.65	-	0.30	-	703
13	?	above face and ribs	7.62 x 5.79 x 2.4	107.6	0	-	782
14	?	above face and ribs	10.66 x 6.09 x 2.74	178	0	6.09	782
15	?	ahead of face and ribs	L x H = 2.39 m ² W = 4.26 m	10	0	first	777
16	?	at face	--- included above ---	---	0	2.13	777

Table A.1 Details of Outbursts From No. 26 Colliery [2.13]

EVENT NO.	DATE	LOCATION	DIRECTION OF DRIVE	TRIGGER MECHANISM	ARCHES DOWN OR DAMAGED	ROCK TYPE EJECTED	BURST ACCOMPANIED BY GAS
17	Mar. 23, 81	14 North Coal Road	West	Shot in coal and stone	4 down	Sandstone	+ 5%, 25 min to clear
18	Mar. 25, 81	14 North Coal Road	West	Not recorded initiation	0	Sandstone	not recorded
19	Apr. 3, 81	14 North Coal Road	West	Unknown	0	Sandstone	No gas reported
20	Apr. 7, 81	14 North Coal Road	West	Unknown	0	Sandstone	No gas reported**
21	Apr. 14, 81	14 North Coal Road	West	Shot in stone	0	Sandstone	5%, 15 min to clear
22	Apr. 27, 81	14 North Coal Road	West	Shot in coal and stone	Unknown	Sandstone	5%, 10 min to clear
23	May 4, 81	14 North Coal Road	West	Shot in coal	1 damaged	Sandstone	5%, 20 min to clear
24	May 7, 81	14 North Coal Road	West	NIL***	1 damaged	Sandstone	3%, 45 min to clear

** 3% gas concentration noted on material level by inside regulator doors on following shift

*** Had nine holes stemmed when brushing face came in, no time to shoot

Table A.1 Details of Outbursts From No. 26 Colliery [2,13]

EVENT NO.	VOLUME OF GAS (m ³)	POSITION OF BURST	DIMENSIONS OF CAVITY (m) L x W x H	ESTIMATED VOLUME OF CAVITY (m ³)	SANDSTONE HEIGHT ABOVE COAL (m)	ADVANCE SINCE LAST FALL (m)	DEPTH BELOW SEA LEVEL
17	?	at face	L x H = 3.45 m ² W = 2.66 m	9	0	2.13	777
18	?	above face	--- included above ---	---	0	0	777
19	-	above face	L = 1.76 m W x H = 2.75 m ²	5	0	5.48	777
20	-	above arch	L x H = 0.276 m ² W = 4.26 m	1	0	3.05	777
21	?	at face	L x H = 4.26 m ² W = 8.53 m	37	0	6.70	777
22	?	at face	L = 1.82 m W x H = 14.40 m ²	27	0	7.90	777
23	?	at face	L x H = 7.04 m ² W = 6.70 m	43	0	4.26	777
24	?	at face	L x H = 11.13 m ² W = 6.62 m	67	0	2.44	777

Table A.1 Details of Outbursts From No. 26 Colliery [2.13]

EVENT NO.	DATE	LOCATION	DIRECTION OF DRIVE	TRIGGER MECHANISM	ARCHES DOWN OR DAMAGED	ROCK TYPE EJECTED	BURST ACCOMPANIED BY GAS
25	May 12, 81	13 North Airway	South	Shooting	0	Sandstone	2 - 2.4% after shooting
26	May 14, 81	14 North Coal Road	West	Shot in Coal	2 down 2 damaged	Sandstone	5%, 40 min to clear
27	June 6, 81	14 North Coal Road	West	Shot in coal	2 damaged	Sandstone	5%, 35 min to clear
28	June 10, 81	14 North Airway	North	Shot in coal and stone	3	Sandstone	5%, 15 min to clear
29	June 19, 81	14 North Coal Road	West	Shot in coal and stone	4 down	Sandstone	5%, 20 min to clear
30	June 26, 81	14 North Coal Road	West	Shot in stone	3 down	Sandstone	5%, 20 min to clear
31	July 14, 81	14 North Airway	North	Shot in stone	2 down	Sandstone	5%, 15 min to clear
32	Nov. 10, 81	14 North Coal Road	West	Shot in coal	0	Sandstone	5%, 25 min to clear

Table A.1 Details of Outbursts From No. 26 Colliery [2.13]

EVENT NO.	VOLUME OF GAS (m ³)	POSITION OF BURST	DIMENSIONS OF CAVITY (m) L x W x H	ESTIMATED VOLUME OF CAVITY (m ³)	SANDSTONE HEIGHT ABOVE COAL (m)	ADVANCE SINCE LAST FALL (m)	DEPTH BELOW SEA LEVEL
25	?	-	?	?	0.6	-	741
26	?	at face	L x H = 15.27 m ² W = 5.25 m	81	0 - 0.4	4.26	777
27	?	at face	L = 4.57 m W x H = 4.39 m ²	20	1.04	6.09	777
28	?	above face	4.57 x 4.26 x 3.04	59	1.52	first	745
29	?	at face	L x H = 1.93 m ² W = 5.86 m	11	1.52	7.92	776
30	?	at face	L = 2.74 m W x H = 9.89 m ²	27	1.52	3.05	776
31	?	above face	3.05 x 4.26 x 2.44	32	.91	17.68	776
32	?	above face	L x H = 6.49 m ² W = 3.65 m	24	2.28	18.29	776

Table A.1 Details of Outbursts From No. 26 Colliery [2.13]

EVENT NO.	DATE	LOCATION	DIRECTION OF DRIVE	TRIGGER MECHANISM	ARCHES DOWN OR DAMAGED	ROCK TYPE EJECTED	BURST ACCOMPANIED BY GAS
33	Dec. 7, 82	Belt Deep	North	Shot in stone and coal	1 damaged	Sandstone	1.5% after shooting
34	Jan. 11, 83	Belt Deep	North	Shot in stone and coal	0	Sandstone	2.65%, 25 min to clear
35	Jan. 19, 83	Belt Deep	North	Shot in stone and coal	7 down	Sandstone	5%, 60 min to clear
36	Nov. 23, 83	Main Deep	North	Shooting	16-18 down	Sandstone	5% after shooting
37	Jan. 6, 84	Main Deep	North	Shooting 12 holes in coal and ribs	15 down	Sandstone	Yes

Table A.1 Details of Outbursts From No. 26 Colliery [2,13]

EVENT NO.	VOLUME OF GAS (m ³)	POSITION OF BURST	DIMENSIONS OF CAVITY (m) L x W x H	ESTIMATED VOLUME OF CAVITY (m ³)	SANDSTONE HEIGHT ABOVE COAL (m)	ADVANCE SINCE LAST FALL (m)	DEPTH BELOW SEA LEVEL
33	?	above face	2.13 x 3.65 x 2.13	17	2.28	?	789
34	?	above face	?	14	2.28	first	789
35	?	above face	4.57 x 4.88 x 3.05	68	1.52	?	789
36	753	above face, and west side rib	Variable	316	0.6 - 2.74	first	789
37	3171	above face, west & east side ribs	Variable	145	0	3.65	790

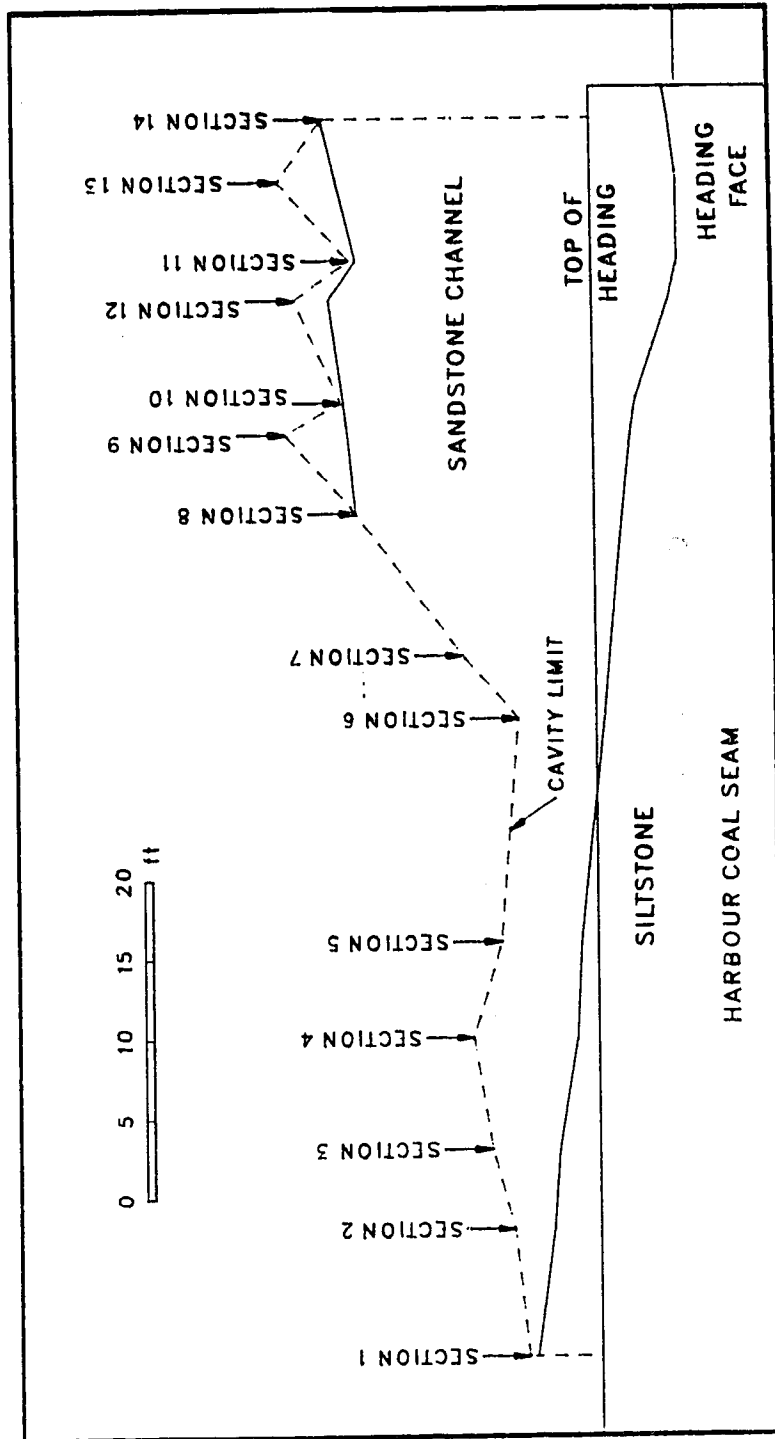
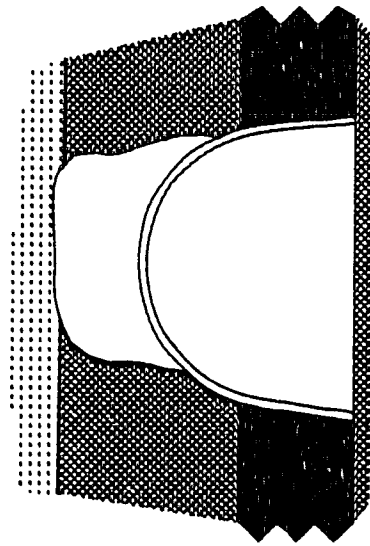
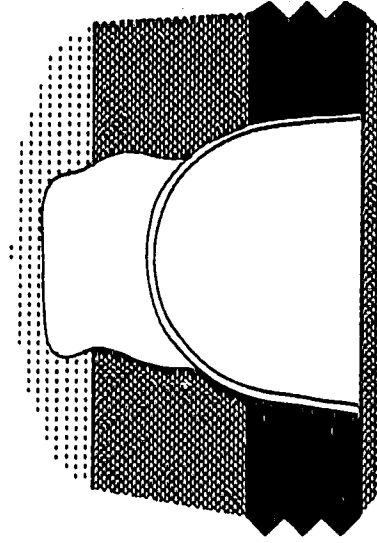


Figure A.1 Longitudinal-Section of the Cavity from Outbursts # 36 and # 37



SECTION 1

Intersection with cross-cut
Cavity Area = 56 sq.ft.



SECTION 2

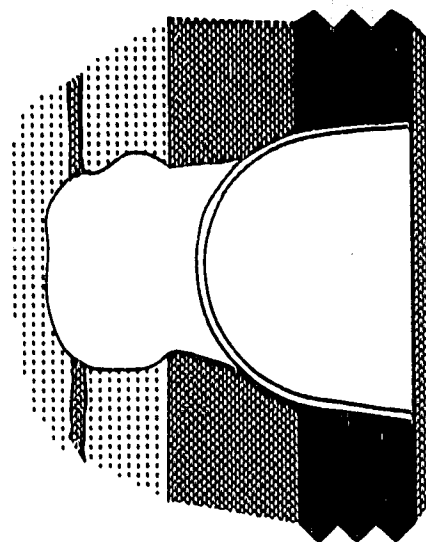
8 feet from cross-cut
Cavity Area = 63 sq.ft.



- SANDSTONE
- SILTSTONE
- COAL

Figure A.2a
(after [2])

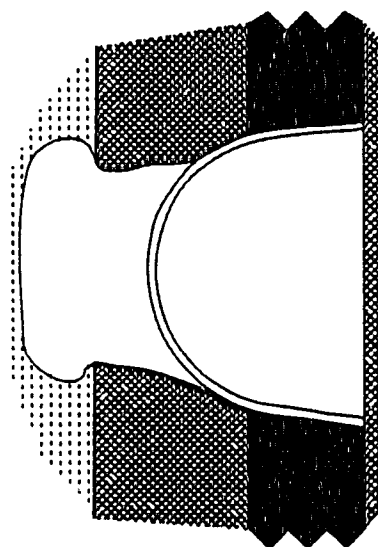
Figure A.2b
(after [2])



SECTION 4

20 feet from cross-cut
Cavity Area = 87 sq. ft.

Figure A.2d
(after [2])



SECTION 3

13 feet from cross-cut
Cavity Area = 80 sq. ft.

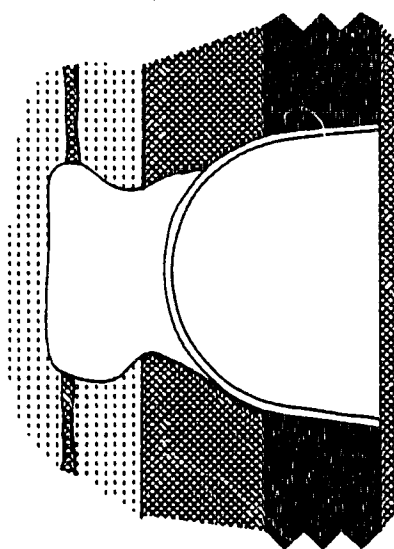
Figure A.2c
(after [2])



SANDSTONE

SILTSTONE

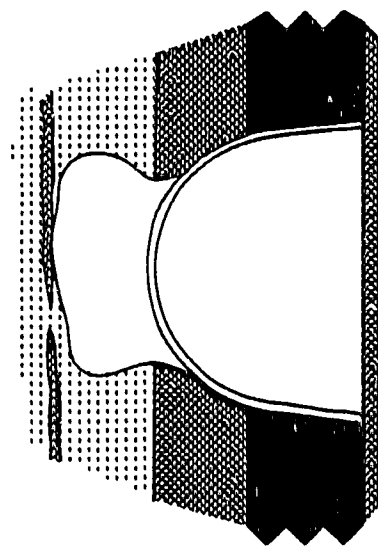
COAL



SECTION 5

26 feet from cross-cut
Cavity Area = 67 sq.ft.

Figure A.2e
(after [2])



SECTION 6

40 feet from cross-cut
Cavity Area = 55 sq.ft.

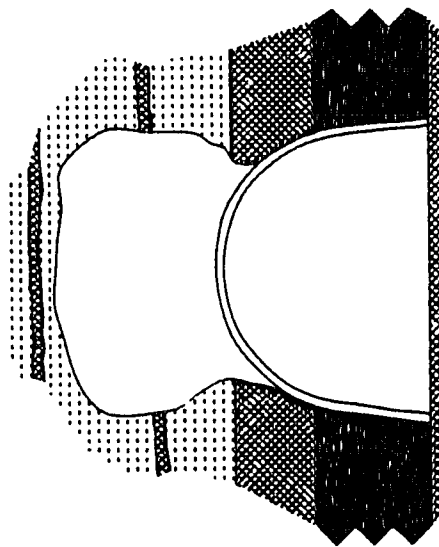
Figure A.2f
(after [2])



SANDSTONE

SILTSTONE

COAL



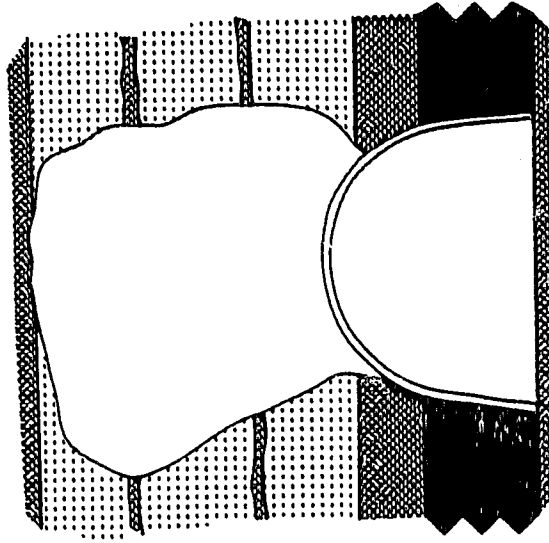
SECTION 7

44 feet from cross-cut
Cavity Area = 116 sq. ft.

Figure A.2g
(after [2])



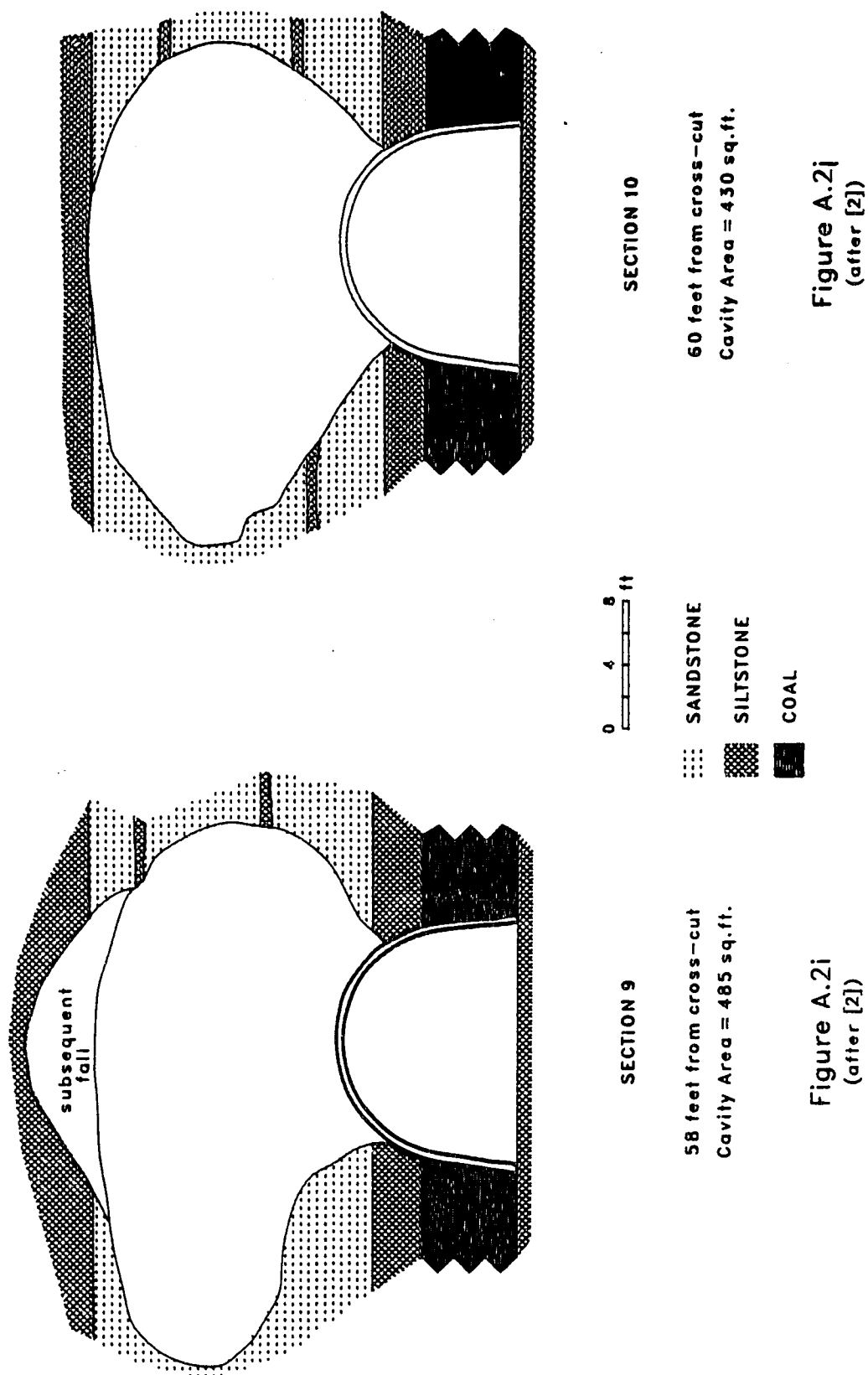
- SANDSTONE
- ▨ SILTSTONE
- COAL

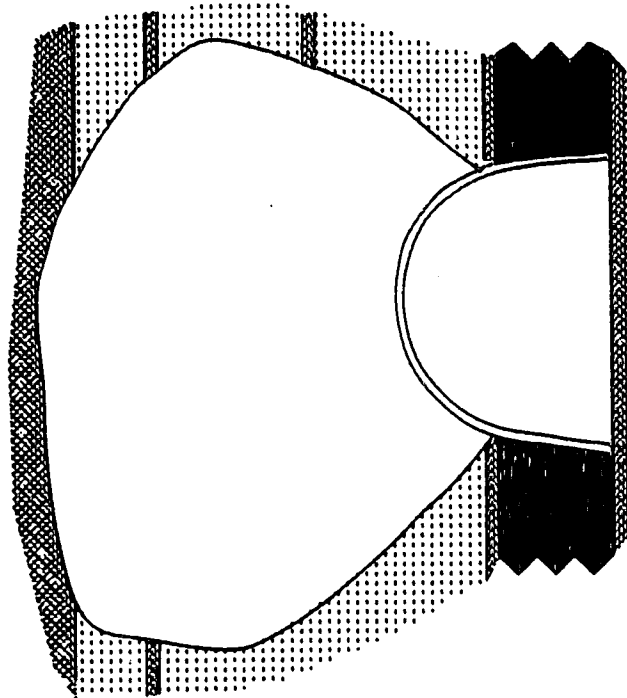


SECTION 8

53 feet from cross-cut
Cavity Area = 253 sq. ft.

Figure A.2h
(after [2])





SECTION 12

66.5 feet from cross-cut
Cavity Area = 542 sq. ft.

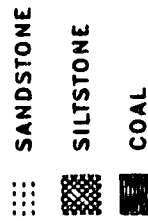
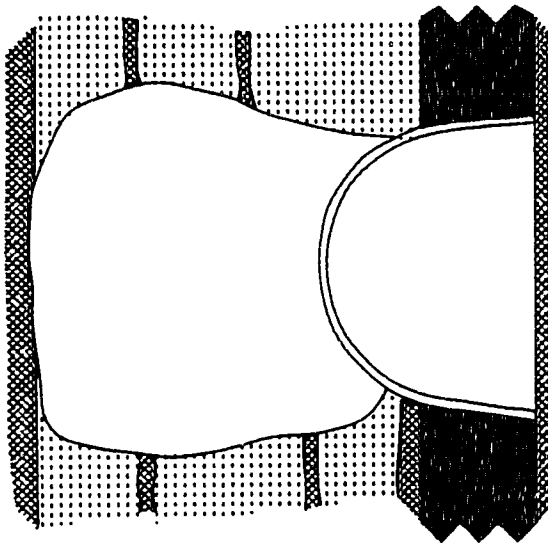


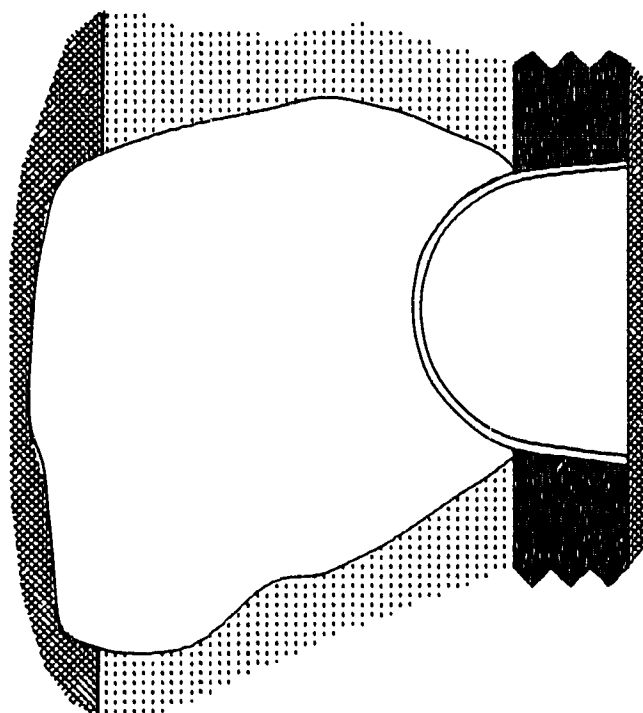
Figure A.2l
(after [2])



SECTION 11

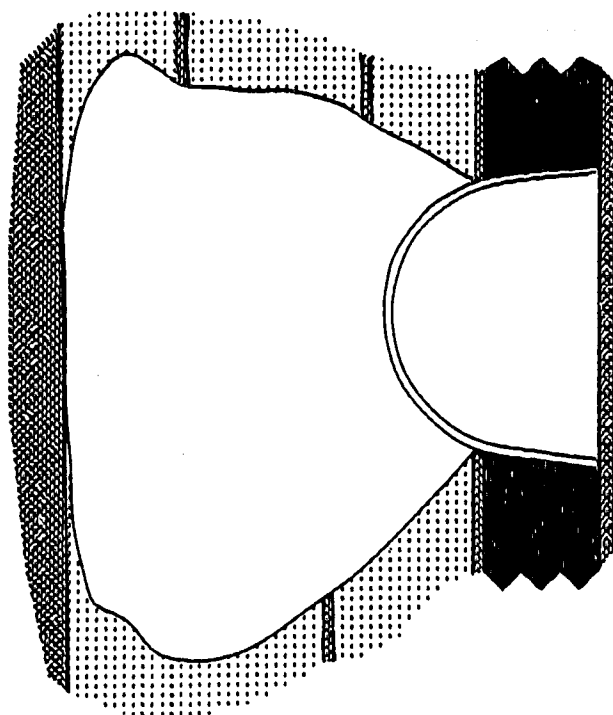
69 feet from cross-cut
Cavity Area = 279 sq. ft.

Figure A.2k
(after [2])



SECTION 13

74 feet from cross-cut
Cavity Area = 518 sq. ft.



SECTION 14

78 feet from cross-cut
Cavity Area = 490 sq. ft.

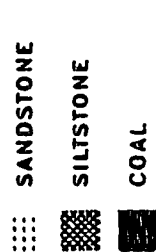


Figure A.2n
(after [2])

Figure A.2m
(after [2])

Appendix B - Insitu Strata Gas Pressures

Packer Test [17]

A packer test was done to attempt to quantify the insitu gas pressure within the sandstone. The test borehole was located between the main and belt deeps, north of the 14 N/S Longwall panels as shown in Figure 5.1, page 24. The borehole was drilled parallel to the deeps and inclined 11° to the horizontal. Discing of the drill cores occurred in several sandstone horizons, indicating spalling and bursting failures were possible in those beds.[39]

To ensure that the measurements were taken in 'undisturbed' ground, the test was conducted at least three tunnel diameters into the rock. Factors that could have affected the equilibrium pressure in the sealed length of the borehole are:

- distance from the test area to the nearest development opening
- seals of equipment, couplings and fittings
- pressure losses due to:
 - a. leakage between the seals and the strata
 - b. leakage through intact wall rock to the unsealed portion of the borehole
 - c. leakage through fracture induced in the strata by drilling
- insitu strata gas pressure

Packers were installed immediately after drilling. The glands (seals) were pressurized to 7.93MPa; after five days, the gland pressure had reduced to 7.72MPa but no pressure build-up had occurred in the test cavity.

It was then decided to inject nitrogen into the cavity to a pressure of 3.45MPa and observe the pressure dissipation. The pressure decreased over the first eight days to 2.62MPa. There it remained for seven days and then increased to 2.76MPa where it stayed through the remainder of the test (to day 45). Figure B.1 shows a plot of the pressure readings.

After the test was completed, gas samples were collected from the test cavity and analyzed. The following constituents were found:

CH ₄	6.5%
O ₂	0.98%
CO	8ppm
N ₂	92.52%

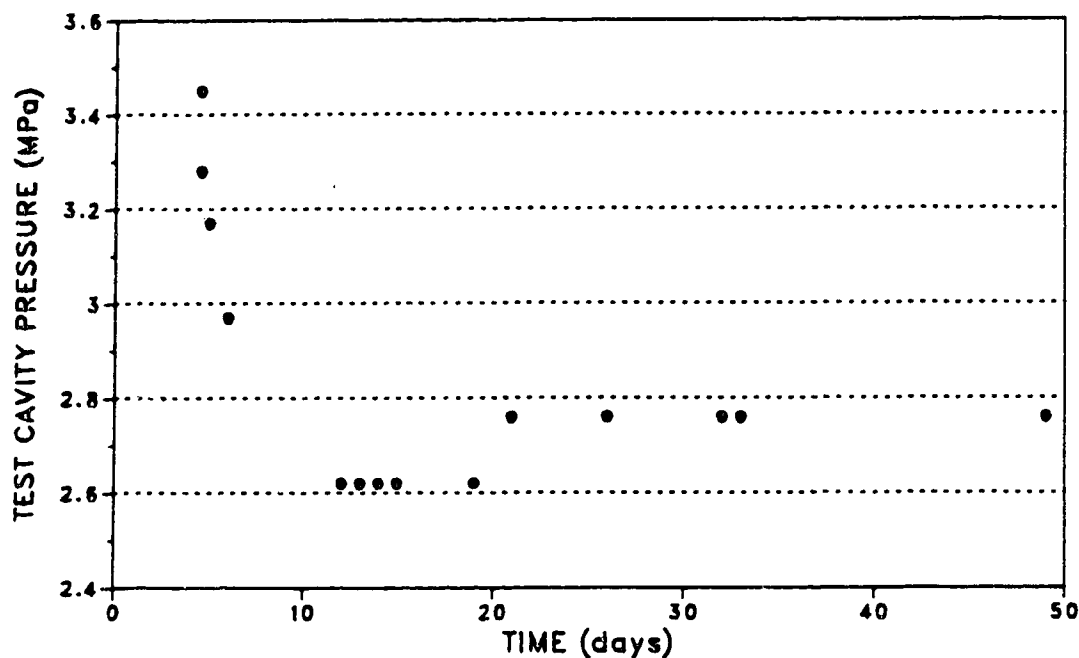


Figure B.1 Test Cavity Pressure During Packer Test (after [17])

Laboratory tests were conducted on the packer equipment and it was discovered that the system leaked gas. The equilibrium pressure of 2.76MPa may have approximated a steady state condition where the leakage around the glands was offset by the gas injection from the strata. The test cavity pressure could also have been in equilibrium with the sandstone gas pressure alone, in which case the insitu gas pressure was 2.76MPa. In either case, the insitu gas pressure must be at least the observed equilibrium value. From the analysis of the gas in the test cavity, only 6.5% was methane. If the system was in equilibrium between strata gas and leakage for 29 days, the strata gas (primarily methane) should, in the author's opinion, be at a much greater proportion than that observed. Therefore, the strata gas pressure could be considered to be approximately 2.76MPa at that point.

Back Analysis with Ideal Gas Law

Aston [3] used the ideal gas equation ($pV=nRT$) in a back analysis in an attempt to determine the insitu gas pressure that must have existed to have evolved the observed increases in methane emissions. Based on the information recorded in Appendix A for the final two outbursts (the volume of rock ejected and the amount of gas associated with it) the pressure of the gas was estimated. Volumes of ejected gas were determined from measurements of percent methane in the return airway and ventilation velocity as shown in Figure B.2.

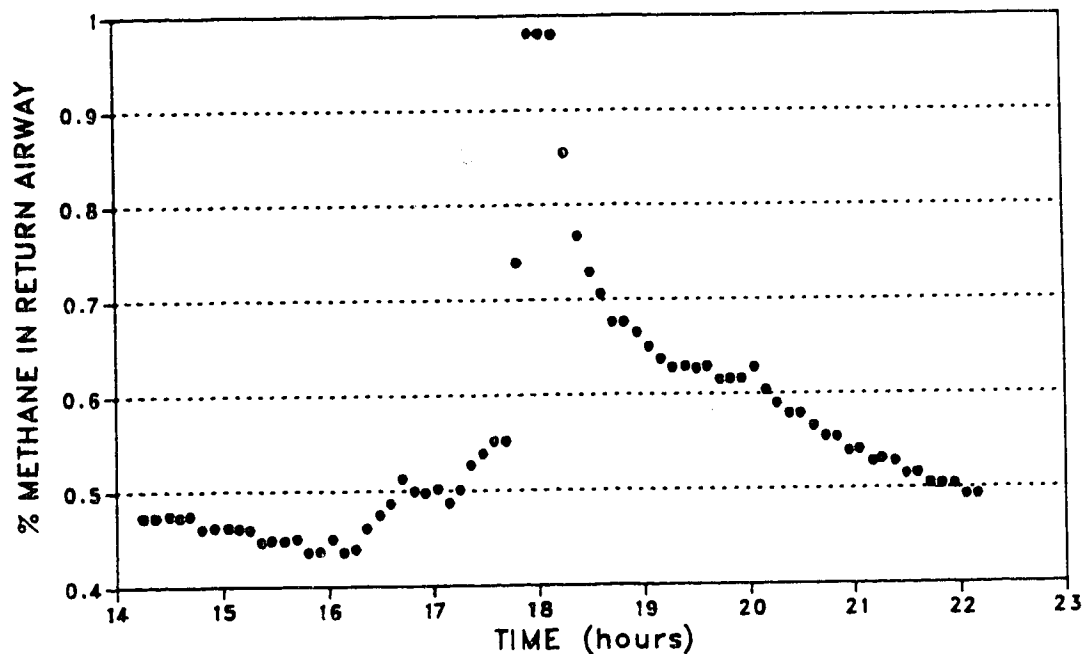


Figure B.2 Methane Content in Return Airway at the Time of Outburst No. 37 (after [2,18])

The analysis carried out in this report was based on the gas collected from the packer test cavity, which was originally pressurized with pure nitrogen, explaining the high content of this gas. The gas mixture noted in the previous section was not indicative of the insitu gas composition involved in the outbursts. The calculations carried out in the report will, however, be noted here.

The ideal gas equation can be modified to account for the compressibility of nonideal gases to give the form $pV=nzRT$. Following the procedure set out by Smith [49] in example 2-5 and accompanying tables, the following table was completed.

GAS COMPONENT	WEIGHT FRACTION	MOLECULAR WEIGHT	moles/lb
N ₂	0.9252	28.013	0.03303
CH ₄	0.0650	16.043	0.00405
O ₂	0.0098	32.000	0.00031*
CO	0.000008	28.000	0.0000003
	1.0000		0.03739

* corrected from Aston

$$\text{Molecular Weight} = \frac{\text{weight}}{\text{moles}} = \frac{1.0000}{0.03739} = 26.748$$

$$\text{Specific Gravity } (\gamma_r) = \frac{\text{mol. weight of gas}}{\text{mol. weight of air}} = \frac{26.748}{28.964} = 0.924$$

From tables provided by Smith, the compressibility of the gas (z) is 0.841. The variables n, R and T are constant for the cases of liberated gas and gas under pressure in the sandstone. From this, the two above mentioned cases can be equated to find the reservoir gas pressure.

$$\frac{p V}{z} = \frac{p' V'}{z'} \quad \text{where}$$

- p' = atmospheric pressure
- V' = measured volume of gas emitted (from Table A.1)
- z' = 1.0
- p = insitu strata gas pressure
- V = sandstone pore volume occupying gas
- = V_r * (porosity) * (1 - S_w)
- V_r = volume of rock ejected (from Table A.1)
- S_w = water saturation (assume 2%)
- z = compressibility of strata gas

For event no. 36:

- p' = 15 psi
- V' = 26500 ft³
- V = 519 ft³
- z = .841

therefore, p = 644 psi or, p = 4.44 MPa

For event no. 37: $p' = 15$ psi
 $V' = 113000$ ft³
 $V = 260$ ft³
 $z = .841$

therefore, $p = 5483$ psi or, $p = 37.8$ MPa

Golder Associates [18] report the strata gas composition to be the following:

CH ₄	75 - 80%
N ₂	≈ 10%
C ₂ H ₆	5 - 10%
other hydrocarbons and CO ₂	2 - 5%

Estimating the composition based on these numbers, the following table has been completed to find the compressibility of this mixture as above.

GAS COMPONENT	WEIGHT FRACTION	MOLECULAR WEIGHT	moles/lb
CH ₄	0.75	16.043	0.04675
N ₂	0.10	28.013	0.00357
C ₂ H ₆	0.10	30.070	0.00333
CO ₂	0.05	44.009	0.00114
	<u>1.00</u>		<u>0.05479</u>

$$\text{Molecular Weight} = \frac{\text{weight}}{\text{moles}} = \frac{1.0000}{0.05479} = 18.252$$

$$\text{Specific Gravity } (\gamma_r) = \frac{\text{mol. weight of gas}}{\text{mol. weight of air}} = \frac{18.252}{28.964} = 0.630$$

from tables provided by Smith, the compressibility of the gas (z) is 0.9294. The strata gas pressure can now be recalculated and was found to be 4.91MPa and 41.78MPa for events 36 and 37 respectively.

Other Estimates on Gas Pressure

Paterson [42] states that the natural gas reservoir formation pressure is expected to be about 23kPa per meter of depth below surface. At the deepest outburst at No. 26 colliery (780m) the estimated gas pressure would be almost 18MPa. This value is probably still too high an estimate as it is several times greater than the tensile strength (Tables C.2a and C.8).

A reservoir engineering rule of thumb is to estimate gas pressures based on the pressure produced by a hydrostatic column of water. This would give an insitu gas pressure of 7.9MPa. Aston and Cair [4] estimate that the most likely range for the gas pressure to be 2.8MPa to 7.9MPa.

Summary

Results from the packer test indicate an insitu gas pressure in the order of 3MPa. This test was conducted in disturbed ground, giving the strata gas time to bleed off between the time of driving the headings and conducting the test.

Back analysis of aquired data produced results of gas pressures ranging from 4.91 to 41.78MPa. Much uncertainty remains about the latter value due to the unreliability of data. A gas pressure of 42MPa far exceeds insitu stress values, and if a pocket of gas at this pressure were present, the pressure pocket would have blown out long before the initiating blast was fired. All that can be said about the gas pressure at this event is that it was high, but it would be unrealistic to put a value to it.

It has been stated by many [42,38] that for an outburst to occur, the effective stress must exceed the uniaxial tensile strength of the rock. Therefore, if we assume that the minimum principal stress is greater than or equal to zero, the gas pressure must be at least equal to the tensile strength of the rock. Therefore, for the purposes of the model presented here, the gas pressure must be at least 2.4MPa (the tensile strength of sandstone chosen for the model). The upper limit of possible gas pressures depends on field stresses and the extent of fracturing around the outburst cavity allowing degassing of that zone. The best estimate is a gas pressure between 2.4MPa and about 10MPa.

Appendix C - Rock Properties

Gorski [22]

Gorski conducted laboratory tests on cores taken from siltstone and sandstone in No. 26 Colliery. The tests consisted of two uniaxial, two triaxial tests, two porosity, two constant head water permeability and one transient pulse water permeability tests. Table C.1a gives the borehole location for these samples, however, these borehole locations could not be identified in terms of location within No. 26 Colliery. The following tables (Tables C.1b,c,d) contain the results of these tests.

In addition to the above mentioned permeability tests, samples were reported to have been tested in a confined state. This was done to simulate the insitu overburden pressure of approximately 24MPa. Although no results are reported, it was concluded the stress relief increases the permeability of the sandstone.

Table C.1a Sample Dry Densities (after [22])

TYPE OF SAMPLE	LOCATION	TYPE OF TEST	DENSITY (g/cm ³)
siltstone	BH5-1	uniaxial	2.7
sandstone	BH4-2	uniaxial	2.5
siltstone	BH5-1	triaxial	2.7
sandstone	BH5-3	triaxial	2.5
siltstone	BH5-1	porosity	2.7
sandstone	BH5-3	porosity	2.5
siltstone	BH5-1	permeability	2.7
sandstone	BH4-2	permeability	2.5

Table C.1b Uniaxial and Triaxial Tests (after [22])

SAMPLE	COMPRESSIVE STRENGTH (MPa)	ELASTIC MODULUS (GPa)	PEAK STRENGTH (MPa)	CONFINING PRESSURE (MPa)	PEAK STRAIN (%)
siltstone	82.31	25.48	172.15	24.13	0.68
sandstone	85.31	20.16	284.86	24.13	1.26

Table C.1c Porosity Test (after [22])

SAMPLE	POROSITY (%)	PORE DIAMETER* (μ)
sandstone	4.7	0.08 - 0.35
siltstone	less than 0.146	less than 0.01

* using the Washburn equation

$$D = \frac{-4 S \cos \theta}{P}$$

D = Pore diameter (Microns)

S = Surface tension of mercury (474 dynes/cm² at 25°C)

θ = Contact angle of mercury (130°)

P = Applied pressure

Table C.1d Constant Head Permeability Tests (after [22])

SAMPLE	END AREA (cm ²)	LENGTH (cm)	P ₁ -P ₂ (atm)	FLOW RATE (cm ³ /sec)	PERMEABILITY* (nanodarcies)
sandstone	14.576	4.103	102.07	0.195x10 ⁻³	500
			119.08	0.239x10 ⁻³	500
			136.09	0.287x10 ⁻³	500
siltstone	15.178	4.042	102.07	0.6x10 ⁻⁶	1.4**
			119.08	0.3x10 ⁻⁶	0.65**
			136.09	0.4x10 ⁻⁶	0.76**

* based on Darcy's law of water permeability

$$k = \frac{\mu Q L}{A (P_1 - P_2)}$$

k = permeability (darcies)

μ = viscosity of water (0.9761 centipoise)

Q = incompressible liquid volume flow rate (cm³/sec)

L = length of core sample (cm)

A = cross-sectional area (cm²)

P₁-P₂ = pressure difference into and out of the sample (atmospheres)

** With such low values, permeability would probably be less than that stated. The transient pulse test was used to check these low readings. The only conclusion stated was that the siltstone is virtually impermeable to water and the permeability is less than 1 nanodarcy.

Table C.2a Strengths and Elastic Properties of D-164 Cores (after [2,13])

SAMPLE	ROCK TYPE	TENSILE STRENGTH (MPa)	COMPRESSIVE STRENGTH (MPa)	ELASTIC MODULUS (MPa)	POISSON RATIO
D164-1	silty mudstone	12.3	-	-	-
D164-2	silty mudstone	-	38.59	28,621	0.30
D164-3	sandstone	2.62	-	-	-
D164-4	sandstone	-	82.16	17,034	0.28
D164-5	sandstone	3.97	72.55	12,897	0.18
D164-6	siltstone	11.49	-	-	-
D164-7	sandstone	6.54	-	-	-
D164-8	sandstone	-	109.60	20,897	0.17
D164-9	sandstone	8.04	-	-	-
D164-10	sandstone	7.74	59.32	16,552	0.09
D164-11	siltstone	12.70	50.52	26,897	0.36
D164-12	mudstone	7.88	29.77	28,966	0.25

Table C.2b Porosity and Permeability of D-164 Cores (after [2,13])

SAMPLE	ROCK TYPE	POROSITY (%)		PERMEABILITY (md)	
		vertical	horizontal	vertical	horizontal
D164-PP-1	siltstone	1.9	1.4	< 0.01	< 0.01
D164-PP-2	sandstone	5.5	5.6	0.03	0.03
D164-PP-3	sandstone	4.7	5.7	0.02	0.05
D164-PP-4	siltstone	0.7	0.8	< 0.01	< 0.01

Coal Strengths [5]

During driveage of the No. 2 Tunnel in the Harbour seam of Donkin-Morien mine, coal samples were collected and tested to build up a data base of Sydney coalfield rock properties. This particular set of tests, conducted in early 1985, consisted of a series of point load index tests. A total of 107 tests were done; fifty parallel and fifty-seven perpendicular to bedding. Table C.3a summarizes these results.

Strengths were determined in the following manner. The point load index, I , was derived from $I=P/D^2$; where P is the point load (MPa) and D is the specimen diameter (mm). The reference diameter is 50mm; because a 54mm diameter core bit size was used, the size correction chart from the pit slope manual [44] was referred to. The following reported correlations (from Hassani [28]) of point load index strengths to compressive and tensile strengths were used:

$$\text{compressive strength: } \sigma_c = 29.24 I_{s4}$$

$$\text{tensile strength: } \sigma_t = 2.78 I_{s4}$$

Table C.3b shows how these values compare with values obtained from other mines in the Sydney Coalfield and the associated coal seams.

Table C.3a Strength of Harbour Seam Coal at Donkin-Morien (after [5])

DIRECTION TO BEDDING	No. OF SAMPLES	TENSILE STRENGTH (MPa)		COMPRESSIVE STRENGTH (MPa)	
		mean	st.dev.	mean	st.dev.
parallel	50	1.05	0.68	11.06	7.10
perpendicular	57	1.43	1.36	15.12	14.28

Table C.3b Strength of Coals From the Sydney Coal Field (after [5])

MINE SITE (SEAM)	DIRECTION TO BEDDING	INDEX STRENGTH $I_{s,4}$ (MPa)	UNIAXIAL COMP. STRENGTH (MPa)	TENSILE STRENGTH (MPa)	ANISOTROPY INDEX $I_{s,4}$
No. 26 (Harbour)	parallel	0.32	9.3	0.89	
	perpend.	0.46	13.5	1.28	1.44
Lingan (Harbour)	parallel	0.58	16.9	1.60	
	perpend.	1.23	35.8	3.41	2.13
Lingan (Harbour)	parallel	0.58	16.9	1.61	
	perpend.	1.22	35.7	3.39	2.10
Prince (Hub)	parallel	0.75	22.0	2.10	
	perpend.	0.41	12.0	1.14	0.54
NOVACO (Main)	parallel	0.26	7.6	0.72	
	perpend.	0.18	5.2	0.50	0.69
Donkin-Morien (Harbor)	parallel	0.38	11.0	1.05	
	perpend.	0.52	15.1	1.44	1.37

Carbon / Carbonate Content in Sandstone [9]

A free carbon / fixed carbon analysis was conducted on six sandstone samples collected at various locations in No. 26 Colliery. An attempt was made to correlate carbon content in sandstone with the outburst locations. Locations of these samples were not specified.

This analysis was based on CO_2 evolution when hydrochloric acid was reacted with carbonate compounds within the sandstone samples. Carbonate content was estimated based on the amount of carbon dioxide evolved, but the ratio of MgCO_3 to CaCO_3 was not known. By assuming the two extreme cases of all one form of carbonate or another, a range of possible percent contents was obtained. This was done based on the molecular masses of the components. Weight percent of CO_2 within MgCO_3 and CaCO_3 are 52.20% and 43.97% respectively. Results of these tests are found in Table C.4.

Table C.4 Test Results for Carbon / Carbonate Content in Sandstone (after [9])

SAMPLE No.	ORIGIN	% CO_2 $\pm 0.1\%$	THEORETICAL CARBONATE (%)	
			(100% MgCO_3)	(100% CaCO_3)
1	disced sandstone	1.4	2.7	3.2
2	burst sandstone	1.2	2.24	2.66
3	borehole sandstone	1.6	3.01	3.57
4	borehole sandstone	1.1	2.05	2.43
5	burst sandstone	0.8	1.51	1.79
6	burst sandstone	1.1	2.05	2.44

Results show no significant difference in the carbon / carbonate content in the burst prone sandstone and the ordinary sandstone that could contribute to the random occurrence of methane pressure pockets.

Proximate Analysis of Sandstone

Aston [3] reported results of a simple Proximate analysis conducted on disced, outburst and ordinary sandstone. This test is based on the weight loss of a sandstone sample due to oxidization of carbon and decomposition of MgCO_3 at 500°C and CaCO_3 at 1000°C . No details have been given on the location from which the samples were taken. Table C.5 contains these results.

Table C.5 Proximate Analysis on Outburst Prone Sandstone (after [3])

TYPE OF SANDSTONE	CARBON (%)	INORGANIC CARBON (%)	CARBONATE (%)
disced sandstone	1.40	1.60	
outburst sandstone	2.11	1.28	2.5 - 3.5
borehole sandstone	2.40	1.03	
	1.97	0.96	

Given an approximate carbon content of 60% for the Harbour coal seam, even if the amount of desorbed gas was $25\text{m}^3 \text{CH}_4/\text{tonne coal}$, carbonaceous material in the sandstone would have had to be as high as 6% for Event 36 and 51% for Event 37 to account for the volumes of gas released.

Rock Properties from the Donkin-Morien Project [19]

In the initial phase of the Donkin-Morien project, a tunnel research project was started to analyze rock behavior with various tunnelling methods. The study included field instrumentation and testing of the strata. Uniaxial compression and Brazilian tests were conducted on the surrounding strata, at depths less than 200m, from boreholes at various points along Tunnels No.2 and No. 3. Elastic modulus and Poisson's ratio were also derived from these tests. A summary of these tests are presented in Table C.6. The rock types noted in this table are as follows:

- I sandstone
- II interbedded sandstone/siltstone
- III siltstone
- IV interbedded siltstone/mudstone
- V mudstone

Table C.6 Strength and Elastic Properties of Various Rock Types from Donkin-Morien (after [19])

ROCK TYPE	σ_c (MPa)		σ_t (MPa)		E (GPa)		ν	
	range	mean	range	mean	range	mean	range	mean
I	44.9 \rightarrow 145.1	93.8	5.6 \rightarrow 9.6	7.5	13.8 \rightarrow 43.7	34.2	0.17 \rightarrow 0.38	0.25
II	47.9 \rightarrow 152.8	121.3	4.7 \rightarrow 11.9	9.0	6.6 \rightarrow 21.9	17.6	-	-
III	13.9 \rightarrow 68.5	53.6	1.9 \rightarrow 4.9	3.5	4.5 \rightarrow 25.3	11.3	-	-
IV	14.7 \rightarrow 62.9	35.8	2.3 \rightarrow 6.3	3.7	4.0 \rightarrow 15.0	9.0	-	-
V	30.9 \rightarrow 42.2	37.2	1.5 \rightarrow 6.0	3.5	8.8 \rightarrow 15.0	11.5	-	-

Borehole D-165 [20]

In early 1985, a series of tests were carried out on rock cores recovered from No. 26 and Lingan Collieries (only the results from the former will be presented). Three areas were to be addressed in this testing program which included:

1. the behaviour of rock under dynamic loading (stress changes) around underground openings
2. the effect of pore gas pressure on the rock strength and mode of failure under various stress conditions
3. failure behaviour under very fast stress changes

Figure 5.1, page 24, shows the location of this borehole in the mine. The orientation of the borehole is not given, however, in the rock type description given below, the bedding planes are parallel to 10° from the core axis. The following is the description of the various rock type found in the cores.

Class D - grey, homogeneous, medium grained sandstone

Class E - same as (D) with isolated pockets of siltstone and mudstone

Class F - alternating bedding of sandstone and siltstone/mudstone. Bedding is inclined approximately 10° to the core axis. The band widths of sandstone and siltstone are 1 to 3mm and 0.1 to 1mm respectively. Some sandstone bands were up to 20mm thick.

Class G - same as (F) with bedding almost parallel to core axis

The log for Borehole D-165 is summarized below. (This is the only description available and is taken from Golder Associates [20])

Horizon 1 2.84m to 5.89m

light grey sandstone; fine to medium grained; thickly bedded with finely laminated dark grey siltstone layers along bedding ranging from 12.7mm to 31.8mm thick. Micaceous. Plant fossils and silty pods. Uneven contact with overlying sandstone.

4.305 to 4.57m: discing - 105 discs/meter

4.57 to 4.87m: core missing

4.87 to 4.89m: discing - 113 discs/meter

Horizon 2 12.09m to 14.65m

laminite-interbedded sandstone/siltstone (65% sand & 35% silt grading up to 55% sand & 45% silt) fine grained, thinly bedded, finely laminated. Micaceous. Gradational contact with overlying siltstone.

Horizon 3 17.07m to 18.39m

medium dark grey siltstone, well bedded and finely laminated, sandy film along lamination. Sandy lenses prevalent throughout. Gradational contact with overlying siltstone. Pyritic. Irregular beds, diagenetic plastic deformation.

Table C.7a gives the depths and descriptions (using the two above systems) for the samples of this borehole. A complete log of the cores is not available.

The strength of the rock was found from a uniaxial and three triaxial tests conducted on four of the samples. Tables C.7b gives the results of these tests and the failure envelope is plotted in Figure C.7a.

It was found that the mode of failure was greatly dependent on the direction of the bedding planes with respect to the core axis. In the case where the two are parallel, axial splitting was observed during uniaxial loading. If the angle of bedding is 10° , axial cracks appear at the ends of the specimen, followed by shearing along a bedding plane. The triaxial tests resulted in failure along single shear planes coincident with the bedding planes of all samples; very little shearing occurred across beds of rock. Some samples failed prematurely due to spalling of a wedge at the ends of the cores.

The strength of the specimen were influenced greatly by their structure. The Lingan samples were also tested at various loading rates and no rate effect was observed. There was no significant difference in the strengths of the No. 26 samples from the various horizons.

Three different permeability tests (using nitrogen gas) were conducted at a range of confining pressures. The first was to find the permeability of sandstone under the following

conditions:

axial stress: $\sigma_a = 4.0$ MPa

radial stress: $\sigma_r = 7.0$ MPa

gas pressure: $P_g = 7.0$ MPa

Table C.7a Classification of Borehole D-165 Cores (after [20])

SAMPLE	DEPTH (m)	DESCRIPTION	
		PROJECT	LOG
D-165-1	3.188 → 3.277	D	Horizon 1
D-165-2	5.486 → 5.575	F	"
D-165-3	5.855 → 5.944	E	"
D-165-4	6.096 → 6.185	F	"
D-165-5	12.344 → 12.433	F	Horizon 2
D-165-6	12.586 → 12.675	F	"
D-165-7	12.675 → 12.764	G	"
D-165-8	12.764 → 12.852	F	"
D-165-9	12.891 → 12.979	F	"
D-165-10	12.979 → 13.068	F	"
D-165-11	13.068 → 13.157	F	"
D-165-12	13.157 → 13.246	F	"
D-165-13	13.335 → 13.424	F	"
D-165-14	13.424 → 13.513	G	"
D-165-15	13.602 → 13.691	F	"
D-165-16	13.691 → 13.780	G	"
D-165-17	13.780 → 13.868	F	"
D-165-18	17.297 → 17.437	F	Horizon 3

Table C.7b Strength of Borehole D-165 Cores (after [20])

SAMPLE No.	INITIAL STRESS LEVEL (MPa)		FAILURE STRESS LEVEL (MPa)		OBSERVED* FAILURE MODE
	σ_3	σ_1	σ_3	σ_1	
D165-12	0	0	0	49.0	AS,SAB
D165-15	10.0	10.0	10.0	118.0	S
D165-10	20.0	20.0	20.0	168.8	S
D165-9	30.0	30.0	30.0	206.3	S

*Modes of Failure: AC: Axial Cracks AS: Axial Splitting
 C: Conjugate planes S: Shear
 SAB: Shear along Bedding MS: Multiple Shear

Under these conditions, and with the gas pressure induced at the top of the sample, after 30 minutes the pressure reading at the bottom of the sample was only 0.07MPa. Forty-eight hours later the pressure had not changed, indicating an extremely low permeability.

The second test was to investigate the change in the permeability with the formation of small cracks in the within the sample. This was accomplished through the cyclic loading and unloading of the radial and axial stresses on the sample. The permeability of the sample did increase with continued cycling but the permeability was still low and restricted to the newly formed cracks. Permeability would only be affected appreciably if the cracking became extensive and interconnected. Also, as expected, the increase in the confining pressure decreased the effective permeability.

The third test consisted of determining the permeability of the sandstone under triaxial stresses at varying gas pressures. The results of these tests are shown in Table C.7c (the last two conditions measure the permeability of cracks induced into the specimen during loading).

One of the objectives of this research program was to observe the failure mechanism of the sandstone under induced pore gas pressures simulating insitu strata conditions. In the

earlier parts of this project, a reference sandstone, Pier Cap Sandstone (obtained locally), was tested for strength under various stresses and internal pore pressures. This rock failed quite violently because its higher porosity and permeability allowed internal pressures to be obtained that were significantly greater than that of the 'bursting' sandstones. The remains of this sandstone was reported to appear very much like the ejected sandstone from the No. 26 Colliery events. The sandstone samples taken from the mine did not exhibit this type of failure because high internal gas pressures could not be attained.

Table C.7c Gas Permeability Tests on Sample D-165-18 (after [20])

APPLIED STRESSES (MPa)			ΔP (atm)	Q (cm ³ /sec)	k* (md)
σ_1	σ_3	P			
10	10	6.9	68.1	-	0.0
30	10	6.9	68.1	-	0.0
30	10	11.0	108.2	-	0.0
50.3	10	7.1	70.1	0.076	11.9
50.3	20	7.1	70.1	0.065	10.2
50.3	25	7.1	70.1	0.060	9.42
62.8	10	6.1	60.2	0.072	12.0
62.8	10	7.0	69.1	0.085	13.4
62.8	20	7.0	69.1	0.073	11.5
62.8	25	7.0	69.1	0.056	8.86

* based on Darcy's law

$$k = \frac{\mu Q L}{A \Delta P}$$

k = permeability (darcies)

μ = viscosity of N₂ (centipoise; varies with applied pressure)

Q = flow rate of nitrogen (cm³/sec)

L = length of core sample (14.3cm)

A = cross-sectional area (17.75cm²)

ΔP = pressure difference into and out of the sample (atmospheres)

The effect of rapid stress changes on the strength of the sandstone was investigated. Samples under a hydrostatic stress of 20.7MPa were observed when the axial stress was increased simultaneously with the decrease of the radial (confining) stress. The rate of increase of σ_1 was kept constant at 43.7MPa/s while the decrease in σ_3 was varied from 0.4 to 32MPa/s. A gas pressure of 7 to 9MPa was applied to the top of the samples during testing. At failure, only five of ten samples showed a gas pressure at the bottom of the samples and of those, only two had pressures in excess of 1MPa. Results are shown in Table C.7d and Figure C.7b. The failure of the samples usually occurred along bedding planes and the more homogeneous the samples, the greater their strength.

"Results of the triaxial tests indicated that none of the samples failed close to the tensile region despite the fact that 7 to 9 MPa of gas pressure was applied at the top of the end of the sample. While the results of the gas permeability tests showed that the permeability of the sample could be increased upon the formation of microcracks within the specimen, the results of this series of tests illustrated that the gas pressure within the sample was insufficient to cause tensile fracture of the specimen. It is believed that gross failure of the sample took place even before the formation of a system of induced microcracks that were sufficiently extensive to allow increased gas permeation. The high loading rate used obviously did not enhance the flow of gas through the sample." (after [20], pp. 23)

Four samples from Lingan Colliery were uniaxially tested with gas pressures being applied at one and both ends of the samples. In the cases of one end under pressure, failure occurred at that end; in the specimen with applied pressure at both ends, failure was more uniform throughout the sample. Tensile failure was noted in these three samples, however, since the gas was not permeated through the samples uniformly, the effective stresses in the samples was unknown. The fourth sample was preloaded to induce microcracking as with the No. 26 samples. This failed by axial splitting along one major fracture at the center and no spalling was observed. It was assumed that the gas permeated through this crack producing and a very nonuniform effective stress within the sample.

The conclusions drawn by Golder Associates with respect to this project are as follows:

1. Rock bursts were simulated in core samples only when the effective stresses became negative (failure with tensile stresses) where gas could be effectively introduced into the samples.
2. In the samples from borehole D-165, there was no clear distinction between the strengths of samples taken from discing and nondiscing sandstone beds.
3. Attempts at inducing a gas pressure into samples produced very irregular internal gas pressures. Uniform gas pressure distribution of the actual field condition could not be simulated in the laboratory.
4. The rapidly changing stress conditions of the samples (to simulate actual stress changes in the field due to excavation) decreased the strength of the sandstone. This occurred because the progressive decrease in confinement of the sample allowed accelerated dilation of the specimen with the onset of failure.
5. Strength of the specimen was dependent on the orientation of the bedding planes to the core axis. More homogeneous samples had higher strengths.

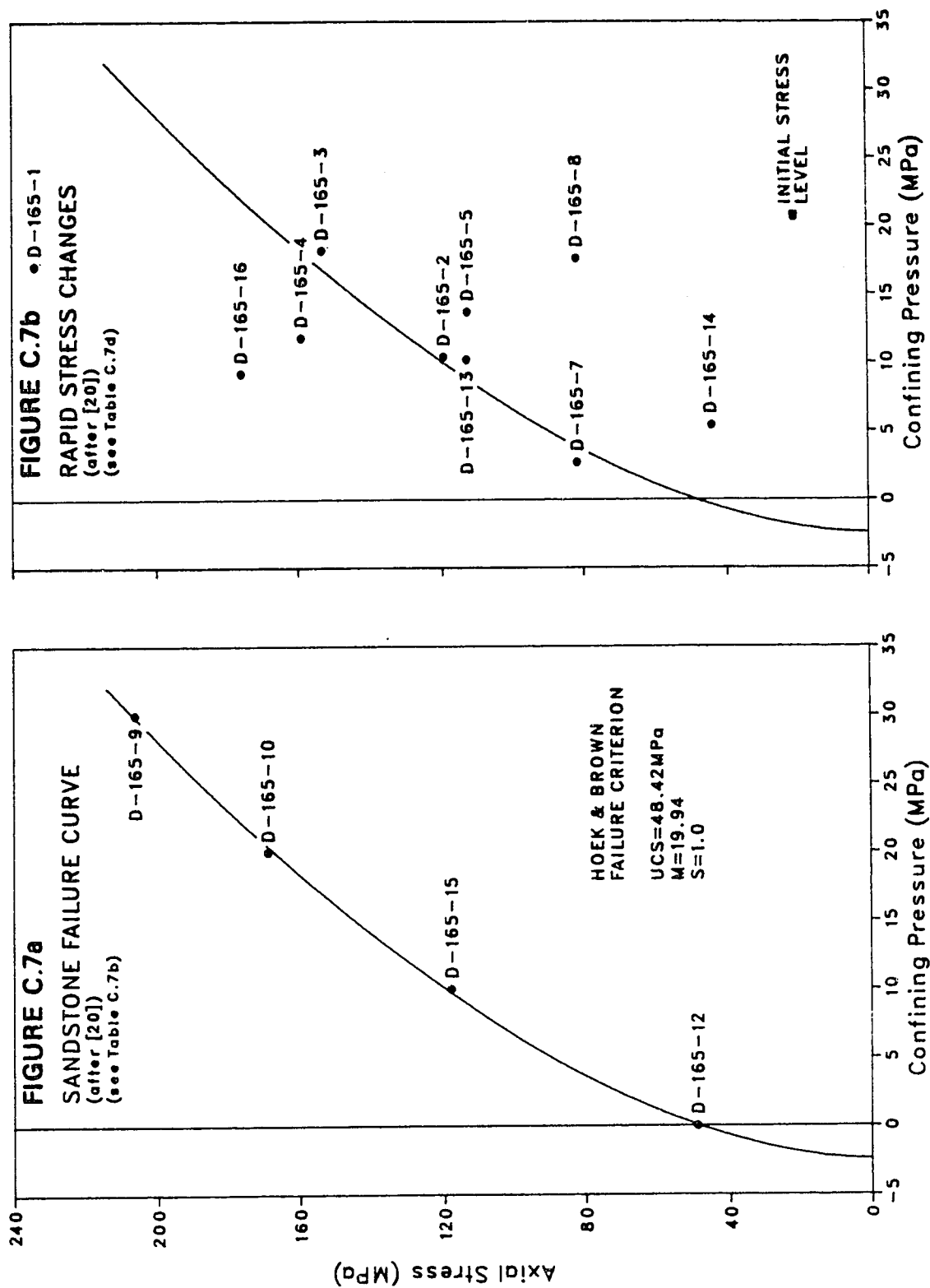


Table C.7d Stress Change Simulation Results (after [20])

SAMPLE No.	PORE GAS PRESSURE (MPa)		STRESSES AT FAILURE (MPa)		OBSERVED* FAILURE MODE	REMARKS
	Upstream	Downstream	σ_3	σ_1		
D-165-1	7.0	0.7	17.1	233.7	S,C,AC	
D-165-3	7.0	1.17	18.2	153.2	S,S	two shear planes along diagonal; one in sandstone (slickensides observed), one perpendicular along siltstone bedding
D-165-8	7.0	0.0	17.6	81.6	MS	approximately 5 shear planes along bedding
D-165-4	9.0	0.0	11.8	158.9	S,C,AS	very little siltstone
D-165-5	9.0	0.0	13.7	112.7	MS	approximately 7 shear planes along bedding
D-165-16	7.0	0.2	9.2	175.7	AS,AC	
D-165-2	7.0	0.4	10.4	119.4	MS	thick siltstone bedding
D-165-13	7.0	0.0	10.2	113.0	MS	
D-165-7	9.0	0.0	2.7	81.6	AS	
D-165-14	7.0	2.4	5.4	44.0	S,AS,AC	

* see Table C.7b for definition

Summary

Little information is available on the rock properties of interest and the data that has been collected produces highly variable rock strengths and elastic properties. This variability could be due to the fact that the tested cores were recovered from different bands of rock in the strata as illustrated in Figure C.2. However, no consistent trends have been found to account for this wide range of properties and these can only be attributed to natural variability. A wide range of properties has also been noted from the tests conducted on rocks from other mines.

The sandstone does have an exceptionally low porosity and permeability, and this has been consistent with all such tests conducted in all types of sandstone (burst, disced, and intact). The large amounts of methane trapped in the sandstone must be under a considerable pressure and does not bleed off at any significant rate (as noted in Appendix B) due to the low effective permeability. Tests for the carbon content in the sandstone indicate that the carbon in the sandstone is insufficient to sorb the amount of methane noted. There is also no significant variation in the carbon content in the burst, disced or intact sandstones.

Only one series of triaxial tests have been conducted on sandstones from No. 26 Colliery. A failure envelope was fitted for the siltstone based solely on the tensile and uniaxial compressive strengths. The same failure criterion (with appropriate parameters) is used for both materials. The failure envelope created from the triaxial tests is non-linear and the Hock and Brown [30] failure criterion fits the data remarkably well, as noted in Figure C.7a. The equation for this curve is:

$$\sigma_1 = \sigma_3 + \sqrt{(m\sigma_c\sigma_3 + s\sigma_c^2)}$$

where: σ_1 is the major principal stress at failure
 σ_3 is the minor principal stress at failure
 σ_c is the uniaxial compressive strength
 m and s are constants that depend on the degree to which the rock is broken.

Because the tests were conducted on intact cores, let $s=1.0$ and σ_c and m were determined by the least squares solution given by Hoek and Brown (Appendix 5 [19]).

Since no triaxial testing was done on the siltstone, a failure curve will have to be fitted based on tensile and uniaxial strengths alone. Of all the data collected from the sandstone, the failure envelope gives a low strength when compared to the uniaxial compression tests. This may be desirable when considering the variability of the material properties. A failure criterion for siltstone was also fitted with a lower than average strength for the same reason. A summary of the strength parameters is given in Table C.8; Figure C.8 compares the rock strength for siltstone and sandstone.

There is also considerable variation in the elastic properties of rock. Final values were chosen based on the means from the samples located in No. 26 Colliery, and are summarized in Table C.8.

Table C.8 Rock Properties

ROCK TYPE	FAILURE ENVELOPE				ELASTIC PROPERTIES	
	$\sigma_c(\text{MPa})$	$\sigma_t(\text{MPa})$	m	s	$E(\text{GPa})$	ν
sandstone	48.42	-2.422	19.94	1.0	18.50	0.18
siltstone	50.50	-11.41	4.20	1.0	26.15	0.36

The properties listed in this table are considered to be the best representation of the rock properties from No. 26 Colliery that can be obtained from the available data. These values have therefore been chosen as rock property input data for the model.

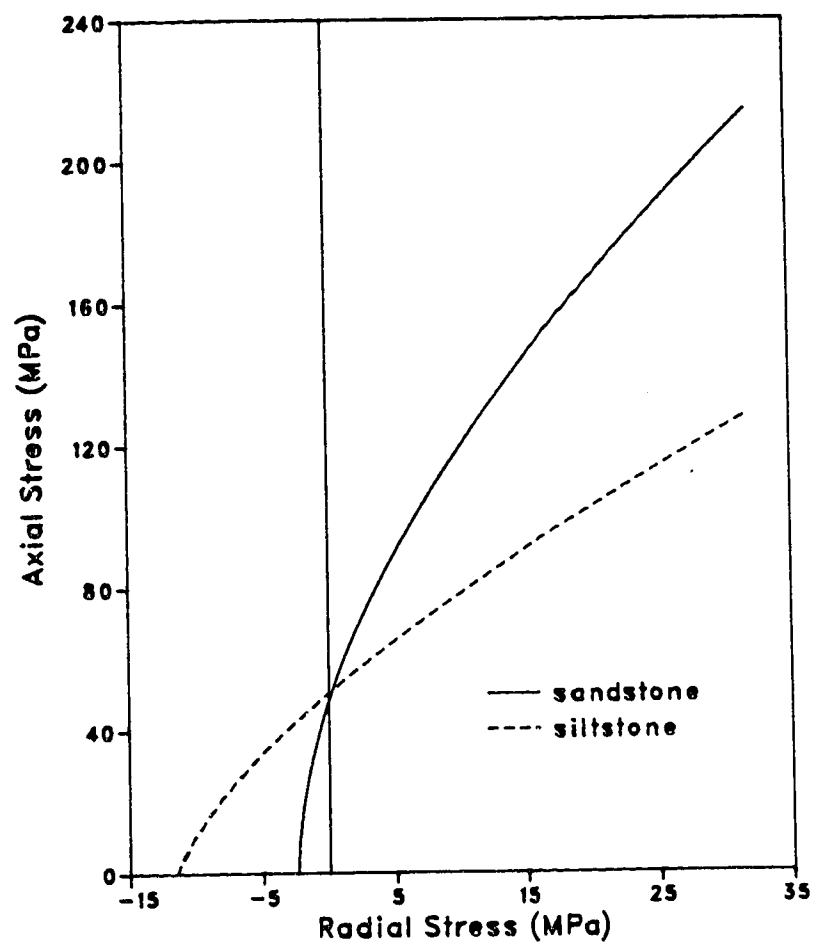


Figure C.8 Sandstone and Siltstone failure envelopes

Appendix D - Insitu Stress Test [21]

Overcoring

Insitu stresses were determined by the overcoring method as layed out by Hooker and Bickel [31] and the calculations were based on the work by Panek [40]. The test was located at the north end of the workings in the 14 South Coal Road as shown in Figure 5.1, page 24. Three overcoring tests were conducted in three drillholes at this location, two in siltstone and one in sandstone. The nearest mine development areas were reported to be 300m away. This was considered to be of sufficient distance to be outside the zone of influence of the longwall panels. It was reported that the test site was in a generally uniform geological environment with no dominant geological features to influence the stress field. Field work was completed in December 1983.

Table D.1 gives the drillhole orientation and the number of tests conducted for each of the drillholes. United States Bureau of Mines (USBM) deformation gauges were installed in areas showing no signs of discontinuities. Deformations were measured in the pilot hole, across three diameters 120° apart, continuously as the pilot hole was being overcored. This allowed for the measurement of the two-dimensional stress field in a plane normal to the drillhole axis.

Biaxial Tests

To find the deformation modulus of the rock being tested, overcored rock specimens were recovered from the test site and a biaxial test was conducted on those cores. The tests were conducted inside a biaxial test cell that required the cores be placed inside a sleeve and hydraulic fluid provided a radial pressure to the outside of that sleeve. The same USBM gauges used in overcoring, were used to measure the deformations of the specimens for a given radial pressure. The equipment was calibrated and corrections were made to the calculations for the overcoring and biaxial tests.

Table D.1 Overcoring Test Locations and Comments (after [21])

DRILL HOLE	TYPE OF ROCK	DRILL HOLE ORIENTATION		TEST No.	SAMPLE DEPTH IN HOLE (m)	COMMENTS ON TESTS
		AZIMUTH	DIP (up)			
1	siltstone	330° (N 30° W)	4°	USBM 1	10.69	a,e
				USBM 2	11.73	b
				USBM 3	12.75	c
				USBM 4	15.14	d,e'
2	siltstone	60° (N 60° E)	4°	USBM 5	11.18	d
				USBM 6	11.84	d
				USBM 7	12.50	d
3	sandstone	60° (N 60° E)	30°	USBM 8	9.4	c
				USBM 9	11.15	d,e

Comments on tests

- a. Test was aborted when USBM gauge was pushed out of the pilot hole due to a surge of water pressure during overcoring.
- b. Rock broke close to (but beyond) the USBM gauge button.
- c. Rock broke before overcoring bit reached USBM gauge button. Gauge rotated with overcore.
- d. Successful test.
- e. Intact overcore samples recovered from test position.
- e'. Intact overcore sample recovered between USBM 3 and USBM 4.

Test Results

A total of nine overcoring tests were attempted, but only five of these were successful as shown in Table D.1. The main cause of failure of these tests was the premature failure of the cores along planes of weakness, usually bedding planes. Figures D.1 to D.4 and D.7 show the deformation of the cores for the five successful results. These figures show the classic deformational responses as the overcore passes by the gauge. The curve reaches a peak when the cutting head of the core is passes buttons of the gauge and then quickly drops to a minimum and becomes constant. The deformation of each of the three buttons was noted.

Only three of the biaxial tests were successful; once again, the main cause of failure of these tests was the premature splitting of the specimen along bedding planes. Two results were obtained from drillhole 1 and one from drillhole 3. Figures D.5, D.6 and D.8 were plotted based on the continuous monitoring of the deformation of the cores during biaxial testing. The curves of the deformation versus pressure are fairly linear for the siltstone but some nonlinearity exists in the sandstone. The deformation in all cases does appear to be elastic as the deformation was recovered when the pressure was reduced.

In all cases, the buttons were oriented in such a way that the deformation U1 was in the plane normal to bedding.

The deformation modulus was determined from the biaxial tests using the following equation (assuming isotropic elasticity).

$$E = \frac{4 r_i r_o^2 P}{(r_o^2 - r_i^2) U}$$

where: E = deformation modulus

P = outer pressure on overcore specimen

U = average diametral deformation

r_i = inner radius of overcore

r_o = outer radius of overcore

Table D.2 shows the results of these tests; the variation of the two results for siltstone was

only about 5%.

Table D.2 Biaxial Test Results (after [21])

DRILL HOLE	ROCK TYPE	BIAXIAL TEST NO.	SAMPLE DEPTH IN HOLE (m)	DEFORMATION MODULUS (GPa)
1	siltstone	1	10.70	33.7
1	siltstone	2	13.80	35.5
3	sandstone	3	11.15	13.1

Poisson's ratio was not measured in these tests. A value of 0.2 was assumed for the purposes of the stress evaluation and no distinction was made between the siltstone and sandstone. Results given in Appendix C (Rock Properties) show that Poisson's ratio for siltstone can be considerably greater than that of sandstone and this can vary significantly.

Evaluation of the stresses was based on the following assumptions:

1. rock was isotropic and homogeneous
2. plane strain conditions exist on the plane normal to the drillhole axes
3. all test results could be combined using a least squares fit to determine the three-dimensional field stress.

The procedure for evaluating the stress tensors has been outlined by Panek [40] and need not be included here. First, the stress components (σ_x , σ_y , σ_z , τ_{xy} , τ_{xz} , τ_{yz}) were found relative to the mine coordinate system (where x, y and z are E-W, N-S, and vertical respectively). These values were evaluated in terms of principal stresses and directions. These results are summarized in Tables D.3.

Table D.3a Input Parameters for Stress Tensor Calculation (after [21])

DRILL HOLE	TEST No.	DIAMETRAL DEFORMATION (μin)			ELASTIC CONSTANTS	
		U3	U1	U2	E (GPa)	ν
1	USBM 4	1885	2058	2010	34.6	0.2
2	USBM 5	1975	2000	1610	34.6	0.2
2	USBM 6	1870	2000	1605	34.6	0.2
2	USBM 7	2045	2455	2110	34.6	0.2
3	USBM 9	5850	3460	5095	13.1	0.2

Table D.3b Average Stress Tensors by Least Squares Solution (after [21])

STRESS	DIRECTION	STRESS TENSOR* (MPa)	
		mean	st.dev.
σ_x	E-W	23.31	3.26
σ_y	N-S	24.98	2.97
σ_z	vertical	25.27	1.16
τ_{xy}	-	0.01	1.80
τ_{yz}	-	-0.05	0.93
τ_{zy}	-	1.21	1.15

* correlation coefficient $R=0.99$

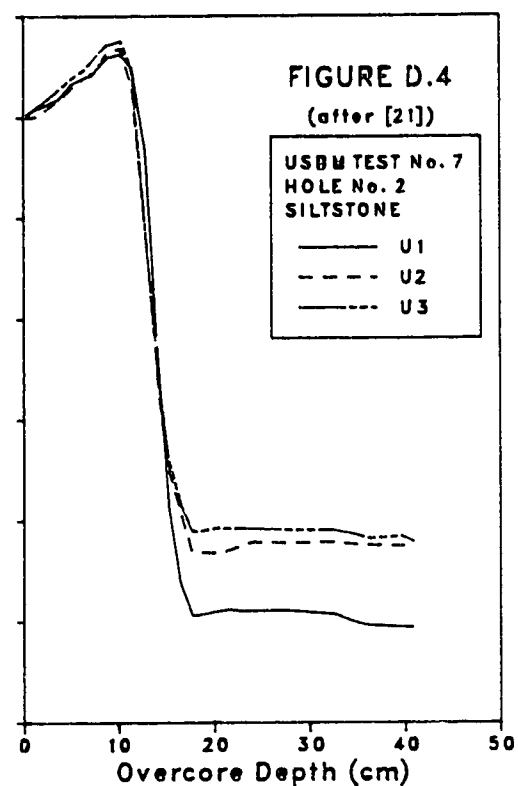
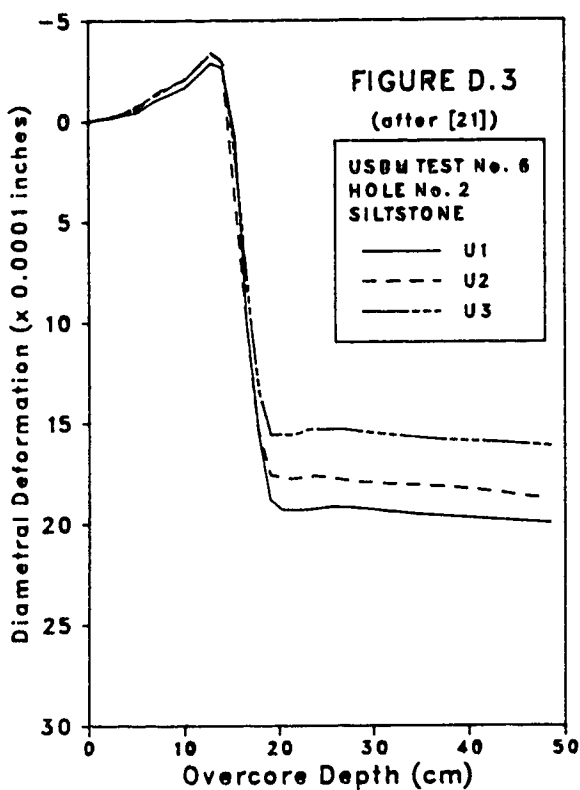
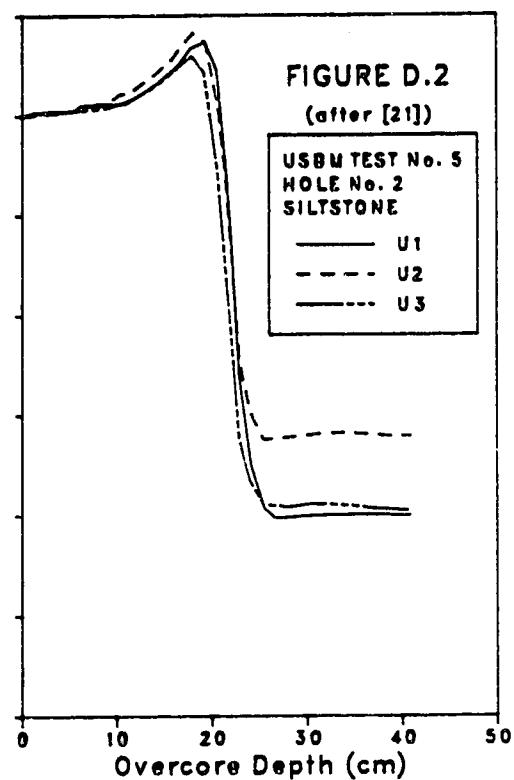
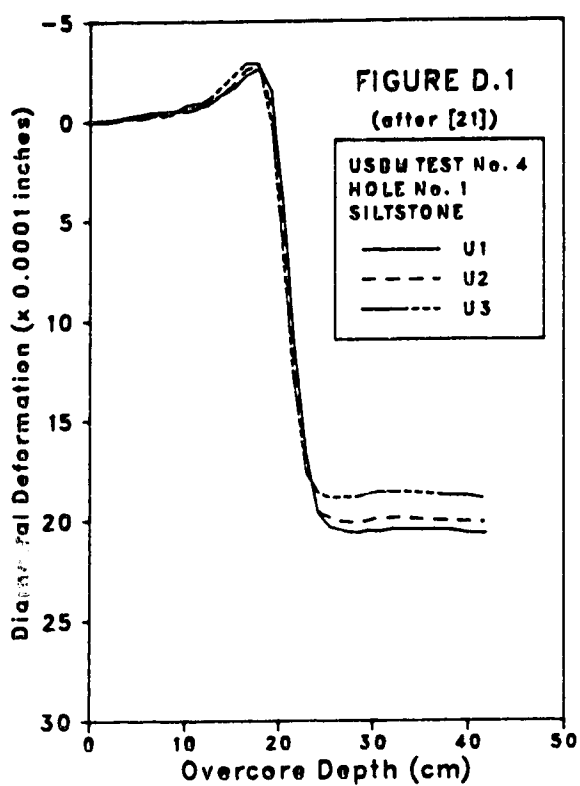
Table D.3c Principal Stress Magnitudes and Directions (after [21])

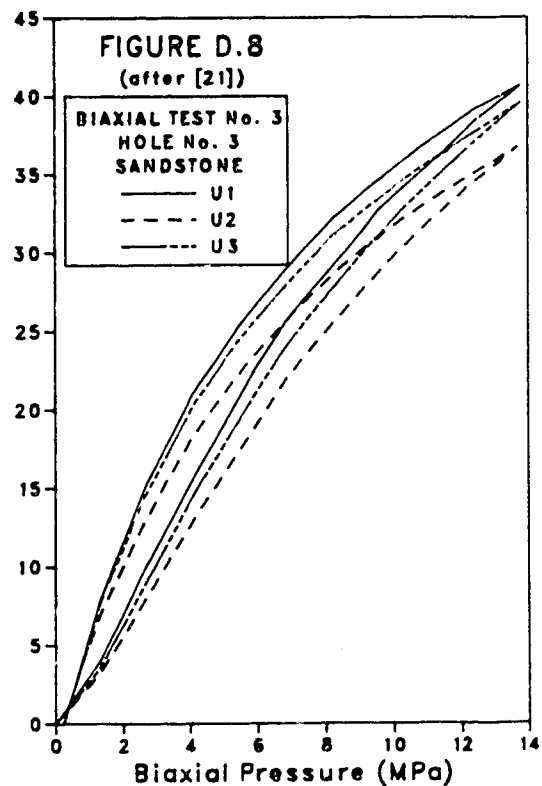
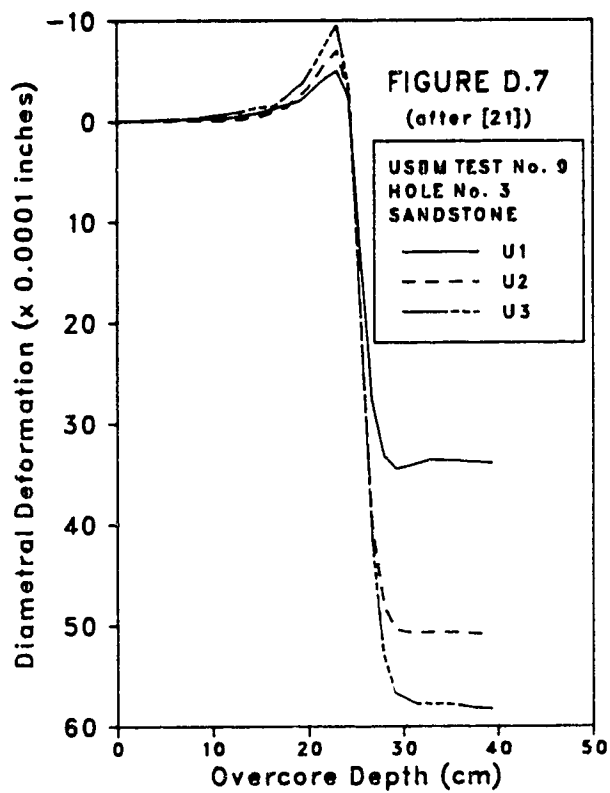
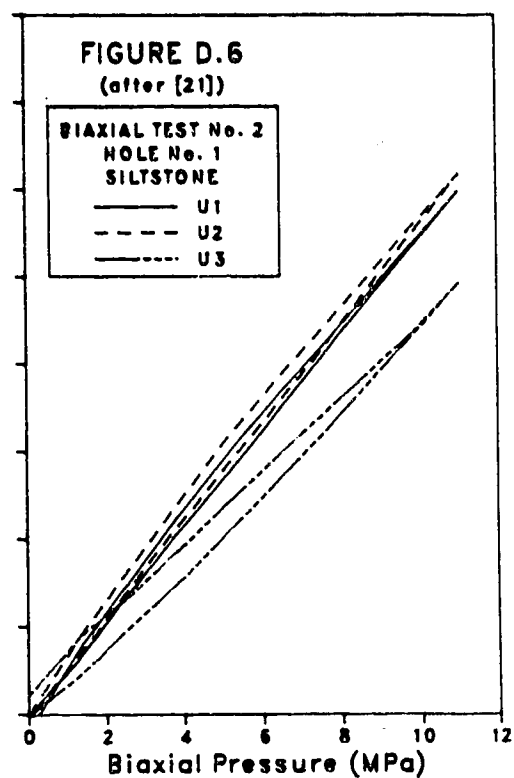
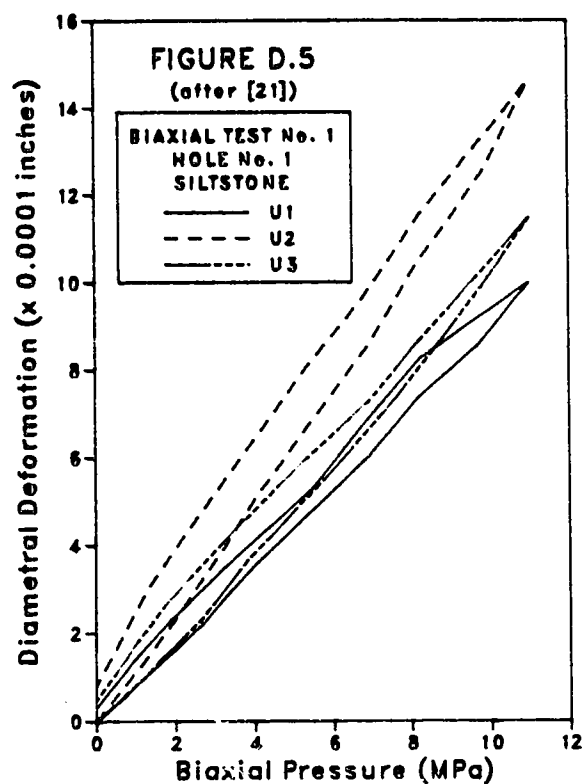
STRESS	MAGNITUDE (MPa)	ORIENTATION	
		AZIMUTH**	DIP (up)
σ_1	26.30	270°	-25°
σ_2	23.20	278°	64°
σ_3	24.05	9°	-13°

** clockwise from North

The following points have been presented by Golder Associates [21] in their discussion of the results of the tests:

- only slight variation exist in deformations in the three diametral directions, with a maximum of 30% at no preferred direction.
- based on the work of Becker and Hooker [31] in comparing isotropic and anisotropic evaluation techniques, it was acceptable to assume isotropic conditions assuming errors to be insignificant for the amount of anisotropy noticed in these results. (No calculations are given to back this up.)
- using the least squares solution for the stress tensors takes into account axial stress along the drillholes. Assuming plane stress conditions produces results 7% greater.
- results in Table D.3b show good correlation between the results from the three drillholes with little standard deviation.
- average vertical stress was 15% greater than the vertical stress based on the weight of overburden.
- the stress field was almost hydrostatic with about 12% variation between the major and minor principal stresses.





Summary

Even though the results from these tests appear to be excellent, some aspects of the tests and calculations leave doubt as to the accuracy of the results.

The first point of question is the location of the test holes; two different materials were chosen in which to conduct the overcoring tests. It should have been known that the elastic properties of siltstone and sandstone could be quite different. The results show that the elastic modulus varies significantly between the two rock types, and it could be expected that the Poisson's ratio would also vary. No tests were conducted to try and quantify Poisson's ratio and a value of 0.2 was used for both rock types. Other tests have shown that this value can vary significantly between the different rock types (Tables C.2a and C.6).

From Figures D.1-D.4 (siltstone), it is clear that deformation normal to the bedding plane (U1) is greater than that parallel to bedding, thus having a lower elastic modulus. Figure D.7 shows that sandstone has a higher modulus normal to the bedding planes. Golder Associates, in their summary mention that the maximum variation in deformation is 30% at no preferred direction. Thirty percent is not insignificant and the rock is behaving anisotropically, however, it has been noted that this should not create significant error.

It has been noted that the tests were conducted in an area more than 300m from the nearest longwall panel and this was considered to be virgin ground. The effect of the roadway itself was not considered by Golder Associates [21] and testing was carried out in an area close enough to the roadway, that the stress field would be influenced.

To attempt to correct this error, a boundary element program was used to re-analyse the result obtained by Golder Associates [21] as follows. The location of the tests was noted with respect to the opening and the stresses at these points were monitored. The insitu stress field (vertical and horizontal stresses) was adjusted until the stresses at the test sites duplicated the test results. The results obtained by Golder Associates were reproduced almost exactly for a stress field with the horizontal and vertical components being the major and minor principal stresses respectively with values of 26.3MPa and 24MPa. This will be considered the virgin insitu stress field for use in the model presented here.

Appendix E - Program SAFCON

This Appendix contains the listing of PROGRAM SAFCON. The purpose of this program is to contour the safety factors of the rock mass around the heading and outburst cavity, define zones of shear and tensile rock failure and produce input files for the next iteration in the spalling process. SAFCON uses as input the stress field results from the boundary element program and shear zone definition from the previous iteration and outputs the new cavity shape, defined as boundary elements for the next run of the boundary element program, coordinates defining the shear zones and a file containing the stresses and safety factors of the boundary elements and field points. Example files are listed in Appendix F.

The contouring performed by SAFCON can be easily done by hand, only with the use of SAFCON, the iteration can be completed within five minutes and the hand method would require about an hour. User interaction is still required to define the shear zone and tensile failure zone because the results from the boundary element program leaves gaps in areas where the stress field cannot be determined.

This appendix is set up in the following manner:

- list of COMMON BLOCKS
- list of INCLUDE files containing some of the COMMON BLOCKS
- listing of the two parameter files PROP.PRM and PLOT.PRM used to initialize variables
- list of global variables (local variables are listed in the appropriate SUBROUTINES)
- an Index of SUBROUTINES with page numbers
- a flow chart of the SUBROUTINES showing how they link together
- listing of the SUBROUTINES

The following COMMON BLOCKS have been used within the program SAFCON:

BOUND	FINDEX
CONST	GASCON
COORD	PLTPRM
F1OLD	STRESS
F1BND	STRGTH
FAIL	WIND

The following is a list of INCLUDE files used within SAFCON; a complete listing of the each file is found at the end of the program.

CONST.INC
PLOT.INC
PLTPRM.INC
WIN.INC
F1CONT.INC
FAIL.INC

The following are the data files used by subroutine INIT to initialize parameters. The first contains rock properties and the second, contouring parameters.

**** PROP.PRM ****

REPOSE:	30.0
FRICL:	30.0
FRICU:	30.0
ELLEN:	0.15
YUPR:	6.0
PP:	6.0

**** PLOT.PRM ****

HGT	.12		
NARC	4		
NDIV	2		
NLEV	7		
ZLEV	LDIG	ICI	INP
0	-1	12	1
1	-3	13	1
1.5	1	11	1
2	-1	11	1
3	-1	11	1
4	-1	11	1
5	-1	11	1

The following is a list and description of the global variables, ones that are used in more than one SUBROUTINE. All other variables are defined within that SUBROUTINE. All variables are listed in alphabetical order.

ALEN	length of the square window to be contoured
BND	an array containing the coordinates of the mid points of the boundary elements, element angle, stresses and safety factor as read in from the boundary element program output file
CONV	conversion factor from degrees to radians
DLEN	distance between field points
ELLEN	boundary element length
ETA	angle of inclination of interface of the two materials (= 0.)
FACT	scaling factor of the contoured plot size
FILE	character variable containing the file name for a given iteration
FLD	an array containing the coordinates of the field points, stresses and safety factor as read in from the boundary element program output file
FRICU,FRICL	friction angles of upper and lower materials respectively
HBMU,HBML	'm' parameter in the Hoek and Brown failure criterion
HBSU,HBSL	's' parameter in the Hoek and Brown failure criterion
INT	number of coordinates entered by the MOUSE defining tensile failed zone
JNT	number of elements defining the boundary
KWIN	type of window
LOC	code used signifying if a field point is within the shear zone LOC= -1 point is outside the shear zone LOC= 0 point is on the shear / intact interface LOC= +1 point is inside the shear zone LOC= +2 point is on shear zone coordinate point
NFCON	signify which zone is being contoured (0 - tensile; 1 - shear failures)
NFIN	number of boundary elements
NFLS	number of points that have failed by shear failure
NFLT	number of points that have failed by tensile failure
NF1	number of points defining the new shear zone
NF10	number of coordinates defining the shear zone
NUMBSF	number of boundary elements
NX,NY	number of field points spaced across the window to be contoured, NX=NY
PI	the exact value of pi (3.141592...)
PP	insitu gas pressure
SF	safety factor: strength / stress
SFGRID	2-D array containing safety factors to be contoured
SLWIN	side length of the field point window
SN	normal stress at a point
STRESS	shear stress at the same point as SN

S1,S3	arrays containing all effective principal stresses
TAU	shear stress at the boundary elements
UCSU,UCSL	uniaxial compressive strengths of upper and lower materials
X,Y	initially contain the coordinates of the end points of the boundary elements which are later replaced by the new boundary elements.
XCONT,YCONT	arrays containing all coordinates at which stresses were evaluated
XFLS,YFLS	arrays containing coordinates of points that have failure by shear
XFLT,YFLT	arrays containing coordinates of points that have failure in tension
XF1,YF1	coordinates of the points entered with the MOUSE
XFIC,YFIC	coordinates of the points defining the entire shear zone
XF1O,YF1O	coordinates of the points defining the shear zone entered by using the mouse.
XMAX,YMAX	maximum coordinates of the square window to be contoured
XMIN,YMIN	minimum coordinates of the square window to be contoured
XMN,YN	coordinates of points defining the contour of tensile failure as entered by the mouse
XOLDB,YOLDB	coordinates of the end points of the boundary elements
XWIN,YWIN	coordinates of the upper left corner of the field point windows
YUPR	upper limit to the sandstone bed

Index of SUBROUTINES

SUBROUTINE / FUNCTION	Page
SAFCON	149
INIT	155
PSB	156
PSF	157
SFCAL	158
FSHEAR	160
PTLOC	161
CONTUR	163
GRIDNG	171
MSECAL	173
MSEWRT	176
MSLAST	176
MSSTOR	177
SYMET	178
FICONT	180
DIST	182
ANGLE	182
PLOT88 SUBROUTINES	
MESSAGE	183
STMODE	183
WAITKY	183
INCLUDE FILES	
CONST.INC	184
PLOT.INC	184
PLTPRM.INC	184
WIN.INC	184
FICONT.INC	184
FAIL.INC	184

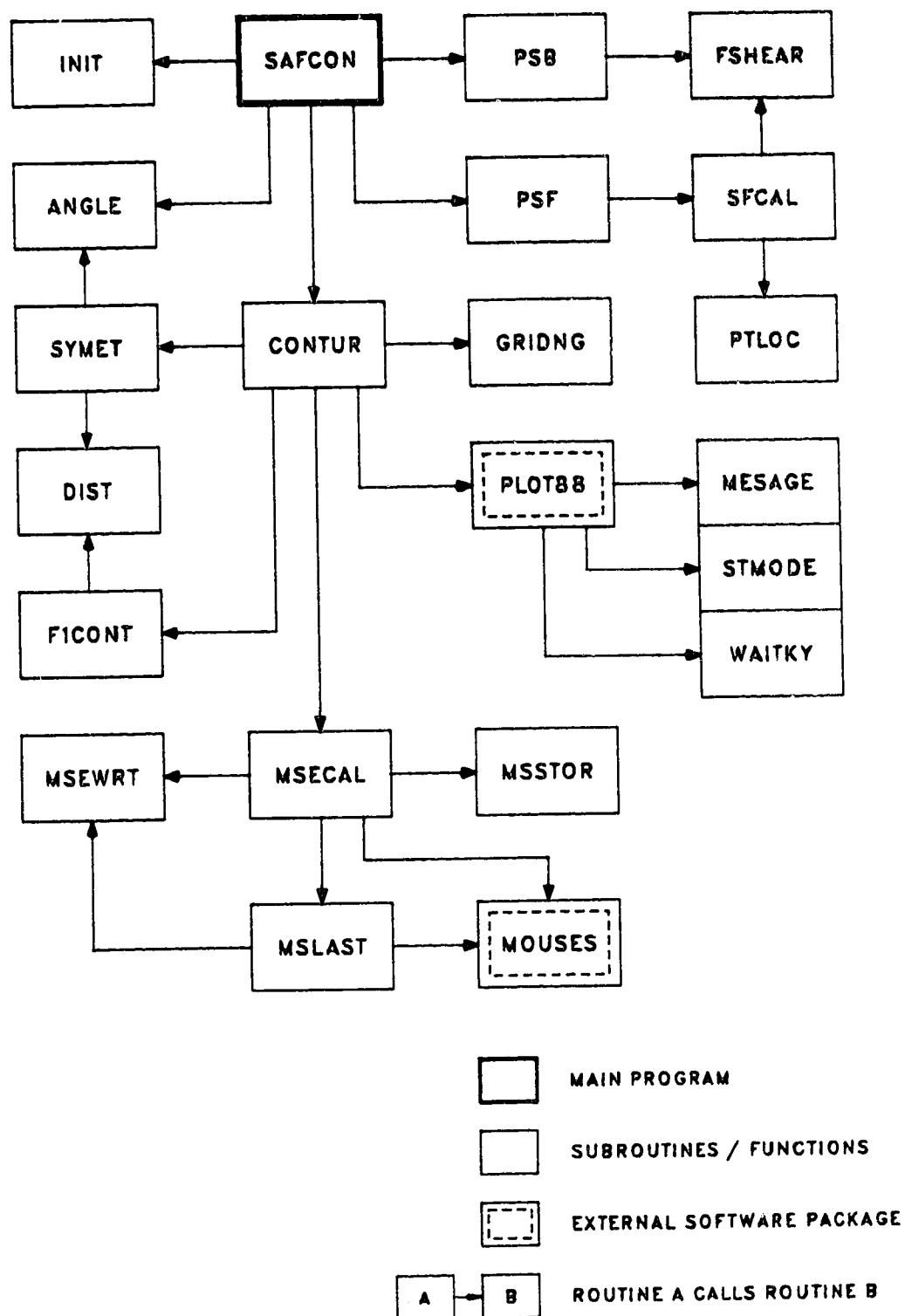


Figure E.1 Flow Chart of Relationship Between SAFCON Routines

PROGRAM SAFCON

Safety Factor CONtouring

This program is run after the boundary element program BESOL/P5005. The results from that program are input to this program, storing the locations and stresses of boundary elements and field points. The effective principal stresses are found by superimposing a gas pressure onto the principal stresses for the rock containing gas. Safety factors are determined for each boundary element and field point. The plotting package PLOT88 is used to contour the safety factors around the opening and plot these contours, heading cross-section, shear zone and sandstone / siltstone interface onto the monitor. The MOUSES subroutine is then called to use a cursor on the monitor to allow the user to input the tensile failure zone and shear zone contours. The tensile failure contour becomes the new boundary for the next iteration and the shear zone gets written off to a file to be used as input for the next iteration.

Many of the variables used within this program are global; they are used if more than one routine. To prevent from having to define these variables within each routine in which they appear, they have been defined previously in the write-up of this appendix. Local variables are defined in the routine they appear.

ROUTINES called: INIT
PSB
PSF
CONTUR
ANGLE

INPUT FILES: RUNAFx.DAT
RUNAFx.OUT
RUNAFx.F1 (will not exist if first iteration)
DATFILE
RUN.INP

OUTPUT FILES: RUNAFx.LST
RUNAFy.DAT (where $y=x+1$, next iteration)
RUNAFy.F1
DATFILE (contains new file name)
RUN.INP (contains new file names)

Local variables: F1EX - logical variable used in INQUIRE statements
NSTRT - first boundary element coordinate within the upper material
NN - counter of boundary elements
NELM - number of field points in a window
NTFP - counter of the total number of field

```

C                               points
C
C
C      REAL X(127), Y(127), XN(200), YN(200)
C
C      Include files containing COMMON blocks to be used between
C      subroutines.
C
C      $INCLUDE:'CONST.INC'
C      $INCLUDE:'PLOT.INC'
C      $INCLUDE:'WIN.INC'
C      $INCLUDE:'F1CONT.INC'
C
C      COMMON /GASCON/ YUPR, PP, ETA
C      COMMON /STRGTH/ UCSU, UCSL, HBMU, HBML, HBSU, HBSL
C      COMMON /COORD/ XN, YN, INT
C      COMMON /BOUND/ X, Y, JNT
C      REAL LENGTH
C      CHARACTER*1 HED1, HED5
C      CHARACTER*5 HED2
C      CHARACTER*7 FILE
C      CHARACTER*12 HED6
C      CHARACTER*24 HED3
C      CHARACTER*60 TITLE
C      CHARACTER*94 HED4
C      LOGICAL F1EX
C
C      Subroutine called to initialize variables
C
C      CALL INIT
C
C      The file DATFILE contains the name of the file containing
C      the P5005 input and output data.
C
C      OPEN (3,FILE='DATFILE')
C      READ (3,10) FILE
C      10 FORMAT (A7)
C
C      The file extension .DAT refers to the P5005 data file,
C      .OUT to the P5005 output file, and .LST is the output
C      file from this program containing the effective principal
C      stresses and safety factors for boundary and field points.
C
C      INQUIRE (FILE=FILE//'.DAT',EXIST=F1EX)
C      IF ( .NOT. F1EX) GO TO 390
C      INQUIRE (FILE=FILE//'.OUT',EXIST=F1EX)
C      IF ( .NOT. F1EX) GO TO 390
C      OPEN (8,FILE=FILE//'.LST')
C      OPEN (4,FILE=FILE//'.OUT')
C      OPEN (5,FILE=FILE//'.DAT')
C
C      Read in all the data from the data file. The variables are
C      defined in Appendix F after the sample input file.
C

```

```

      READ(5,20) TITLE
20  FORMAT (T11, A60)
      READ(5,*) KPROB, NSTEPS, NUMSTV, NFILL
      READ(5,*) NUMBSD, NUMBSF, NUMWIN, KFAIL, KDREF
      READ(5,*) PRL, EL, PRU, EU, ETA, XREF, YREF, UXFIX, UYFIX
      READ(5,*) AXX, BXX, AYY, BYY, AXY, BXY
      READ(5,*) UCSL, HBML, HBSL, UCSU, HBMU, HBSU
      NN = 0

```

C
C
C

Read in boundary element end points.

```

      DO 40 L = 1, NUMBSF
      READ (5,*) NUM, KODE, XBEG, YBEG, XEND, YEND
      IF (NN .EQ. 0) THEN
        X(1) = XBEG
        Y(1) = YBEG
        XOLDB(1) = XBEG
        YOLDB(1) = YBEG
      END IF
      XLEN = (XEND - XBEG) / NUM
      YLEN = (YEND - YBEG) / NUM

```

C
C
C

Break up multiple element segments into individual elements

```

      DO 30 K = 1, NUM
      AK = K
      X(K + NN + 1) = XBEG + AK * XLEN
      Y(K + NN + 1) = YBEG + AK * YLEN
      XOLDB(K + NN + 1) = XBEG + AK * XLEN
      YOLDB(K + NN + 1) = YBEG + AK * YLEN

```

C
C
C

Find the midpoint of the elements

```

      BND(K + NN,1) = XBEG + (AK - .5) * XLEN
      BND(K + NN,2) = YBEG + (AK - .5) * YLEN
      BND(K + NN,3) = ANGLE(XBEG,YBEG,XEND,YEND)
      IF (Y(K + NN + 1) .EQ. 0.0 .AND. Y(K + NN) .LT. 0.)
      +   NSTRT = K + NN + 1
30  CONTINUE
      NN = NN + NUM
40  CONTINUE
      NFIN = NN

```

C
C
C
C

Scan the output file for the required results for boundary elements and field points.

```

50  READ (4,60,END=390) HED6
60  FORMAT (T2, A12)
      IF (HED6 .NE. 'ELEMENT      ') GO TO 50
      DO 70 L = 1, NFIN
      READ (4,*) IB, BX, BY, UXJ, UYJ, USJ, UNJ, SXX, SYJ,
      +   SXY, SS, BND(L,5), BND(L,4), BND(L,6)
70  CONTINUE

```

C

C Print out heading for .LST file.

C

```

      WRITE (8,80) PP, YUPR
80  FORMAT (/, '      GAS PRESSURE WITHIN SANDSTONE IS', F8.3,
+         ' MPa', /, '      UPPER LIMIT TO GAS IN SANDSTONE ',
+         F8.3, ' m', //, 70(' - '), /)
      WRITE (8,*) '      MID POINTS OF BOUNDARY ELEMENTS'
      WRITE (8,90)
90  FORMAT (/, ' POINT          X          Y          S1          ',
+         ' S3          SN          SHEAR          SF' //)

```

C

C The file extension .F1 contains the coordinates of the
 C polygon defining the shear zone around the opening. If
 C this file does not exist, the shear zone is not defined.

C

```

      INQUIRE (FILE=FILE//' .F1', EXIST=F1EX)
      IF ( .NOT. F1EX) GO TO 120
      OPEN (7, FILE=FILE//' .F1')
      NF10 = 1
100  READ (7,*, END=110) XF10(NF10), YF10(NF10)
      NF10 = NF10 + 1
      GO TO 100
110  NF10 = NF10 - 1
      CLOSE (7)
      GO TO 140

```

C

C If the shear zone was not defined, the boundary defining
 C the opening will also be the shear zone.

C

```

120  DO 130 NF10 = 1, NFIN
      XF10(NF10) = XOLDB(NF10)
130  YF10(NF10) = YOLDB(NF10)
      NF10 = NF10 - 1

```

C

C This subroutine calculates the principal stresses and
 C safety factors on the boundary.

C

```

140  CALL PSB

```

C

```

      DO 150 L = 1, NUMWIN
150  READ (5,*) XWIN(L), YWIN(L), SLWIN(L), KWIN(L)
      CLOSE (5)
      NTFP = 0

```

C

C Reading in field point data from .OUT file.

C

```

      DO 220 N = 1, NUMWIN
      IF (KWIN(N) .EQ. 1) NELM = 121
      IF (KWIN(N) .EQ. 2) NELM = 441
      IF (KWIN(N) .GE. 3) NELM = 11
160  READ (4,170) HED2
170  FORMAT (T4, A5)
      IF (HED2 .NE. ' POINT') GO TO 160
      DO 210 L = 1, NELM

```

```

180     READ (4,190,END=230) HED3, HED1, HED4, HED5
190     FORMAT (A24, A1, A94, A1)
      IF (HED1 .EQ. '-' ) GO TO 180
      IF (HED5 .EQ. '*' ) GO TO 210
      NTFP = NTFP + 1
      BACKSPACE 4
      READ (4,200) IPT, FLD(NTFP,1), FLD(NTFP,2), UX, UY,
+         EX, EY, EZ, SX, SY, SZ, FLD(NTFP,3), FLD(NTFP,4),
+         TH1, FLD(NTFP,5)
200     FORMAT(I8, 2F8.1, 1X, F7.4, F8.4, 3F8.3, 6F8.1, F8.2)
210     CONTINUE
220 CONTINUE
230 CLOSE (4)
C
      WRITE (8,240)
240     FORMAT (/ , 70(' -' ), / , '  FIELD POINT RESULTS' , /)
      WRITE (8,250)
250     FORMAT (/ , '          X          Y          S1          ' ,
+         '          S3          FI' /)
C
C   This subroutine calculates the effective principal stresses
C   for the field points.
C
      CALL PSF
C
C   The CONTOUR subroutine takes all the data and contours
C   field point safety factors, calls the MOUSES routine to
C   allow the user to define the tensile and shear zones and
C   then sets up these zones such that it is symmetrical about
C   the Y-axis.
C
      CALL CONTUR(FILE)
      CLOSE (8)
C
C   Set up the new file name by incrementing a value by 1 for
C   the next set of iterations. The filename contains a two-
C   digit number that can be incremented.
C
      JNT = JNT - 1
      REWIND 3
      READ (3,260) HED2, I
260     FORMAT (A5, I2)
      I = I + 1
      REWIND 3
      WRITE (3,260) HED2, I
      REWIND 3
      READ (3,10) FILE
      CLOSE (3)
C
C   The RUN.INP file contains the file name of the input and
C   output file required by the P5005 program. Running of this
C   program is done through a batch file and this .INP file
C   contains the required information.
C

```

```

OPEN (2, FILE='RUN.INP')
WRITE (2, 270) FILE, FILE
270 FORMAT (/, A7, ' .DAT', /, A7, ' .OUT', //)
CLOSE (2)

```

```

      SUBROUTINE INIT
C
C   Initialize the rock properties and PLOT88 plotting
C   parameters.
C
C   Called from ROUTINE SAFCON
C
C   INPUT FILES: PROP.PRM
C                 PLOT.PRM
C
C   $INCLUDE:'CONST.INC'
C   $INCLUDE:'PLTPRM.INC'
C   COMMON /GASCON/ YUPR, PP, ETA
C
C   PI = ATAN(1.) * 4.
C   OPEN (2,FILE='PROP.PRM',STATUS='OLD')
C   READ (2,10) FRICL, FRICU, ELLEN, YUPR, PP
10  FORMAT (4(T10,F8.3,/), (T10,F8.3))
C   FRICL = FRICL / 180. * PI
C   FRICU = FRICU / 180. * PI
C   CLOSE (2)
C
C   Plotting paramters used by PLOT88.
C   See manual for definition.
C
C   OPEN (2,FILE='PLOT.PRM',STATUS='OLD')
C   READ (2,20) HGT, NARC, NDIV, NLEV
20  FORMAT (T10, F8.3/, 3(T10,I2,/))
C   DO 30 I = 1, NLEV
C     READ (2,*) ZLEV(I), LDIG(I), ICI, INP
30  LWGT(I) = ICI * 100 + INP
C   CLOSE (2)
C
C   RETURN
C   END

```

```

SUBROUTINE PSB
C
C Determine the principal stresses and safety factor for the
C boundary elements and then write out the results to the
C .LST file. Since the boundary is assumed to be relieved of
C gas pressure, this does not have to be considered. A check
C is make for tensile failures. The subroutine FSHEAR
C calculates the safety factor.
C
C Called from ROUTINE SAFCON
C
C ROUTINES called: FSHEAR
C
$INCLUDE:'CONST.INC'
$INCLUDE:'PLOT.INC'
$INCLUDE:'FAIL.INC'
  NFLS = 0
  NFLT = 0
  DO 20 N = 1, NFIN
    S1(N) = BND(N,4)
    S3(N) = BND(N,5)
    XCONT(N) = BND(N,1)
    YCONT(N) = BND(N,2)
    CALL FSHEAR(S1(N),S3(N),XCONT(N),YCONT(N),SN,TAU,SF)
    IF (SF .LT. 0.) THEN
      NFLT = NFLT + 1
      XFLT(NFLT) = XCONT(N)
      YFLT(NFLT) = YCONT(N)
    END IF
    WRITE(8,10)N,XCONT(N),YCONT(N),S1(N),S3(N),SN,TAU,SF
10  FORMAT (I4, T9, 2F9.3, 3F10.2, F9.2, F8.2)
20 CONTINUE
  RETURN
  END

```


SUBROUTINE PSF

```

C
C Determine the effective principal stresses and safety
C factor for the field points and then write out the results
C to the .LST file. The points are checked to see if they
C fall within the previous shear zone and if so, gas
C pressures are not applied and an astrix (*) is put next
C to the results. The function SFCAL calculates the safety
C factors. Points of shear and tensile failure are stored
C in separate variables to be plotted later.
C
C Called from ROUTINE SAFCON
C
C ROUTINES called: SFCAL
C
C Local variables: IR - value passed from SFCAL identifying
C                   points within the shear zone
C                   FI - safety factor
C                   K - assigned a format number to allow two write
C                     format, one for field points in the shear
C                     zone and one outside
C
C $INCLUDE: 'CONST.INC'
C $INCLUDE: 'PLOT.INC'
C $INCLUDE: 'FAIL.INC'
C   DO 40 N = 1, NTFP
C     XCONT(NFIN + N) = FLD(N,1)
C     YCONT(NFIN + N) = FLD(N,2)
C     S1(NFIN + N) = FLD(N,3)
C     S3(NFIN + N) = FLD(N,4)
C     IR = 0
C     FI = SFCAL(S1(NFIN + N),S3(NFIN + N),XCONT(NFIN + N),
+      YCONT(NFIN + N),IR)
C     IF (FI .LT. 0.) THEN
C       NFLT = NFLT + 1
C       XFLT(NFLT) = XCONT(NFIN + N)
C       YFLT(NFLT) = YCONT(NFIN + N)
C       GO TO 10
C     END IF
C     IF (FI .LT. 1.) THEN
C       NFLS = NFLS + 1
C       XFLS(NFLS) = XCONT(NFIN + N)
C       YFLS(NFLS) = YCONT(NFIN + N)
C     END IF
C 10  IF (IR .EQ. 2) ASSIGN 20 TO K
C     IF (IR .NE. 2) ASSIGN 30 TO K
C     WRITE (8,K) XCONT(NFIN+N), YCONT(NFIN+N), S1(NFIN+N),
+      S3(NFIN+N), FI
C 20  FORMAT (T9, 2F9.3, 2F10.2, F12.3, '  *' )
C 30  FORMAT (T9, 2F9.3, 2F10.2, F12.3)
C 40  CONTINUE
C     RETURN
C     END

```

```

C      FUNCTION SFCAL(S1, S3, X, Y, N)
C
C      The purpose of this Function is to calculate the effective
C      principal stresses and then apply the appropriate failure
C      criterion and assess the safety factor of a field point.
C      The point is checked if it is within the sheared zone and
C      the type of rock.
C
C      Called from ROUTINE PSF
C
C      ROUTINES called: PTLOC
C                      FSHEAR
C
C      Local variables: X,Y - coordinates of the point evaluated
C                      M,S,UCS - parameters of the Hoek and Brown
C                          failure criterion
C                      ST - tensile strength
C                      A,B,C - variables used to solve a quadratic
C                          equation
C                      S3F - given S1, this is the S3 to fail
C                      S1F - given S3, this is the S1 to fail
C
C
C      REAL M
C      $INCLUDE:'CONST.INC'
C      COMMON /STRGTH/ UCSU, UCSL, HBMU, HBML, HBSU, HBSL
C      COMMON /GASCON/ YUPR, PP, ETA
C      CONV = PI / 180.
C
C      The subroutine PTLOC checks each field point to determine
C      if it within the shear zone defined by a simple polygon.
C
C      CALL PTLOC(X, Y, LOC)
C      IF (LOC .NE. (-1)) GO TO 10
C      UCS = UCSL
C      M = HBML
C      S = HBSL
C
C      Check if the point is within sandstone; if so, superimpose
C      the gas pressure.
C
C      IF (Y .GE. X*TAN(ETA*CONV) .AND. Y .LE. YUPR) THEN
C          IF (N .EQ. 0) S1 = S1 - PP
C          IF (N .EQ. 0) S3 = S3 - PP
C          UCS = UCSU
C          M = HBMU
C          S = HBSU
C      END IF
C
C      If the point has failed in tension (ie. the minor principal
C      stress, S3, is larger, negatively, than the tensile
C      strength, ST) default the safety factor to -.2.
C
C      ST = (M*UCS - SQRT(((M*UCS)**2) + 4.*S*UCS**2)) / 2.

```

```

      IF (S3 .LT. ST) THEN
        SFCAL = -.2
        RETURN
      END IF

C
C   If the point is completely stress relieved, the safety
C   factor defaults to 2. to prevent divide by zero in later
C   calculations.
C
      IF (S1 .EQ. 0. .AND. S3 .EQ. 0.) THEN
        SFCAL = 2.
        RETURN
      END IF

C
C   Find the minor principal stress on the Hoek and Brown
C   failure curve (S3F) that corresponds to the major principal
C   stress. This is done for S1 less than 0.1.
C
      IF (S1 .LT. 0.1) THEN
        A = -1.
        B = 2. * S1 + M * UCS
        C = S * UCS ** 2 - S1 ** 2
        S3F = (-B + SQRT(B**2 - 4.*A*C)) / (2.*A)
        SFCAL = S3F / S3
        RETURN
      END IF

C
C   Find the major principal stress on the Hoek and Brown
C   failure curve (S1F) that corresponds to the minor principal
C   stress. This is done for S1 greater than or equal to 0.1.
C
      S1F = S3 + SQRT(M*UCS*S3 + S*UCS**2)
      SFCAL = S1F / S1
      RETURN

C
C   If the point is within the sheared zone, the Coulomb-Navier
C   failure criterion is used to define the safety factor. This
C   assumes that the rock has lost cohesion and strength is
C   provided through friction only.
C
10 CALL FSHEAR(S1, S3, X, Y, SN, STRESS, SFCAL)
   IF (S1 .LT. 0.) SFCAL = -SFCAL
   N = 2
   RETURN
END

```

```
SUBROUTINE FSHEAR(S1, S3, X, Y, SN, STRESS, SF)
```

```

C This subroutine finds the safety factor of a point within a
C previously defined shear zone. The Coulomb - Navier failure
C criterion is applied. A check is made for points in
C sandstone or siltstone.

```

```

C Called from ROUTINE PSB
C SFCAL

```

```

C Local variables: X,Y - coordinates of point evaluated
C STRGTH - shear strength at given point
C BETA - angle between fracture plane and minor
C principal stress

```

```

C $INCLUDE:'CONST.INC'

```

```

COMMON /GASCON/ YUPR, PP, ETA
CONV = PI / 180.

```

```

IF (Y .GE. X*TAN(ETA*CONV) .AND. Y .LE. YUPR)
+   BETA = PI / 4. + FRICU / 2

```

```

IF (Y .LT. X*TAN(ETA*CONV) .OR. Y .GT. YUPR)
+   BETA = PI / 4. + FRICL / 2

```

```

SN = (S1 + S3) / 2. + (S1 - S3) / 2. * COS(2.*BETA)

```

```

STRESS = (S1 - S3) / 2. * SIN(2.*BETA)

```

```

STRGTH = SN * TAN(2.*(BETA - PI/4.))

```

```

SF = STRGTH / STRESS

```

```

C RETURN
END

```

SUBROUTINE PTLOC(XP, YP, LOC)

C
C This is a routine to determine the position of a point
C on a plane with respect to a simple closed polygon on the
C same plane. The method and most of the coding has been
C taken directly from Hall, John K., 'PTLOC-A Fortran
C Subroutine for Determining the Position of a Point
C Relative to a Closed Boundary', Mathematical Geology,
C Vol 7, No 1, 1975 pp. 75-78.

C
C Called from ROUTINE SFCAL

C
C Local variables: R1,R2 - euclidean lengths of polygon
C sides
C X1,Y1,X2,Y2 - coordinate locations of
C the current side 1-2
C VPL - product of R1*R2
C ST - cross product SIDE 1 SIDE 2
C CT - dot product SIDE 1 SIDE 2
C C180 - real constant set to detent a COS(180)
C to within real accuracy
C TSC - summation of COSINES
C I - indexing integer
C IP - auxilliary indexing integer for previous
C index
C ISR - defines the rotational sense of the
C boundary points if and only if LOC=+1
C ISR=+1 bounding points are in clockwise
C order
C ISR=-1 bounding points are in counter-
C clockwise order

C
C \$INCLUDE:'F1CONT.INC'

C DATA C180 /0.9999999998/

C
FUZZ = 0.001
I1 = 0
I2 = 0
ISR = 0
IEC = 0
TSC = 0.
SC = 0.
TCC = 1.
CC = 1.
IP = NP
X1 = XF10(NF10) - XP
Y1 = YF10(NF10) - YP
R1 = SQRT(X1*X1 + Y1*Y1)
DO 70 I = 1, NF10
X2 = XF10(I) - XP
Y2 = YF10(I) - YP
R2 = SQRT(X2*X2 + Y2*Y2)
VPL = R1 * R2

```

        IF (R1 .LE. FUZZ) GO TO 110
        IF (R2 .LE. FUZZ) GO TO 110
        ST = (X1*Y2 - X2*Y1) / VPL
        CT = (X1*X2 + Y1*Y2) / VPL
        IF (CT + C180) 90, 90, 10
10      IF (I - NF10) 30, 20, 20
20      IF ((IEC/2)*2 - IEC) 100, 80, 80
30      TSC = SC * CT + CC * ST
        TCC = CC * CT - SC * ST
        IF (TSC*SC) 40, 40, 60
40      IF (TSC*ST) 50, 60, 60
50      IEC = IEC + 1
60      SC = TSC
        CC = TCC
        X1 = X2
        Y1 = Y2
        R1 = R2
        IP = I
70      CONTINUE
80      LOC = -1
        RETURN
90      LOC = 0
        I1 = IP
        I2 = I
        RETURN
100     ISR = 1
        LOC = 1
        IF (SC .LT. 0.) ISR = -1
        RETURN
110     LOC = 2
        I1 = I
        I2 = I
        IF (R1 .NE. 0.) RETURN
        I1 = IP
        I2 = IP
C
        RETURN
        END

```

SUBROUTINE CONTUR(FILE)

C
C This subroutine takes the field point safety factors,
C contours them and calls all the required PLOT88 subroutines
C to plot the results on the monitor. The contouring window
C can be controlled to allow the user to zoom in on any area
C of the window he wishes. The plots can also be directed to
C an HP7475 pen plotter, printer and a file to allow the
C figure to be plotted later on the printer or plotter.

C
C Called from ROUTINE SAFCON

C
C ROUTINES called: GRIDNG
C PLOT88
C MSECAL
C SYMET
C F1CONT

C
C OUTPUT FILES: RUNaFx.PLT (only to write off a plot to a
C file)

C
C Local variables: SYM - character variable used in plotting
C contours
C NPTS - total number of points evaluated,
C boundary and field
C IF1,IF0 - for shear and tensile failure zones
C respectively; =0 if points not entered
C or not contoured; =1 if contoured
C IPTD - identify the IOPORT, MODEL
C XLEN,YLEN - length (in inches) of the contour
C window
C ISEK - initially =0; set to 1 if contour window
C origin or dimensions have been changed
C ISEL - used to select desired functions to
C alter the contour or contouring operation
C XPT,YPT - location on the contour window
C MDL - if a plot is to be written off to a file
C this variable contains the model number
C that the plot will be later output to

C
C Note: several variables used by PLOT88 are defined in the
C user manual and need not be defined here

C
C
C REAL XN(200), YN(200), XPIJ(600), SF(600), X(127), Y(127)
C INTEGER*2 KNXT(600)
C INTEGER IOPORT(4), MODEL(4)
C CHARACTER SYM
C DIMENSION SFGRID(128,128)
C \$INCLUDE:'CONST.INC'
C \$INCLUDE:'PLOT.INC'
C \$INCLUDE:'WIN.INC'
C \$INCLUDE:'PLTPRM.INC'
C \$INCLUDE:'F1CONT.INC'

```
$INCLUDE:'FAIL.INC'
```

```
COMMON /GASCON/ YUPR, PP, ETA
```

```
COMMON /COORD/ XN, YN, INT
```

```
COMMON /BOUND/ X, Y, JNT
```

```
DATA IOPT /97, 9602, 0, 10/, MODEL /97, 30, 5, 30/
```

```
DATA NFCON, IF1, IFO /3*0/
```

```
DATA XLEN, YLEN /2*7./
```

```
NPTS = NFIN + NTFP
```

```
CONV = PI / 180.
```

```
NSM = 0
```

```
JNT = 0
```

```
NF1 = 1
```

```
INT = 1
```

```
10 IPTD = 1
```

```
FACT = 1.
```

```
C
```

```
C
```

```
C
```

```
C
```

```
C
```

The subroutine SCREEN is from FORTRAN UTILITIES and will clear and set the monitor to the desired mode. The argument '3' represents the regular 80 column text mode.

```
CALL SCREEN(3)
```

```
C
```

```
C
```

```
C
```

```
C
```

The contouring window limits are initially set to extreme values which are later redefined.

```
XMIN = 100.
```

```
XMAX = -100.
```

```
YMIN = 100.
```

```
YMAX = -100.
```

```
C
```

```
C
```

```
C
```

```
C
```

The window limits are defined to include all the field points around the cavity.

```
DO 20 I = 1, NUMWIN
```

```
  XMIN = AMIN1(XMIN,XWIN(I))
```

```
  XMAX = AMAX1(XMAX,XWIN(I) + SLWIN(I))
```

```
  YMIN = AMIN1(YMIN,YWIN(I) - SLWIN(I))
```

```
  YMAX = AMAX1(YMAX,YWIN(I))
```

```
20 CONTINUE
```

```
C
```

```
C
```

```
C
```

```
C
```

```
C
```

The contouring window is square so the side length of the window is set to the maximum range of field points, either in the X or Y direction.

```
ALEN = AMAX1(XMAX - XMIN,YMAX - YMIN)
```

```
30 ISEK = 0
```

```
C
```

```
C
```

```
C
```

```
C
```

```
C
```

The GRIDNG subroutine will set the field points up into an array that will be used by a PLOT88 subroutine to contour the safety factors.

```
CALL GRIDNG(XMAX, YMAX, ALEN, SFGRID, XMIN, YMIN, NX, NY)
```

```
XFACT = (XMAX - XMIN) / XLEN
```

```
YFACT = (YMAX - YMIN) / YLEN
```



```

C
C   For lines to be plotted on the monitor, the arrays must
C   contain the values of the origin of the window and the
C   scaling factors entered into the array after the data
C   points.
C
      XOLDB(NFIN + 1) = XMIN
      YOLDB(NFIN + 1) = YMIN
      XOLDB(NFIN + 2) = XFACT
      YOLDB(NFIN + 2) = YFACT
C
C   The PLOTS subroutine requires input regarding the device
C   onto which the data is to be plotted.
C
40 CALL PLOTS(0, IOPORT(IPTD), MODEL(IPTD))
   CALL PLOT(0,0,-3)
   CALL FACTOR(FACT)
C
C   Define the window size, by coordinates, then draw lines
C   around the perimeter.
C
      CALL WINDOW(0, 0, XLEN, YLEN)
      CALL PLOT(0, 0, 3)
      CALL PLOT(0, YLEN, 2)
      CALL PLOT(XLEN, YLEN, 2)
      CALL PLOT(XLEN, 0, 2)
      CALL PLOT(0, 0, 2)
C
C   Plotting the sandstone / siltstone interface, the upper
C   limit to the sandstone bed and the axis of symmetry
C   (Y axis).
C
      CALL OFFSET(XMIN, XFACT, YMIN, YFACT)
      CALL COLOR(10, IERR)
      CALL PLOT(XMIN, XMIN*SIN(ETA*CONV), 13)
      CALL WHERE(XP1, YP1, ZFACT)
      CALL PLOT(XMAX, XMAX*SIN(ETA*CONV), 13)
      CALL PLOT(XP1, YP1, 2)
      CALL PLOT(XMIN, YUPR, 13)
      CALL WHERE(XP1, YP1, ZFACT)
      CALL PLOT(XMAX, YUPR, 13)
      CALL PLOT(XP1, YP1, 2)
      CALL PLOT(0., YMIN, 13)
      CALL WHERE(XP1, YP1, ZFACT)
      CALL PLOT(0., YMAX, 13)
      CALL PLOT(XP1, YP1, 2)
C
      CALL COLOR(7, IERR)
      CALL LINE(XOLDB, YOLDB, NFIN, 1, 1, 15)
C
C   If points have been entered for the tensile failure zone,
C   does the user wish it to be plotted?
C   INKEY is a FORTRAN UTILITY subroutine that can be used to
C   wait for a keyboard key to be pressed, and stores the

```

C character of the key.

```

C
  IF (JNT .EQ. 0 .OR. IF0 .EQ. 0) GO TO 70
  WRITE (*,50)
50  FORMAT (///'  PLOT NEW BOUNDARY? ',\ )
60  IF (INKEY(SYM,SCAN) .EQ. 0) GO TO 60
  WRITE (*,130) SYM
  IF (SYM .EQ. 'Y' .OR. SYM .EQ. 'y') THEN
    X(JNT + 1) = XMIN
    Y(JNT + 1) = YMIN
    X(JNT + 2) = XFACT
    Y(JNT + 2) = YFACT
    CALL COLOR(12, IERR)
    CALL LINE(X, Y, JNT, 1, 0, 0)
  END IF

```

C Prompts the user whether or not to plot the new shear zone
 C contour, if it exists.

```

C
70  IF (NF1 .EQ. 1 .OR. IF1 .EQ. 0) GO TO 100
  WRITE (*,80)
80  FORMAT (///'  PLOT NEW F1 CONTOUR? ',\ )
90  IF (INKEY(SYM,SCAN) .EQ. 0) GO TO 90
  WRITE (*,130) SYM
  IF (SYM .EQ. 'Y' .OR. SYM .EQ. 'y') THEN
    XF1C(NF1 + 1) = XMIN
    YF1C(NF1 + 1) = YMIN
    XF1C(NF1 + 2) = XFACT
    YF1C(NF1 + 2) = YFACT
    CALL COLOR(13, IERR)
    CALL LINE(XF1C, YF1C, NF1, 1, 0, 0)
  END IF

```

C Prompts the user whether or not to plot the old shear zone
 C contour.

```

C
100 WRITE (*,110)
110  FORMAT (///'  PLOT OLD F1 CONTOUR? ',\ )
120  IF (INKEY(SYM,SCAN) .EQ. 0) GO TO 120
  WRITE (*,130) SYM
130  FORMAT (A1,\ )
  IF (SYM .EQ. 'Y' .OR. SYM .EQ. 'y') THEN
    XF1O(NF1O + 1) = XMIN
    YF1O(NF1O + 1) = YMIN
    XF1O(NF1O + 2) = XFACT
    YF1O(NF1O + 2) = YFACT
    CALL COLOR(5, IERR)
    CALL LINE(XF1O, YF1O, NF1O, 1, 0, 0)
  END IF

```

C This subroutine takes the gridded safety factors in SFGRID
 C and smooths the data NSM number of times for smoother
 C contours.

C

```

      CALL ZSMTH(SFGRID, 128, 128, NX, NY, NSM)
      NSM = 0
C
C   This subroutine contours the safety factors.
C
      CALL ZCSEG(SFGRID, 128, 128, NX, NY, 0, 0, XLEN, YLEN,
+             ZLEV, LDIG, LWGT, NLEV, HGT, NDIV, NARC)
C
C   The field points are plotted onto the monitor only, not
C   the plotter or printer.
C
      IF (IPTD .NE. 1) GO TO 150
      SYM = CHAR(3)
      CALL COLOR(14, IERR)
      DO 140 I = 1, NX
        DO 140 J = 1, NY
          IF (SFGRID(I,J) .GT. 1.0E30) GO TO 140
          XPT = XMIN + (I - 1) * (XMAX - XMIN) / FLOAT(NX - 1)
          YPT = YMIN + (J - 1) * (YMAX - YMIN) / FLOAT(NY - 1)
          CALL PLOT(XPT, YPT, 13)
          CALL WHERE(XPT, YPT, ZFACT)
          CALL SYMBOL(XPT, YPT, .12, SYM, 0., -1)
140    CONTINUE
C
C   All points that have failed in tension are plotted on all
C   devices.
C
150  IF (NFLT .EQ. 0) GO TO 170
      SYM = CHAR(15)
      CALL COLOR(12, IERR)
      DO 160 I = 1, NFLT
        CALL PLOT(XFLT(I), YFLT(I), 13)
        CALL WHERE(XPT, YPT, ZFACT)
160  CALL SYMBOL(XPT, YPT, .1, SYM, 0., -1)
C
C   All points that have failed in shear are plotted on all
C   devices.
C
170  IF (NFLS .EQ. 0) GO TO 190
      SYM = CHAR(15)
      CALL COLOR(13, IERR)
      DO 180 I = 1, NFLS
        CALL PLOT(XFLS(I), YFLS(I), 13)
        CALL WHERE(XPT, YPT, ZFACT)
180  CALL SYMBOL(XPT, YPT, .1, SYM, 0., -1)
C
C   Set the monitor into graphics mode for the final plot.
C
190  IF (IPTD .EQ. 1) CALL SCREEN(16)
C
C   When this subroutine is called, the entire plot is put
C   onto the monitor at once.
C
      CALL PLOT(0., 0., 999)

```

```

C
C   If the contouring is completed for this window, press any
C   key to erase the plot and reset the monitor to text mode.
C
      IF (IFO .EQ. 1 .AND. IF1 .EQ. 1) THEN
        CALL LOCATE(0, 0, 0)
200    IF (INKEY(SYM,SCAN) .EQ. 0) GO TO 200
        GO TO 210
      END IF

C
C   If contouring is not complete, call the MSECAL subroutine
C   and mouse can be used to define shear and tensile failure
C   contours.
C
      IF (IPTD .EQ. 1) THEN
        CALL MSECAL(ALEN, XMIN, YMIN, FACT, NFCON)
      END IF

C
C   Menu to select the next option. MS FORTRAN ver. 4.01 is
C   being used so selection #4 allows the user to go back to
C   DOS without quitting the program. Type COMMAND to get into
C   DOS and EXIT to get back into the program. A contour can be
C   redefined if the user does not like the previous attempt.
C   Option #6 will take points entered from the MSECAL
C   subroutine and produce a contour to be plotted. If both
C   contours are complete MSECAL will not be recalled unless
C   specified by option #8 or #9. When both contours are
C   completed, entering #6, continue, the program will leave
C   the contouring phase and produce the input files for the
C   next iteration of the model.
C
210 CALL SCREEN(3)
      WRITE (*,220)
220 FORMAT (//, '  1  PLOT ON NEW DEVICE'//,
+          '  2  CHANGE PLOT SIZE'//,
+          '  3  CHANGE WINDOW SIZE'//,
+          '  4  DOS\> COMMAND / EXIT'//,
+          '  5  REPLOT'//,
+          '  6  CONTINUE'//,
+          '  7  TERMINATE PROGRAM'//,
+          '  8  CONTOUR F=0.0'//,
+          '  9  CONTOUR F=1.0'//,
+          ' 10  SMOOTHING'//, '  ENTER SELECTION: ',\ )
      READ (*,*) ISEL
230 IF (ISEK .EQ. 1 .AND. ISEL .EQ. 5) GO TO 30
      GOTO(280, 310, 330, 360, 40, 370, 380, 240, 250, 260)ISEL

C
C   Enter the coordinates for the tensile failure contour.
C
240 NFCON = 0
      IFO = 0
      INT = 1
      ISEL = 5
      GO TO 230

```

```

C
C   Enter the coordinates for the shear zone contour.
C
250 NFCON = 1
    IF1 = 0
    NF1 = 1
    ISEL = 5
    GO TO 230
C
260 WRITE (*,270)
270 FORMAT (//, '   HOW MANY TIMES TO SMOOTH? ',\ )
    READ (*,*) NSM
    GO TO 40
C
C   Select the desired output device. A plot can be written
C   off to a file to be plotted later. This file will have
C   a name corresponding to this iteration with the extension
C   of .PLT and in binary form. Only one file can be saved per
C   iteration unless option 4 from FORMAT statement 220 is used
C   to enter DOS and rename this file so a new plot can be
C   saved under the .PLT name.
C
280 WRITE (*,290)
290 FORMAT (//, ' PLOTTING DEVICE: ',\ ,
+         '      1  SCREEN' /\ ,
+         '      2  PLOTTER' /\ ,
+         '      3  PRINTER' /\ ,
+         '      4  FILE' /\ , ' ENTER SELECTION: ',\ )
    READ (*,*) IPTD
    IF (IPTD .EQ. 4) THEN
        WRITE (*,300)
300    FORMAT (//, ' ENTER MODEL: ',\ )
        READ (*,*) MDL
        MODEL(4) = MODEL(MDL)
        OPEN (90,FILE=FILE//'.PLT',FORM='BINARY')
    END IF
    GO TO 210
C
C   Reduce or enlarge a window by the desired FACTor.
C
310 WRITE (*,320)
320 FORMAT (//, ' ENTER FACTOR: ',\ )
    READ (*,*) FACT
    GO TO 210
C
C   Set the limits to the window size.
C
330 WRITE (*,340) XMIN, YMIN, XMAX, YMAX
340 FORMAT (//, ' XMIN = ', F8.3, ' YMIN = ', F8.3, /
+         ' XMAX = ', F8.3, ' YMAX = ', F8.3)
    WRITE (*,350)
350 FORMAT (//, ' ENTER XMIN,YMIN,ALEN', /\ ' ',\ )
    READ (*,*) XMIN, YMIN, ALEN
    ISEK = 1

```

```

      GO TO 210
C
C   Allow to enter DOS. Useful to look up specific values in
C   in the .OUT or .LST files.
C
360 PAUSE ' '
      GO TO 210
C
C   Convert the entered coordinates from the MSECAL subroutine
C   to a symmetric contour.
C
370 IF (IFO .EQ. 1 .AND. IF1 .EQ. 1) RETURN
      IF (IFO .EQ. 0 .AND. INT .GT. 1) THEN
C
C   SYMET is called to take the entered coordinates and produce
C   a contour of equal length elements. The results from this
C   subroutine will become the new boundary for input to the
C   boundary element program.
C
      CALL SYMET
      IFO = 1
      END IF
      IF (IF1 .EQ. 0 .AND. NF1 .GT. 1) THEN
C
C   F1CONT takes the coordinates entered defining the shear
C   zone and produces a symmetric contour around the opening.
C
      CALL F1CONT
      IF1 = 1
      END IF
      IF (IFO .EQ. 0 .AND. IF1 .EQ. 1) NFCON = 0
      IF (IFO .EQ. 1 .AND. IF1 .EQ. 0) NFCON = 1
      GO TO 10
C
380 STOP
      END

```

```

SUBROUTINE GRIDNG(XMAX,YMAX,ALEN,SFGRID,XMIN,YMIN,NX,NY)
C
C This subroutine takes all the field points and stores their
C safety factors in a two-dimensional array that will later
C be used by PLOT88 subroutines to contour the safety
C factors. All the field points from the boundary element
C program must be equally spaced when combining points from
C more than one window. The coordinates are converted to
C positions within the array for the final contour window.
C
C Called from ROUTINE CONTUR
C
C Local variables: KL - counts the number of field points
C                   within the contour window
C                   NWIN - NUMWIN-1
C                   XCAL,YCAL - coordinates of points being
C                               counted across the contour window
C                   MXP,MYP - number of points across the contour
C                               window
C                   XDIST,YDIST - distance between X,YMIN & X,YCAL
C                   K,L - convert X and Y coordinate, respectively,
C                           into positions within array SFGRID
C
C
C   REAL SFGRID(128,128)
C   REAL*8 DLEN
C $INCLUDE:'WIN.INC'
C $INCLUDE:'PLOT.INC'
C $INCLUDE:'CONST.INC'
C   DATA MXP,MYP /2*0/, IA /1/, IB /128/, XDIST,YDIST /2*10./
C
C From the side length of a field point window and the
C number of points along that side, the distance between
C points can be found (DLEN).
C
C   IF (KWIN(1) .EQ. 2) NWIN = 20
C   IF (KWIN(1) .NE. 2) NWIN = 10
C   DLEN = DBLE(SLWIN(1)/FLOAT(NWIN))
C
C Determine the maximum number of points (separated by a
C distance of DLEN) required in the X direction. This will
C be stored in MXP.
C
C   DO 10 I = IA, IB
C     XCAL = XMIN + DLEN * FLOAT(I - 1)
C     IF (XDIST .GT. ABS(XMIN - XCAL)) THEN
C       XDIST = ABS(XMIN - XCAL)
C       MXP = I
C     END IF
C 10 CONTINUE
C
C Determine the maximum number of points (separated by a
C distance of DLEN) required in the Y direction. This will
C be stored in MYP.

```

```

C
DO 20 I = IA, IB
  YCAL = YMIN + DLEN * FLOAT(I - 1)
  IF (YDIST .GT. ABS(YMIN - YCAL)) THEN
    YDIST = ABS(YMIN - YCAL)
    MYP = I
  END IF
20 CONTINUE

C
C From the desired width of contour, ALEN, and the distance
C between points, DLEN, the number of points in the
C contouring window can be found and stored in NX and NY,
C since a square window is being used. The minimum and
C maximum points are then found.
C
  NX = ANINT(ALEN/DLEN) + 1.0001
  NY = NX
  XMIN = DBLE(XMIN+DLEN*FLOAT(MXP-1))
  YMIN = DBLE(YMIN+DLEN*FLOAT(MYP-1))
  XMAX = DBLE(XMIN+DLEN*FLOAT(MXP-1))+DLEN * FLOAT(NX-1)
  YMAX = DBLE(YMIN+DLEN*FLOAT(MYP-1))+DLEN * FLOAT(NY-1)
  ALEN = DLEN * FLOAT(NX - 1)

C
C Any point outside this contouring window is given the value
C 1.E35, which the contouring subroutine will not contour in.
C
  DO 30 J = 1, NY
    DO 30 I = 1, NX
30 SFGRID(I,J) = 1.0E35

C
C The coordinates of the field points within the window will
C be converted to locations within the array to store the
C safety factors.
C
  KL = 0
  DO 40 I = NFIN + 1, NFIN + NTFP
    X = XCONT(I)
    Y = YCONT(I)
    IF ((X - XMAX).LT.0.01.AND.(XMIN - X).LT.0.01 .AND.
      + (Y - YMAX).LT.0.01.AND.(YMIN - Y).LT.0.01) THEN
      K = (X - XMIN) * (NX - 1) / (XMAX - XMIN) + 1.01
      L = (Y - YMIN) * (NY - 1) / (YMAX - YMIN) + 1.01
      SFGRID(K,L) = SFCAL(S1(I),S3(I),X,Y,1)
      KL = KL + 1
    END IF
  40 CONTINUE

C
  RETURN
  END

```



```

SUBROUTINE MSECAL(ALEN, XMIN, YMIN, FACT, NFCON)
C
C This subroutine contains all the calls to the MOUSES
C subroutine for manually contouring the tensile and shear
C failure zones. This subroutine sets up the cursor on the
C monitor and allows the user to move the cursor with the
C mouse and coutour the desired zone. The M1 argument of the
C subroutine controls the type of function to be carried out.
C
C Called from ROUTINE CONTUR
C
C ROUTINES called: MOUSES
C                  MSLAST
C                  MSEWRT
C                  MSSTOR
C
C Local variables: CURSOR - array defining graphics cursor
C                  shape
C                  M1,M2,M3,M4 - parameters used by MOUSES
C                  ROUTINE
C
C      EXTERNAL MOUSES
C      REAL XN(200), YN(200)
C      INTEGER*2 CURSOR(16,2)
C $INCLUDE:'F1CONT.INC'
C      COMMON /COORD/ XN, YN, INT
C      DATA CURSOR/ 16*65535, 32768, 57344, 63488, 65024,
C      +             3072, 1536, 10* 0/
C
C      Call for a graphics cursor for the monitor with a shape
C      defined by the binary data in the CURSOR array.
C
C      M1 = 9
C      M2 = 0
C      M3 = 0
C      CALL MOUSES(M1, M2, M3, CURSOR(1,1))
C      M1 = 1
C
C      Show the cursor.
C
C      CALL MOUSES(M1, M2, M3, M4)
C      calls to FUNCTION 5 to set M2 (button presses) to zero
C      M1 = 5
C      M2 = 0
C      CALL MOUSES(M1, M2, M3, M4)
C      M1 = 5
C      M2 = 1
C      CALL MOUSES(M1, M2, M3, M4)
C
C      Set minimum and maximum positions that the cursor can move
C      in the horizontal direction on the monitor. 448 pixels
C      corresponds to seven inches on an IBM PS/2 MODEL 60, VGA
C      graphics card. Minimum point is 0 and the maximum is 448,
C      from left to right. FACT is a plotting scaling factor used

```

```

C   by PLOT88.
C
C       M1 = 7
C       M3 = 0
C       M4 = 448 * FACT
C       CALL MOUSES(M1, M2, M3, M4)
C
C   Set minimum and maximum positions that the cursor can move
C   in the vertical direction on the monitor. 314 pixels
C   corresponds to seven inches on an IBM PS/2 MODEL 60, VGA
C   graphics card. Minimum point is 35 and the maximum is 349,
C   from top to bottom.
C
C       M1 = 8
C       M3 = 349 - 314 * FACT
C       M4 = 349
C       CALL MOUSES(M1, M2, M3, M4)
C
C   Set mouse cursor to last entered point. This is used when
C   contouring in sections and viewing different areas of the
C   contoured window.
C
C       IF (NFCN .EQ. 1) GO TO 10
C
C   This subroutine writes out the final point entered when
C   contouring the tensile failure zone.
C
C       CALL MSLAST(XN(INT-1),YN(INT-1),XMIN,YMIN,ALEN,FACT)
C       GO TO 20
C
C   This subroutine writes out the final point entered when
C   contouring the sheared zone.
C
C   10 CALL MSLAST(XF1(NF1-1),YF1(NF1-1),XMIN,YMIN,ALEN,FACT)
C
C   The LOCATE subroutine is from the FORTRAN UTILITIES which
C   allows the user to specify the location of the cursor on
C   the monitor. In this case, the cursor is placed on the
C   last entered point of contouring.
C
C   20 CALL LOCATE(0, 0, 40)
C       WRITE (*,60) NFCN
C   60 FORMAT(' CONTOURINGF=' ,11,' .0' ,\ )
C
C   30 M1 = 3
C       CALL MOUSES(M1, M2, M3, M4)
C
C   This subroutine continuously writes out, on the monitor,
C   the present position of the cursor.
C
C       CALL MSEWRT(M3, M4, ALEN, XMIN, YMIN, FACT)
C
C   Check if the right button has been pressed. If so, exit
C   this phase of entering contour points. GOTO 30.

```

```

C
  M1 = 5
  M2 = 1
  CALL MOUSES(M1, M2, M3, M4)
  IF (M2 .NE. 0) GO TO 50
C
C   Check if the left button has been pressed. If not, GOTO 21.
C   This iterating allows for the continued writing out of the
C   cursor position to the monitor.
C
  M1 = 5
  M2 = 0
  CALL MOUSES(M1, M2, M3, M4)
  IF (M2 .EQ. 0) GO TO 30
C
C   If the left button was pressed, the coordinates will be
C   stored by the subroutine MSSTOR if contouring the tensile
C   failure zone - (NFCN = 0), into XN and YN
C
  IF (NFCN .EQ. 1) GO TO 40
  CALL MSSTOR(M3,M4,ALEN,FACT,XMIN,YMIN,XN(INT),YN(INT))
  INT = INT + 1
  GO TO 20
C
C   If the shear zone is being contoured, the position the
C   button was last pushed will be stored into XF1 and YF1.
C
  40 CALL MSSTOR(M3,M4,ALEN,FACT,XMIN,YMIN,XF1(NF1),YF1(NF1))
  NF1 = NF1 + 1
C
C   This cycling continues until all the desired points are
C   entered and the right button is pushed.
C
  GO TO 20
C
  50 RETURN
  END

```

```
SUBROUTINE MSEWRT(M3, M4, ALEN, XMIN, YMIN, FACT)
```

```
Writes out the X and Y location of the cursor on the
monitor. The X and Y points from the mouse are converted
to the actual coordinates of the plot.
```

```
Called from ROUTINE MSECAL
MSLAST
```

```
Local variables: X,Y - coordinates of the cursor in inches
with respect to the original plot
```

```
X = (REAL(M3)*ALEN/448.) / FACT + XMIN
Y = (REAL(349 - M4)*ALEN/314.) / FACT + YMIN
CALL LOCATE(0, 0, 0)
WRITE (*,10) X, Y
10 FORMAT('X=',F8.3,' Y =',F8.3,\)
RETURN
END
```

```
-----
SUBROUTINE MSLAST(X, Y, XM, YM, A, F)
```

```
Writes out, on the monitor, the location of the last point
entered by the mouse. The cursor is then set to that
position.
```

```
Called from ROUTINE MSECAL
```

```
ROUTINES called: MSEWRT
```

```
Local variables: X,Y - coordinates of the last entered
point
XM,YM - XMIN,YMIN
A - ALEN
F - FACT
```

```
M1 = 4
M3 = NINT((X - XM)*F*448./A)
M4 = NINT(349. - ((Y - YM)*F*314./A))
CALL MOUSES(M1, M2, M3, M4)
CALL MSEWRT(M3, M4, A, XM, YM, F)
CALL LOCATE(0, 1, 0)
WRITE (*,10) X, Y
10 FORMAT(' LAST POINT ENTERED: X =', F8.3,', Y =', F8.3,\)
RETURN
END
```

```

SUBROUTINE MSSTOR(M3, M4, A, F, XM, YM, X, Y)

```

```

C Stores the coordinates of the contours into their
C respective arrays. This must be done in a separate
C subroutine because the MOUSE routines store the entered
C points in a manner that would conflict with other data
C stored in computer RAM.

```

```

C Called from ROUTINE MSECAL

```

```

C Local variables: X,Y - coordinates of the last entered
C point

```

```

C XM,YM - XMIN,YMIN

```

```

C A - ALEN

```

```

C F - FACT

```

```

C X = (REAL(M3)*A/448.) / F + XM

```

```

C Y = (REAL(349 - M4)*A/314.) / F + YM

```

```

C CALL LOCATE(0, 1, 0)

```

```

C WRITE (*,10) X, Y

```

```

10 FORMAT(' LAST POINT ENTERED: X =', F8.3,', Y =', F8.3,\)

```

```

C RETURN

```

```

C END

```

SUBROUTINE SYMET

This subroutine takes the coordinates that have been entered for tensile zone contour and produces a symmetrical boundary. When the points are initially entered using the mouse, only the points on the right side of the cavity are required, the left side is produced here as a mirror image of the right. This guarantees the symmetry of the problem.

Called from ROUTINE CONTUR

ROUTINES called: DIST
ANGLE

Local variables: DIS - distance between two points
TH - angle of the boundary element defined by length DIS
B - Y intercept for the equation defining the boundary element
SA1,SA2,SA3 - side lengths of a triangle
A1,A2,A3 - included angle between adjacent sides of the triangle
T2,T3 - absolute angle of the side lengths of the triangle (counter-clockwise from 3:00 is positive.)

```
REAL XN(200), YN(200), X(127), Y(127)
$INCLUDE:'CONST.INC'
$INCLUDE:'PLOT.INC'
COMMON /COORD/ XN, YN, INT
COMMON /BOUND/ X, Y, JNT
```

The first point entered when contouring the tensile zone is the point at which the contour deviates from the original opening. In terms of an outburst, this is where the ejected tensile material is forced through the shear zone at the boundary. This loop finds the closest boundary point to this first point entered. The old boundary is stored in XOLDB and YOLDB. XN and YN contain the points entered from the mouse.

```
DIS = 100.
DO 10 I = 1, NFIN
  IF (DIS .GT. DIST(XN(1),YN(1),XOLDB(I),YOLDB(I))) THEN
    JNT = I
    DIS = DIST(XN(1),YN(1),XOLDB(I),YOLDB(I))
  END IF
10 CONTINUE
XN(1) = XOLDB(JNT)
YN(1) = YOLDB(JNT)
```

This loop takes the series of points entered by the mouse and produces a set of evenly spaced coordinates (of length

C ELLEN) that will represent the new boundary. These
 C coordinates are stored in arrays X and Y.
 C

```

DO 30 I = 2, INT
20 IF (DIST(XN(I),YN(I),X(JNT),Y(JNT)) .LT. ELLEN) GOTO 30
  SA1 = ELLEN
  SA2 = DIST(XN(I - 1),YN(I - 1),X(JNT),Y(JNT))
  T2 = ANGLE(XN(I - 1),YN(I - 1),X(JNT),Y(JNT))
  T3 = ANGLE(XN(I - 1),YN(I - 1),XN(I),YN(I))
  A2 = T2 - T3
  A3 = ASIN(SA2/SA1*SIN(A2))
  A1 = ACOS(-COS(A2 + A3))
  SA3 = SA1 * COS(A3) + SA2 * COS(A2)
  JNT = JNT + 1
  X(JNT) = XN(I - 1) + COS(T3) * SA3
  Y(JNT) = YN(I - 1) + SIN(T3) * SA3
  IF (ABS(Y(JNT)) .LT. 0.01) Y(JNT) = 0.
  IF (X(JNT) .LT. 0.) GO TO 40
  GO TO 20
30 CONTINUE

```

C The final point used to define the right side of the cavity
 C is on the Y-AXIS. If the distance between this point and
 C the previous point is less than half the element length,
 C the previous point is eliminated and one longer element
 C is made.
 C

```

40 TH = ANGLE(X(JNT - 1),Y(JNT - 1),X(JNT),Y(JNT))
  B = Y(JNT) - X(JNT) * TAN(TH)
  X(JNT) = 0.
  Y(JNT) = X(JNT) * TAN(TH) + B
  IF (DIST(X(JNT),Y(JNT),X(JNT-1),Y(JNT-1)) .LT. ELLEN/2.)
  + THEN
    JNT = JNT - 1
    X(JNT) = X(JNT + 1)
    Y(JNT) = Y(JNT + 1)
  END IF

```

C This loop now completes the mirror image of the right side
 C to the left and ends when the cavity is fully defined.
 C

```

  K = JNT - 1
  DO 50 J = K, 1, -1
    JNT = JNT + 1
    X(JNT) = X(J) * (-1.)
    Y(JNT) = Y(J)
    IF (X(JNT) .EQ. X(1) .AND. Y(JNT) .EQ. Y(1)) GOTO 60
50 CONTINUE

```

C
 C 60 RETURN
 C END

SUBROUTINE F1CONT

```

C
C   This subroutine does for the shear zone what SYMET did for
C   the tensile zone. The left side of the cavity is made a
C   mirror image of the right. However, the sides defining the
C   contour need not be the same length.
C
C   Called from ROUTINE CONTUR
C
C   ROUTINES called ANGLE
C
C   Local variables: DIS - distance between two points
C
C   $INCLUDE:'PLOT.INC'
C   $INCLUDE:'CONST.INC'
C   $INCLUDE:'F1CONT.INC'
C
C   The first point entered by the contouring is where the new
C   shear zone deviates from the old. The closest point is
C   found.
C
      DIS = 100.
      DO 10 I = 1, NF10
        IF (DIS .GT. DIST(XF1(1),YF1(1),XF10(I),YF10(I))) THEN
          JNT = I
          DIS = DIST(XF1(1),YF1(1),XF10(I),YF10(I))
        END IF
      10 CONTINUE
C
C   All the points defining the old shear zone prior to the
C   deviation are stored into arrays XF1C and YF1C.
C
      DO 20 I = 1, JNT
        XF1C(I) = XF10(I)
      20 YF1C(I) = YF10(I)
C
C   The points entered by the contouring with the mouse are
C   now into the same variables as above.
C
      30 DO 40 I = 2, NF1
        IF (XF1(I) .LT. 0.) GO TO 50
        XF1C(JNT + I - 1) = XF1(I)
      40 YF1C(JNT + I - 1) = YF1(I)
C
C   The shear contour on the left side of the cavity is now
C   made a mirror image of the right.
C
      50 I = I - 2
      K = JNT + I
      KK = JNT + I
      DO 60 J = KK, 1, -1
        K = K + 1
        XF1C(K) = XF1C(J) * (-1.)

```



```
      YF1C(K) = YF1C(J)
      IF (XF1C(K) .EQ. XF1C(1) .AND. YF1C(K) .EQ. YF1C(1))
+      GO TO 70
60 CONTINUE
C
C  NF1 is the total number of shear points defining the shear
C  zone.
C
70 NF1 = K - 1
   RETURN
   END
```

```

C      FUNCTION DIST(X1, Y1, X2, Y2)
C      This is a function to calculate the distance between two
C      points.
C      Called from ROUTINE SYMET
C      F1CONT
C      Local variables: X1,Y1 - coordinates of first point
C      X2,Y2 - coordinates of second point
C
C      DIST = SQRT((X1 - X2)**2 + (Y1 - Y2)**2)
C      RETURN
C      END
C
C      -----
C      FUNCTION ANGLE(X1, Y1, X2, Y2)
C      This subroutine defines the angle between any two points
C      where the angle of 0 degrees points at three o'clock and
C      counter - clockwise is the positive angle.
C      Called from ROUTINE SAFCON
C      SYMET
C      Local variables: X1,Y1 - coordinates of first point
C      X2,Y2 - coordinates of second point
C      XX,YY - distance between two points in X
C      and Y components
C
C      $INCLUDE:'CONST.INC'
C      XX = X2 - X1
C      YY = Y2 - Y1
C      IF (XX .EQ. 0.0 .AND. YY .GE. 0.) THEN
C          ANGLE = PI / 2.
C          RETURN
C      ELSE IF (XX .EQ. 0.0 .AND. YY .LT. 0.) THEN
C          ANGLE = 3. * PI / 2.
C          RETURN
C      END IF
C      ANGLE = ATAN(YY/XX)
C      IF (XX .LT. 0.) THEN
C          ANGLE = ANGLE + PI
C          RETURN
C      ELSE IF (XX .GT. 0.0 .AND. YY .LT. 0.) THEN
C          ANGLE = ANGLE + 2. * PI
C          RETURN
C      END IF
C      RETURN
C      END

```

C The following three subroutines were written to override
C the subroutines from PLOT88. A call to one PLOT88
C subroutine sets the monitor into graphics mode, plots the
C figure, and then one key press will erase the plot as the
C screen mode changes back to text. The following
C subroutines (that also appear in PLOT88) will now prevent
C the plot from being erased and allow user contouring of
C the shear and tensile zones.
C
C

C -----
C SUBROUTINE MESSAGE

C The PLOT88 version of this subroutine causes a message to
C be displayed to strike any key to continue.
C
C RETURN
C END

C -----
C SUBROUTINE STMODE

C The PLOT88 version of this subroutine causes the screen
C mode to change from graphics to text. FORTRAN UTILITIES
C will be used to do this within the CONTUR subroutine when
C required.
C
C RETURN
C END

C -----
C SUBROUTINE WAITKY

C The PLOT88 version of this subroutine waits for a key to
C be pressed to erase the plot off the monitor.
C
C RETURN
C END

```

C   The following six files are the include files containing
C   COMMON blocks for different aspects of the program
C
C   -----
C   CONST.INC - contains a string of constants used by most
C               subroutines.
C
C       REAL BND(126,6),FLD(500,5)
C       COMMON /CONST/ PI,REP,FRICL,FRICU,ELLEN,NSTRT,NFIN,NTFP
C       COMMON /FINDEX/ BND,FLD
C
C   -----
C   PLOT.INC - contains the coordinates of boundary elements
C               and field points to be plotted. Principal
C               stresses are also passed.
C
C       REAL XOLDB(127),YOLDB(127),XCONT(600),YCONT(600)
C       REAL S1(600),S3(600)
C       COMMON /STRESS/ XOLDB,YOLDB,XCONT,YCONT,S1,S3,NUMBSF
C
C   -----
C   PLTPRM.INC - contains plotting parameters used by PLOT88
C               subroutines.
C
C       REAL ZLEV(51)
C       INTEGER*2 LDIG(51)
C       INTEGER LWGT(51)
C       COMMON /PLTPRM/ NLEV,HGT,NARC,NDIV,ZLEV,LDIG,LWGT
C
C   -----
C   WIN.INC - contains the coordinates and side length of the
C               windows of field points.
C
C       REAL XWIN(10),YWIN(10),SLWIN(10)
C       INTEGER KWIN(10)
C       COMMON /WIND/ XWIN,YWIN,SLWIN,KWIN,NUMWIN
C
C   -----
C   F1CONT.INC - contains the arrays containing the coordinates
C               of the old shear zone, new shear zone and the
C               points entered by the mouse (right side of
C               cavity only).
C
C       REAL XF1(180),YF1(180),XF1C(200),YF1C(200)
C       REAL XF1O(200),YF1O(200)
C       COMMON /F1OLD/ XF1O,YF1O,NF1O
C       COMMON /F1BND/ XF1C,YF1C,XF1,YF1,NF1
C
C   -----
C   FAIL.INC - contains array that store the coordinates of
C               points that have failed in shear and tension.
C
C       REAL XFLS(40),YFLS(40),XFLT(40),YFLT(40)
C       COMMON /FAIL/ XFLS,YFLS,NFLS,XFLT,YFLT,NFLT

```

Appendix F - Sample Input and Output For Computer Programs

The following are sample input and output files for the computer programs used in the model. The first will be the files for the boundary element program BESOL/P5005 (version 1.1) then SAFCON. The complete listing of the file will be given with a description of the contents. The P5005 program allows several options for the type of evaluation desired. Any item that is not related to the operation of the program as required by the model, will not be explained. The files presented here are those from Figure 7.5c, Sample Run: Iteration #3, page 47.

A note on the filing system used for these runs. With the hundreds of computer runs carried out, some sort of organized filing system was required. First, to designate the files in a given run, the following file extensions were used: .DAT is the boundary element program input file, .OUT is the boundary element program output file, .LST is the output file from SAFCON containing effective stresses and safety factors and .F1 is an output file from SAFCON containing the coordinates of the shear zone. The user has the option to write off the plot to a file to be printer or plotter later. This file has the extension .PLT and is in binary code. SAFCON outputs the next .DAT file which is input for the next iteration of P5005. All files are in the form RUNaFb.ext where '.ext' are the extensions listed above, 'b' is a two-digit file number that is incremented by one for each iteration and 'a' is a character which represents a given field stress condition. The value of 'a' is arbitrarily chosen for a given stress field and all computer runs with that stress field will use that value of 'a'. For a set of runs, the initial file number is chosen by the user, and from there on, SAFCON increments it by one for each iteration, until that series of runs is completed.

The file DATFILE contains the name of the file (in the form RUNaFb) to be run. The file RUN.INP is an input file for the P5005 program containing the input sequence required to run that program. The run command is P5005 <RUN.INP . This is convenient for running the model in batch mode.

Input file for P5005 - filename: RUNFF32.DAT

```

1  RUNFF32-FINAL ROCK PROPERTIES-K=1.0-GAS PRESSURE=6.6MPa
2      2      1      0      0
3      0 68      2      2      3
4      .36 26150.      .18 18500.      0.      0.      0.      0.      0.
5      25.000      .000 25.000      .000      .000      .000
6      50.5 4.2 1.00 48.4 19.9 1.00
7      8      1 -2.250      .000 -2.250 -2.000      0.      0.
8      18      1 -2.250 -2.000      2.250 -2.000      0.      0.
9      8      1      2.250 -2.000      2.250      .000      0.      0.
10     1      1      2.250      .000      2.348      .230      0.      0.
11     1      1      2.348      .230      2.408      .473      0.      0.
12     1      1      2.408      .473      2.439      .721      0.      0.
13     1      1      2.439      .721      2.419      .970      0.      0.
14     1      1      2.419      .970      2.383      1.217      0.      0.
15     1      1      2.383      1.217      2.276      1.443      0.      0.
16     1      1      2.276      1.443      2.157      1.663      0.      0.
17     1      1      2.157      1.663      2.009      1.865      0.      0.
18     1      1      2.009      1.865      1.823      2.032      0.      0.
19     1      1      1.823      2.032      1.618      2.176      0.      0.
20     1      1      1.618      2.176      1.407      2.309      0.      0.
21     1      1      1.407      2.309      1.180      2.414      0.      0.
22     1      1      1.180      2.414      .945      2.498      0.      0.
23     1      1      .945      2.498      .705      2.570      0.      0.
24     1      1      .705      2.570      .459      2.614      0.      0.
25     1      1      .459      2.614      .211      2.642      0.      0.
26     1      1      .211      2.642      .000      2.654      0.      0.
27     1      1      .000      2.654      -.211      2.642      0.      0.
28     1      1      -.211      2.642      -.459      2.614      0.      0.
29     1      1      -.459      2.614      -.705      2.570      0.      0.
30     1      1      -.705      2.570      -.945      2.498      0.      0.
31     1      1      -.945      2.498      -1.180      2.414      0.      0.
32     1      1      -1.180      2.414      -1.407      2.309      0.      0.
33     1      1      -1.407      2.309      -1.618      2.176      0.      0.
34     1      1      -1.618      2.176      -1.823      2.032      0.      0.
35     1      1      -1.823      2.032      -2.009      1.865      0.      0.
36     1      1      -2.009      1.865      -2.157      1.663      0.      0.
37     1      1      -2.157      1.663      -2.276      1.443      0.      0.
38     1      1      -2.276      1.443      -2.383      1.217      0.      0.
39     1      1      -2.383      1.217      -2.419      .970      0.      0.
40     1      1      -2.419      .970      -2.439      .721      0.      0.
41     1      1      -2.439      .721      -2.408      .473      0.      0.
42     1      1      -2.408      .473      -2.348      .230      0.      0.
43     1      1      -2.348      .230      -2.250      .000      0.      0.
44     -.60      5.00      3.00      1
45     1.80      2.60      3.00      1

```

The parameters of the data file on the preceding page will be defined line by line (line numbers are included for convenience). A description will be given for the relevant parameters only. The variable names are found to the right of the line numbers.

line 1 TITLE or description of the problem analysed, allowed 80 characters

control parameters

line 2 KPROB (=2) the type of problem that will relax the stresses on the boundary elements to zero. (KPROB = 1 is a simulation of mining or sequential excavation.)

 NSTEPS number of increments of stress relaxation on the boundary

 NUMSTV required if considering artificial support

 NFILL required if considering backfill

control parameters

line 3 NUMBSD (=0) number of displacement discontinuity elements used

 NUMBFS number of fictitious stress element used. This element type is used to to define boundary element around an excavation.

 KFAIL type of failure criterion used (1 = Mohr-Coulomb and 2 = Hoek and Brown)

 KDREF a reference point for displacements, ie. all displacements will be given with respect to a defined point (given on line 4)

elastic properties of rock mass

line 4 PRL Poisson's ratio of lower material

 EL Elastic modulus of lower material

 PRU Poisson's ratio of upper material

 EU Elastic modulus of upper material

 ETA angle of inclination of interface of the two materials. In this model, the angle is always 0°, to keep symmetry about the Y-axis.

 XREF x coordinate of displacement reference point

 YREF y coordinate of displacement reference point

 UXFIX value of the x-displacement at the reference point

 UYFIX value of the y-displacement at the reference point

insitu stress field

line 5 AXX horizontal field stress at $y=0$.
 BXX rate of change of horizontal stress with depth
 AYY vertical field stress at $y=0$.
 BYY rate of change of vertical stress with depth
 AXY shear stress at $y=0$.
 BXY rate of change of shear stress with depth

failure criterion - Hoek and Brown parameters

line 6 UCSL uniaxial compressive strength of lower material
 HBML parameter 'm' of lower material
 HBSL parameter 's' of lower material
 UCSU uniaxial compressive strength of upper material
 HBMU parameter 'm' of upper material
 HBSU parameter 's' of upper material

define excavation opening and boundary conditions

line 7-43 NUM number of element into which this segment is to be divided
 CODE boundary conditions imposed on the boundary element: $KODE=1$,
 relax normal and shear stresses to prescribed values given later by BVS
 and BVN.
 XBEG x coordinate of the start point of line segment
 YBEG y coordinate of the start point of line segment
 XEND x coordinate of the end point of line segment
 YEND y coordinate of the end point of line segment
 BVS resulting shear stress on boundary element
 BVN resulting normal stress on boundary element

define location and type of field point window

line 44,45 XWIN x coordinate of upper left corner of field point window
 YWIN y coordinate of upper left corner of field point window
 SLWIN side length of window
 KWIN type of window (1 is an 11x11 point square grid, 2 is a 21x21 square
 grid, 3 is a horizontal line of 11 points, and 4 is a vertical line of 11
 points).

The following is a listing of the boundary element output file RUNFF32.OUT. Very little needs to be said about the output file, it is all self explanatory. First are the ownership details of the program, then a descriptive listing of the input data, then the results; first from the boundary elements, then from each of the field point windows. The variables used as headings for the boundary and field point results are defines below.

X,Y	coordinates of the midpoints of the boundary elements and mid points
UX,UY	displacements in the X and Y directions
US,UN	shear and normal displacements of the boundary elements
SXX,SYY,SXY	stresses in the X and Y directions and the associated shear stresses
SS,SN,ST	shear, normal and tangential stresses on the boundary element
FI	failure index defined by the Crouch Research Inc.
EXX,EYY,EXY	strains in the X and Y directions and associated shear strain
S1,S2	major and minor principal stresses
TH1	the angle of the major principal to the positive X axis, counter-clock-wise is positive

The BESOL System: Boundary Element Solutions
for Rock Mechanics Problems

BESOL/P5005 version 1.1

Serial Number: 3057660636071

Registered Owner: THE UNIVERSITY OF ALBERTA
DEPT. OF MINERAL ENGINEERING
EDMONTON, ALBERTA, CANADA

(C) Copyright Crouch Research, Inc. 1985, 1986.

Portions (C) Copyright Microsoft Corporation 1981, 1983, 1984, 1985.

All Rights Reserved.

RUNFF32 - FINAL ROCK PROPERTIES - K=1.0 - GAS PRESSURE=6.6MPa

FILE NAMES:

RUNFF32.DAT (INPUT DATA FILE)
RUNFF32.OUT (OUTPUT FILE)

KIND OF PROBLEM BEING SOLVED = TYPE 2 (STEPWISE RELAXATION OF RESULTANT BOUNDARY TRACTION TO ZERO)
NUMBER OF STRAIGHT LINE BOUNDARY SEGMENTS USED TO DEFINE DISPLACEMENT DISCONTINUITY ELEMENTS (NUMBSD) = 0
NUMBER OF STRAIGHT LINE BOUNDARY SEGMENTS USED TO DEFINE FICTITIOUS STRESS ELEMENTS (NUMBSF) = 68
NUMBER OF WINDOWS FOR FIELD POINT CALCULATIONS (NUMWIN) = 2

INCLINATION OF INTERFACE, ETA = .00 DEGREES

ELASTIC CONSTANTS FOR LOWER HALF-PLANE (Y' LE O) -

POISSON'S RATIO = .36
YOUNG'S MODULUS = .2615E+05

ELASTIC CONSTANTS FOR UPPER HALF-PLANE (Y' GE O) -

POISSON'S RATIO = .18
YOUNG'S MODULUS = .1850E+05

ROCK FAILURE PARAMETERS FOR LOWER HALF-PLANE (Y' LE O) -

UNIAXIAL COMPRESSIVE STRENGTH OF INTACT ROCK = .5050E+02
HOEK-BROWN FAILURE PARAMETERS: M = 4.20 S = 1.0000

ROCK FAILURE PARAMETERS FOR UPPER HALF-PLANE (Y' GE O) -

UNIAXIAL COMPRESSIVE STRENGTH OF INTACT ROCK = .4840E+02
 HOEK-BROWN FAILURE PARAMETERS: M = 19.90 S = 1.0000

XX-COMPONENT OF FIELD STRESS = .2500E+02 + (.0000E+00)*Y

YY-COMPONENT OF FIELD STRESS = .2500E+02 + (.0000E+00)*Y

XY-COMPONENT OF FIELD STRESS = .0000E+00 + (.0000E+00)*Y

THE DISPLACEMENT UY = UYFIX = .0000 IS GIVEN AT THE POINT X = XREF = .0, Y = YREF = .0

BOUNDARY ELEMENT DATA, FICTITIOUS STRESS ELEMENTS.

ELEMENT	KODE	XBEG	YBEG	XEND	YEND	LENGTH	ANGLE	BVS	BVN
1	1	-2.3	.0	-2.3	-.3	.25	-90.00	.0000E+00	.0000E+00
2	1	-2.3	-.3	-2.3	-.5	.25	-90.00	.0000E+00	.0000E+00
3	1	-2.3	-.5	-2.3	-.8	.25	-90.00	.0000E+00	.0000E+00
4	1	-2.3	-.8	-2.3	-1.0	.25	-90.00	.0000E+00	.0000E+00
5	1	-2.3	-1.0	-2.3	-1.3	.25	-90.00	.0000E+00	.0000E+00
6	1	-2.3	-1.3	-2.3	-1.5	.25	-90.00	.0000E+00	.0000E+00
7	1	-2.3	-1.5	-2.3	-1.8	.25	-90.00	.0000E+00	.0000E+00
8	1	-2.3	-1.8	-2.3	-2.0	.25	-90.00	.0000E+00	.0000E+00
9	1	-2.3	-2.0	-2.0	-2.0	.25	.00	.0000E+00	.0000E+00
10	1	-2.0	-2.0	-1.8	-2.0	.25	.00	.0000E+00	.0000E+00
11	1	-1.8	-2.0	-1.5	-2.0	.25	.00	.0000E+00	.0000E+00
12	1	-1.5	-2.0	-1.3	-2.0	.25	.00	.0000E+00	.0000E+00
13	1	-1.3	-2.0	-1.0	-2.0	.25	.00	.0000E+00	.0000E+00
14	1	-1.0	-2.0	-.8	-2.0	.25	.00	.0000E+00	.0000E+00
15	1	-.8	-2.0	-.5	-2.0	.25	.00	.0000E+00	.0000E+00
16	1	-.5	-2.0	-.3	-2.0	.25	.00	.0000E+00	.0000E+00
17	1	-.3	-2.0	.0	-2.0	.25	.00	.0000E+00	.0000E+00
18	1	.0	-2.0	.3	-2.0	.25	.00	.0000E+00	.0000E+00
19	1	.3	-2.0	.5	-2.0	.25	.00	.0000E+00	.0000E+00
20	1	.5	-2.0	.8	-2.0	.25	.00	.0000E+00	.0000E+00
21	1	.8	-2.0	1.0	-2.0	.25	.00	.0000E+00	.0000E+00
22	1	1.0	-2.0	1.3	-2.0	.25	.00	.0000E+00	.0000E+00
23	1	1.3	-2.0	1.5	-2.0	.25	.00	.0000E+00	.0000E+00
24	1	1.5	-2.0	1.8	-2.0	.25	.00	.0000E+00	.0000E+00
25	1	1.8	-2.0	2.0	-2.0	.25	.00	.0000E+00	.0000E+00
26	1	2.0	-2.0	2.3	-2.0	.25	.00	.0000E+00	.0000E+00
27	1	2.3	-2.0	2.3	-1.8	.25	90.00	.0000E+00	.0000E+00
28	1	2.3	-1.8	2.3	-1.5	.25	90.00	.0000E+00	.0000E+00
29	1	2.3	-1.5	2.3	-1.3	.25	90.00	.0000E+00	.0000E+00
30	1	2.3	-1.3	2.3	-1.0	.25	90.00	.0000E+00	.0000E+00
31	1	2.3	-1.0	2.3	-.8	.25	90.00	.0000E+00	.0000E+00
32	1	2.3	-.8	2.3	-.5	.25	90.00	.0000E+00	.0000E+00
33	1	2.3	-.5	2.3	-.3	.25	90.00	.0000E+00	.0000E+00
34	1	2.3	-.3	2.3	.0	.25	90.00	.0000E+00	.0000E+00
35	1	2.3	.0	2.3	.2	.25	66.92	.0000E+00	.0000E+00
36	1	2.3	.2	2.4	.5	.25	76.13	.0000E+00	.0000E+00
37	1	2.4	.5	2.4	.7	.25	82.88	.0000E+00	.0000E+00

POINT	X	Y	UX	UY	EXX	EYX	EXY	SXX	SVY	SVY	SVY	S1	S2	TH1	FI
62	-2.2	1.6	.00338	-.00455	.00239	.00514	12.5	42.7	23.1	.0	.0	.0	55.2	.88	9.39
63	-2.3	1.3	.00363	-.00416	.00220	.00506	10.3	46.2	21.9	.0	.0	.0	56.5	.86	9.25
64	-2.4	1.1	.00389	-.00367	.00307	.00438	1.1	52.2	7.6	.0	.0	.0	53.3	.91	9.20
65	-2.4	.8	.00411	-.00331	.00297	.00436	.3	46.1	3.7	.0	.0	.0	46.4	1.04	9.25
66	-2.4	.6	.00428	-.00297	.00348	.00388	.6	39.3	-4.9	.0	.0	.0	39.9	1.21	9.39
67	-2.4	.4	.00440	-.00275	.00372	.00361	1.8	30.3	-7.5	.0	.0	.0	32.1	1.51	9.63
68	-2.3	.1	.00441	-.00261	.00413	.00303	5.3	29.1	-12.4	.0	.0	.0	34.4	1.41	9.96
RESULTS FOR FIELD POINTS, WINDOW 1, STEP NUMBER 1. (ALL STRAINS ARE MULTIPLIED BY 1000.)															
1	-6	5.0	.0003	-.0047	.433	-.471	.117	31.6	17.4	1.8	1.8	31.9	17.2	7.2	7.97
2	-3	5.0	.0001	-.0048	.449	-.489	.060	31.9	17.2	.9	.9	31.9	17.1	3.6	8.12
3	0	5.0	.0000	-.0048	.455	-.495	.000	31.9	17.1	.0	.0	31.9	17.1	.0	8.35
4	.3	5.0	-.0001	-.0048	.449	-.489	-.060	31.9	17.2	-.9	-.9	31.9	17.1	-3.6	8.69
5	.6	5.0	-.0003	-.0047	.433	-.471	-.117	31.6	17.4	-1.8	-1.8	31.9	17.2	-7.2	9.12
6	.9	5.0	-.0004	-.0047	.408	-.443	-.168	31.2	17.9	-2.6	-2.6	31.7	17.4	-10.8	9.66
7	1.2	5.0	-.0005	-.0046	.375	-.407	-.213	30.7	18.5	-3.3	-3.3	31.6	17.6	-14.3	10.40
8	1.5	5.0	-.0006	-.0046	.337	-.365	-.248	30.2	19.2	-4.3	-4.3	31.4	17.9	-17.6	10.93
9	1.8	5.0	-.0007	-.0045	.296	-.319	-.274	29.5	19.9	-5.0	-5.0	31.2	18.3	-20.8	11.56
10	2.1	5.0	-.0008	-.0044	.254	-.274	-.291	28.9	20.6	-5.3	-5.3	30.9	18.6	-23.9	12.29
11	2.4	5.0	-.0009	-.0043	.213	-.229	-.300	28.3	21.3	-5.4	-5.4	30.6	19.0	-26.8	7.7
12	-6	4.7	.0003	-.0049	.486	-.530	.140	32.4	16.5	1.1	1.1	32.7	16.2	3.9	7.97
13	-3	4.7	.0002	-.0049	.506	-.552	.072	32.7	16.1	.0	.0	32.8	16.1	.0	7.93
14	0	4.7	.0000	-.0049	.513	-.560	.000	32.8	16.0	-1.1	-1.1	32.8	16.0	-3.9	7.97
15	.3	4.7	-.0002	-.0049	.506	-.552	-.072	32.7	16.1	-2.2	-2.2	32.7	16.1	-7.7	8.12
16	.6	4.7	-.0003	-.0048	.486	-.530	-.140	32.4	16.5	-3.1	-3.1	32.6	16.4	-11.4	8.35
17	.9	4.7	-.0004	-.0048	.454	-.494	-.200	31.9	17.1	-3.9	-3.9	32.4	16.7	-15.1	8.69
18	1.2	4.7	-.0006	-.0048	.414	-.449	-.251	31.3	17.8	-4.6	-4.6	32.2	17.1	-18.7	9.12
19	1.5	4.7	-.0007	-.0047	.367	-.396	-.291	30.6	18.7	-5.0	-5.0	31.9	17.5	-22.1	9.66
20	1.8	4.7	-.0008	-.0046	.316	-.341	-.319	29.9	19.5	-5.3	-5.3	31.6	18.0	-25.3	10.30
21	2.1	4.7	-.0009	-.0045	.266	-.286	-.335	29.1	20.4	-5.4	-5.4	31.2	18.4	-28.3	11.03
22	2.4	4.7	-.0010	-.0043	.218	-.234	-.342	28.4	21.3	2.6	2.6	33.8	15.0	8.2	6.92
23	-6	4.4	.0003	-.0051	.548	-.599	.168	33.4	15.4	1.4	1.4	33.9	14.8	4.1	6.78
24	-3	4.4	.0002	-.0051	.574	-.627	.086	33.8	14.9	.0	.0	33.9	14.8	.0	6.74
25	0	4.4	.0000	-.0051	.582	-.637	.000	33.9	14.8	-1.4	-1.4	33.9	14.8	-4.1	6.78
26	.3	4.4	-.0002	-.0051	.574	-.627	-.086	33.8	14.9	-2.6	-2.6	33.8	15.0	-8.2	6.92
27	.6	4.4	-.0003	-.0051	.548	-.599	-.168	33.4	15.4	-3.8	-3.8	33.6	15.3	-12.2	7.15
28	.9	4.4	-.0005	-.0050	.509	-.554	-.240	32.8	16.1	-4.7	-4.7	33.4	15.7	-16.1	7.48
29	1.2	4.4	-.0006	-.0049	.458	-.496	-.299	32.0	17.1	-5.4	-5.4	33.1	16.2	-19.8	7.92
30	1.5	4.4	-.0008	-.0048	.399	-.431	-.344	31.1	18.1	-5.8	-5.8	32.7	16.7	-23.4	8.46
31	1.8	4.4	-.0009	-.0047	.338	-.363	-.373	30.2	19.2	-6.1	-6.1	32.3	17.2	-26.8	9.10
32	2.1	4.4	-.0010	-.0045	.277	-.296	-.388	29.3	20.3	-6.1	-6.1	31.9	17.7	-29.9	9.84
33	2.4	4.4	-.0011	-.0044	.221	-.234	-.390	28.4	21.3	1.6	1.6	35.0	13.6	8.7	5.80
34	-6	4.1	.0004	-.0053	.623	-.681	.203	34.5	14.1	.0	.0	35.1	13.3	4.3	5.67
35	-3	4.1	.0002	-.0053	.654	-.718	.105	35.0	13.5	-1.6	-1.6	35.1	13.3	.0	5.62
36	0	4.1	.0000	-.0053	.665	-.730	.000	35.1	13.3	-3.2	-3.2	35.1	13.3	-4.3	5.67
37	.3	4.1	-.0002	-.0053	.654	-.718	-.105	35.0	13.5	-3.2	-3.2	35.0	13.3	-8.7	5.80
38	.6	4.1	-.0004	-.0053	.623	-.681	-.203	34.5	14.1	-5.6	-5.6	34.8	13.9	-12.9	6.03
39	.9	4.1	-.0006	-.0052	.573	-.624	-.290	33.7	15.0	.0	.0	34.5	14.4	-17.1	6.35
40	1.2	4.1	-.0007	-.0051	.508	-.551	-.359	32.8	16.2	.0	.0	34.5	14.4	.0	6.35

19	3.9	2.3	- .0020	- .0037	- .239	.239	-.464	21.3	28.8	-7.3	33.2	16.8	-58.6	8.32
20	4.2	2.3	- .0020	- .0035	- .241	.236	-.407	21.2	28.7	-6.4	32.3	17.5	-60.2	9.37
21	4.5	2.3	- .0019	- .0034	- .241	.231	-.358	21.2	28.6	-5.6	31.6	18.2	-61.7	10.48
22	4.8	2.3	- .0018	- .0033	- .237	.226	-.315	21.2	28.5	-4.9	31.0	18.7	-63.2	11.65
23	1.8	2.0	THIS POINT IS TOO CLOSE TO A BOUNDARY											
24	2.1	2.0	THIS POINT IS TOO CLOSE TO A BOUNDARY											
25	2.4	2.0	- .0026	- .0046	- .220	.380	-1.171	22.3	31.7	-18.4	45.9	8.0	-52.2	2.64
26	2.7	2.0	- .0026	- .0043	- .296	.394	-.921	20.8	31.6	-14.4	41.6	10.8	-55.3	3.66
27	3.0	2.0	- .0025	- .0041	- .316	.370	-.749	20.3	31.0	-11.7	38.6	12.8	-57.3	4.68
28	3.3	2.0	- .0024	- .0039	- .319	.342	-.629	20.1	30.5	-9.9	36.4	14.2	-58.9	5.67
29	3.6	2.0	- .0023	- .0037	- .317	.321	-.539	20.1	30.1	-8.4	34.9	15.2	-60.3	6.65
30	3.9	2.0	- .0022	- .0036	- .312	.305	-.466	20.1	29.8	-7.3	33.7	16.2	-61.8	7.63
31	4.2	2.0	- .0021	- .0035	- .305	.292	-.405	20.2	29.5	-6.3	32.7	17.0	-63.2	8.67
32	4.5	2.0	- .0020	- .0033	- .295	.281	-.352	20.3	29.3	-5.5	32.0	17.7	-64.6	9.76
33	4.8	2.0	- .0019	- .0032	- .284	.269	-.306	20.5	29.2	-4.8	31.3	18.3	-66.0	10.93
34	1.8	1.7	THIS POINT IS NOT IN THE REGION OF INTEREST											
35	2.1	1.7	THIS POINT IS TOO CLOSE TO A BOUNDARY											
36	2.4	1.7	THIS POINT IS TOO CLOSE TO A BOUNDARY											
37	2.7	1.7	- .0029	- .0042	- .522	.625	-.939	17.3	35.3	-14.7	43.5	9.0	-60.7	3.04
38	3.0	1.7	- .0027	- .0039	- .475	.520	-.746	17.7	33.3	-11.7	39.6	11.5	-61.9	4.12
39	3.3	1.7	- .0026	- .0038	- .442	.451	-.622	18.1	32.1	-9.8	37.1	13.1	-62.8	5.09
40	3.6	1.7	- .0024	- .0036	- .417	.407	-.530	18.4	31.3	-8.3	35.4	14.3	-63.9	6.04
41	3.9	1.7	- .0023	- .0035	- .396	.377	-.455	18.7	30.8	-7.1	34.1	15.4	-65.2	7.00
42	4.2	1.7	- .0022	- .0034	- .376	.353	-.391	19.0	30.4	-6.1	33.1	16.3	-66.5	8.02
43	4.5	1.7	- .0021	- .0033	- .355	.333	-.337	19.3	30.1	-5.3	32.3	17.2	-67.8	9.11
44	4.8	1.7	- .0020	- .0032	- .334	.314	-.290	19.7	29.8	-4.5	31.6	17.9	-69.1	10.28
45	1.8	1.4	THIS POINT IS NOT IN THE REGION OF INTEREST											
46	2.1	1.4	THIS POINT IS TOO CLOSE TO A BOUNDARY											
47	2.4	1.4	THIS POINT IS TOO CLOSE TO A BOUNDARY											
48	2.7	1.4	- .0032	- .0039	- .788	.872	-.850	13.0	39.0	-13.3	44.6	7.4	-67.2	2.61
49	3.0	1.4	- .0030	- .0038	- .658	.668	-.691	14.7	35.5	-10.8	40.1	10.1	-66.9	3.66
50	3.3	1.4	- .0028	- .0036	- .582	.559	-.585	15.8	33.7	-9.2	37.5	11.9	-67.1	4.59
51	3.6	1.4	- .0026	- .0035	- .530	.495	-.500	16.5	32.6	-7.8	35.8	13.4	-67.9	5.50
52	3.9	1.4	- .0025	- .0034	- .488	.450	-.427	17.2	31.9	-6.7	34.5	14.6	-68.9	6.44
53	4.2	1.4	- .0023	- .0032	- .451	.416	-.363	17.8	31.4	-5.7	33.4	15.7	-70.0	7.45
54	4.5	1.4	- .0022	- .0031	- .417	.386	-.309	18.3	30.9	-4.8	32.6	16.7	-71.2	8.54
55	4.8	1.4	- .0021	- .0031	- .385	.359	-.263	18.8	30.5	-4.1	31.8	17.5	-72.4	9.71
56	1.8	1.1	THIS POINT IS NOT IN THE REGION OF INTEREST											
57	2.1	1.1	THIS POINT IS NOT IN THE REGION OF INTEREST											
58	2.4	1.1	THIS POINT IS TOO CLOSE TO A BOUNDARY											
59	2.7	1.1	- .0035	- .0036	-1.057	1.046	-.644	8.4	41.4	-10.1	44.2	5.5	-74.3	2.27
60	3.0	1.1	- .0032	- .0035	- .847	.786	-.580	11.5	37.1	-9.1	40.0	8.6	-72.3	3.28
61	3.3	1.1	- .0030	- .0034	- .729	.656	-.511	13.3	35.0	-8.0	37.6	10.6	-71.8	4.16
62	3.6	1.1	- .0028	- .0033	- .647	.578	-.441	14.6	33.8	-6.9	36.0	12.3	-72.1	5.04
63	3.9	1.1	- .0026	- .0032	- .582	.522	-.376	15.6	32.9	-5.9	34.7	13.8	-72.9	5.96
64	4.2	1.1	- .0024	- .0031	- .527	.477	-.318	16.5	32.3	-5.0	33.7	15.1	-73.8	6.97
65	4.5	1.1	- .0023	- .0030	- .478	.437	-.268	17.3	31.7	-4.2	32.8	16.2	-74.8	8.05
66	4.8	1.1	- .0021	- .0029	- .434	.402	-.225	18.0	31.2	-3.5	32.0	17.2	-75.9	9.24
67	1.8	.8	THIS POINT IS NOT IN THE REGION OF INTEREST											
68	2.1	.8	THIS POINT IS NOT IN THE REGION OF INTEREST											
69	2.4	.8	THIS POINT IS TOO CLOSE TO A BOUNDARY											
70	2.7	.8	- .0038	- .0033	-1.236	1.044	-.341	4.8	40.5	-5.3	41.3	4.0	-81.7	2.11

71	3.0	.8	-.0034	-.0033	-1.008	.843	-.412	8.5	37.5	-6.5	38.9	7.1	-78.0	3.02
72	3.3	.8	-.0032	-.0032	-.862	.727	-.397	10.9	35.8	-6.2	37.3	9.4	-76.7	3.84
73	3.6	.8	-.0029	-.0031	-.755	.648	-.353	12.7	34.7	-5.5	36.0	11.4	-76.6	4.68
74	3.9	.8	-.0027	-.0030	-.669	.585	-.303	14.1	33.8	-4.8	34.9	13.1	-77.1	5.59
75	4.2	.8	-.0025	-.0030	-.596	.531	-.254	15.4	33.0	-4.0	33.9	14.5	-77.9	6.59
76	4.5	.8	-.0023	-.0029	-.533	.483	-.211	16.4	32.4	-3.3	33.0	15.8	-78.7	7.67
77	4.8	.8	-.0022	-.0028	-.477	.440	-.175	17.4	31.7	-2.7	32.2	16.9	-79.6	8.86
78	1.8	.5	THIS POINT IS NOT IN THE REGION OF INTEREST											
79	2.1	.5	THIS POINT IS NOT IN THE REGION OF INTEREST											
80	2.4	.5	THIS POINT IS TOO CLOSE TO A BOUNDARY											
81	2.7	.5	-.0039	-.0030	-1.269	.881	-.073	3.4	37.1	-1.1	37.1	3.3	-88.1	2.21
82	3.0	.5	-.0036	-.0030	-1.096	.826	-.224	6.6	36.8	-3.5	37.2	6.2	-83.4	2.95
83	3.3	.5	-.0033	-.0030	-.954	.760	-.257	9.2	36.1	-4.0	36.7	8.6	-81.7	3.67
84	3.6	.5	-.0030	-.0029	-.837	.696	-.241	11.3	35.3	-3.8	35.9	10.7	-81.3	4.46
85	3.9	.5	-.0028	-.0029	-.737	.634	-.209	13.0	34.5	-3.3	35.0	12.5	-81.5	5.34
86	4.2	.5	-.0026	-.0028	-.650	.575	-.174	14.5	33.7	-2.7	34.1	14.1	-82.1	6.32
87	4.5	.5	-.0024	-.0027	-.575	.520	-.142	15.8	32.9	-2.2	33.2	15.5	-82.7	7.41
88	4.8	.5	-.0022	-.0027	-.509	.470	-.115	16.8	32.2	-1.8	32.4	16.6	-83.4	8.60
89	1.8	.2	THIS POINT IS NOT IN THE REGION OF INTEREST											
90	2.1	.2	THIS POINT IS TOO CLOSE TO A BOUNDARY											
91	2.4	.2	THIS POINT IS TOO CLOSE TO A BOUNDARY											
92	2.7	.2	-.0040	-.0028	-1.165	.656	.100	4.5	33.0	1.6	33.1	4.4	86.9	2.82
93	3.0	.2	-.0037	-.0028	-1.095	.756	-.062	6.3	35.4	-1.0	35.4	6.3	-88.1	3.16
94	3.3	.2	-.0033	-.0028	-.989	.758	-.114	8.5	35.9	-1.8	36.0	8.4	-86.3	3.69
95	3.6	.2	-.0031	-.0027	-.879	.719	-.118	10.5	35.6	-1.8	35.7	10.4	-85.8	4.39
96	3.9	.2	-.0028	-.0027	-.775	.663	-.102	12.3	34.9	-1.6	35.0	12.2	-86.0	5.22
97	4.2	.2	-.0026	-.0026	-.681	.603	-.082	14.0	34.1	-1.3	34.2	13.9	-86.4	6.18
98	4.5	.2	-.0024	-.0026	-.599	.544	-.062	15.4	33.3	-1.0	33.3	15.3	-86.9	7.26
99	4.8	.2	-.0022	-.0025	-.527	.489	-.047	16.6	32.5	-.7	32.5	16.5	-87.4	8.46
100	1.8	-.1	THIS POINT IS NOT IN THE REGION OF INTEREST											
101	2.1	-.1	THIS POINT IS TOO CLOSE TO A BOUNDARY											
102	2.4	-.1	THIS POINT IS TOO CLOSE TO A BOUNDARY											
103	2.7	-.1	-.0039	-.0026	-1.025	.696	.114	-2.9	30.2	2.2	30.4	-3.0	86.2	-1.09
104	3.0	-.1	-.0036	-.0026	-1.039	.793	.052	-1.1	34.2	1.0	34.2	-1.1	88.4	-1.11
105	3.3	-.1	-.0033	-.0025	-.976	.789	.026	1.6	35.5	.5	35.6	1.6	89.2	1.58
106	3.6	-.1	-.0030	-.0025	-.881	.738	.020	4.5	35.6	.4	35.6	4.5	89.3	1.90
107	3.9	-.1	-.0028	-.0025	-.781	.669	.022	7.2	35.1	.4	35.1	7.2	89.1	2.29
108	4.2	-.1	-.0026	-.0024	-.685	.597	.026	9.6	34.3	.5	34.3	9.6	88.9	2.75
109	4.5	-.1	-.0024	-.0024	-.600	.530	.028	11.7	33.5	.5	33.5	11.7	88.6	3.26
110	4.8	-.1	-.0022	-.0024	-.526	.469	.029	13.5	32.6	.6	32.6	13.5	88.3	3.84
111	1.8	-.4	THIS POINT IS NOT IN THE REGION OF INTEREST											
112	2.1	-.4	THIS POINT IS TOO CLOSE TO A BOUNDARY											
113	2.4	-.4	THIS POINT IS TOO CLOSE TO A BOUNDARY											
114	2.7	-.4	-.0038	-.0024	-.959	.645	.159	-1.2	29.7	3.1	29.9	-1.5	84.4	-1.14
115	3.0	-.4	-.0035	-.0023	-.988	.755	.169	.3	33.8	3.2	34.1	.0	84.5	1.48
116	3.3	-.4	-.0032	-.0023	-.936	.763	.170	2.7	35.4	3.3	35.7	2.4	84.3	1.66
117	3.6	-.4	-.0030	-.0023	-.847	.716	.165	5.5	35.6	3.2	35.9	5.2	84.0	1.97
118	3.9	-.4	-.0027	-.0022	-.749	.649	.155	8.1	35.0	3.0	35.3	7.8	83.8	2.36
119	4.2	-.4	-.0025	-.0022	-.656	.578	.141	10.5	34.2	2.7	34.5	10.2	83.6	2.82
120	4.5	-.4	-.0023	-.0022	-.574	.512	.126	12.4	33.3	2.4	33.6	12.2	83.5	3.34
121	4.8	-.4	-.0022	-.0022	-.503	.453	.111	14.1	32.5	2.1	32.7	13.9	83.5	3.93

Once the boundary element program run is completed, SAFCON uses the two files listed above as input. The first output file from SAFCON is one containing the effective principal stresses and new safety factors once the gas pressure has been superimposed onto the principal stresses. This file is named RUNFF32.LST. Since the boundary is considered sheared, the Coulomb-Navier failure criterion is used, requiring the determination of the normal and shear stresses. These have been included in the output as SN and SHEAR respectively. The safety factor is defined as shear strength over shear stress. The X axis ($Y=0$) represents the interface between the two different materials. Stresses evaluated on the interface are assumed to be sandstone and therefore, a gas pressure is superimposed. The field points with an astrix (*), indicate field points that fall within the previously defined shear zone. These points are sheared and no gas pressure is applied.

Listed at the top of this file is the applied gas pressure and the upper limit to the sandstone bed. If this upper limit is not desired, it is made large enough such that it will not affect the spalling process.

The following is a listing of SAFCON output file RUNFF32.LST.

GAS PRESSURE WITHIN SANDSTONE IS 6.600MPa
 UPPER LIMIT TO GAS IN SANDSTONE 6.000m

 MID POINTS OF BOUNDARY ELEMENTS

POINT	X	Y	S1	S3	SN	SHEAR	SF
1	-2.250	-.125	5.00	.00	1.25	2.17	.33
2	-2.250	-.375	17.90	.00	4.47	7.75	.33
3	-2.250	-.625	21.40	.00	5.35	9.27	.33
4	-2.250	-.875	23.80	.00	5.95	10.31	.33
5	-2.250	-1.125	26.80	.00	6.70	11.60	.33
6	-2.250	-1.375	31.40	.00	7.85	13.60	.33
7	-2.250	-1.625	41.30	.00	10.32	17.88	.33
8	-2.250	-1.875	90.50	.00	22.62	39.19	.33
9	-2.125	-2.000	86.90	.00	21.72	37.63	.33
10	-1.875	-2.000	38.20	.00	9.55	16.54	.33
11	-1.625	-2.000	28.50	.00	7.12	12.34	.33
12	-1.375	-2.000	24.10	.00	6.02	10.44	.33
13	-1.125	-2.000	21.60	.00	5.40	9.35	.33
14	-.875	-2.000	20.00	.00	5.00	8.66	.33
15	-.625	-2.000	19.00	.00	4.75	8.23	.33
16	-.375	-2.000	18.40	.00	4.60	7.97	.33
17	-.125	-2.000	18.10	.00	4.52	7.84	.33
18	.125	-2.000	18.10	.00	4.52	7.84	.33
19	.375	-2.000	18.40	.00	4.60	7.97	.33
20	.625	-2.000	19.00	.00	4.75	8.23	.33
21	.875	-2.000	20.00	.00	5.00	8.66	.33
22	1.125	-2.000	21.60	.00	5.40	9.35	.33
23	1.375	-2.000	24.10	.00	6.02	10.44	.33
24	1.625	-2.000	28.50	.00	7.12	12.34	.33
25	1.875	-2.000	38.20	.00	9.55	16.54	.33
26	2.125	-2.000	86.90	.00	21.72	37.63	.33
27	2.250	-1.875	90.50	.00	22.62	39.19	.33
28	2.250	-1.625	41.30	.00	10.32	17.88	.33
29	2.250	-1.375	31.40	.00	7.85	13.60	.33
30	2.250	-1.125	26.80	.00	6.70	11.60	.33
31	2.250	-.875	23.80	.00	5.95	10.31	.33
32	2.250	-.625	21.40	.00	5.35	9.27	.33
33	2.250	-.375	17.90	.00	4.47	7.75	.33
34	2.250	-.125	5.00	.00	1.25	2.17	.33
35	2.299	.115	34.40	.00	8.60	14.90	.33
36	2.378	.352	32.10	.00	8.02	13.90	.33
37	2.424	.597	39.90	.00	9.97	17.28	.33
38	2.429	.845	46.40	.00	11.60	20.09	.33
39	2.401	1.094	53.30	.00	13.32	23.08	.33
40	2.329	1.330	56.50	.00	14.12	24.47	.33
41	2.217	1.553	55.20	.00	13.80	23.90	.33
42	2.083	1.764	58.60	.00	14.65	25.37	.33
43	1.916	1.949	57.10	.00	14.27	24.73	.33
44	1.720	2.104	52.00	.00	13.00	22.52	.33
45	1.513	2.243	50.40	.00	12.60	21.82	.33
46	1.293	2.362	49.30	.00	12.32	21.35	.33
47	1.063	2.456	46.90	.00	11.72	20.31	.33

48	.825	2.534	46.40	.00	11.60	20.09	.33
49	.582	2.592	45.90	.00	11.47	19.88	.33
50	.335	2.628	45.00	.00	11.25	19.49	.33
51	.105	2.648	46.10	.00	11.52	19.96	.33
52	-.105	2.648	46.10	.00	11.52	19.96	.33
53	-.335	2.628	45.00	.00	11.25	19.49	.33
54	-.582	2.592	45.90	.00	11.47	19.88	.33
55	-.825	2.534	46.40	.00	11.60	20.09	.33
56	-1.063	2.456	46.90	.00	11.72	20.31	.33
57	-1.293	2.362	49.30	.00	12.32	21.35	.33
58	-1.513	2.243	50.40	.00	12.60	21.82	.33
59	-1.720	2.104	52.00	.00	13.00	22.52	.33
60	-1.916	1.949	57.10	.00	14.27	24.73	.33
61	-2.083	1.764	58.60	.00	14.65	25.37	.33
62	-2.217	1.553	55.20	.00	13.80	23.90	.33
63	-2.329	1.330	56.50	.00	14.12	24.47	.33
64	-2.401	1.094	53.30	.00	13.32	23.08	.33
65	-2.429	.845	46.40	.00	11.60	20.09	.33
66	-2.424	.597	39.90	.00	9.97	17.28	.33
67	-2.378	.352	32.10	.00	8.02	13.90	.33
68	-2.299	.115	34.40	.00	8.60	14.90	.33

FIELD POINT RESULTS

X	Y	S1	S3	FI
-.600	5.000	25.30	10.60	4.847
-.300	5.000	25.30	10.50	4.826
.000	5.000	25.30	10.50	4.826
.300	5.000	25.30	10.50	4.826
.600	5.000	25.30	10.60	4.847
.900	5.000	25.10	10.80	4.926
1.200	5.000	25.00	11.00	4.930
1.500	5.000	24.80	11.30	5.093
1.800	5.000	24.60	11.70	5.218
2.100	5.000	24.30	12.00	5.346
2.400	5.000	24.00	12.40	5.497
-.600	4.700	26.10	9.60	4.492
-.300	4.700	26.20	9.50	4.454
.000	4.700	26.20	9.40	4.433
.300	4.700	26.20	9.50	4.454
.600	4.700	26.10	9.60	4.492
.900	4.700	26.00	9.80	4.552
1.200	4.700	25.80	10.10	4.650
1.500	4.700	25.60	10.50	4.770
1.800	4.700	25.30	10.90	4.910
2.100	4.700	25.00	11.40	5.073
2.400	4.700	24.60	11.80	5.239
-.600	4.400	27.20	8.40	4.064
-.300	4.400	27.30	8.20	4.007
.000	4.400	27.30	8.20	4.007
.300	4.400	27.30	8.20	4.007
.600	4.400	27.20	8.40	4.064

.900	4.400	27.00	8.70	4.157
1.200	4.400	26.80	9.10	4.272
1.500	4.400	26.50	9.60	4.425
1.800	4.400	26.10	10.10	4.596
2.100	4.400	25.70	10.60	4.772
2.400	4.400	25.30	11.10	4.951
-.600	4.100	28.40	7.00	3.603
-.300	4.100	28.50	6.70	3.526
.000	4.100	28.50	6.70	3.526
.300	4.100	28.50	6.70	3.526
.600	4.100	28.40	7.00	3.603
.900	4.100	28.20	7.30	3.692
1.200	4.100	27.90	7.80	3.838
1.500	4.100	27.60	8.40	4.005
1.800	4.100	27.10	9.10	4.225
2.100	4.100	26.60	9.80	4.449
2.400	4.100	26.10	10.40	4.658
-.600	3.800	29.90	5.20	3.041
-.300	3.800	30.00	4.90	2.965
.000	3.800	30.00	4.80	2.942
.300	3.800	30.00	4.90	2.965
.600	3.800	29.90	5.20	3.041
.900	3.800	29.60	5.70	3.182
1.200	3.800	29.30	6.30	3.345
1.500	3.800	28.90	7.10	3.561
1.800	3.800	28.30	7.90	3.804
2.100	3.800	27.70	8.80	4.073
2.400	3.800	27.10	9.60	4.327
-.600	3.500	31.70	3.10	2.400
-.300	3.500	31.80	2.70	2.296
.000	3.500	31.90	2.60	2.264
.300	3.500	31.80	2.70	2.296
.600	3.500	31.70	3.10	2.400
.900	3.500	31.40	3.70	2.565
1.200	3.500	31.00	4.50	2.781
1.500	3.500	30.50	5.50	3.046
1.800	3.500	29.80	6.50	3.331
2.100	3.500	29.00	7.60	3.652
2.400	3.500	28.20	8.70	3.980
-.600	3.200	33.80	.40	1.557
-.300	3.200	34.00	.00	1.424
.000	3.200	34.00	-.20	1.358
.300	3.200	34.00	.00	1.424
.600	3.200	33.80	.40	1.557
.900	3.200	33.60	1.10	1.769
1.200	3.200	33.20	2.20	2.078
1.500	3.200	32.50	3.50	2.433
1.800	3.200	31.70	4.90	2.806
2.100	3.200	30.70	6.30	3.192
2.400	3.200	29.50	7.60	3.590
-.600	2.900	36.40	-2.90	-.200
-.300	2.900	36.60	-3.50	-.200
.000	2.900	36.70	-3.50	-.200
.300	2.900	36.60	-3.50	-.200

.600	2.900	36.40	-2.90	-.200
.900	2.900	36.20	-2.00	.508
1.200	2.900	35.80	-.70	1.121
1.500	2.900	35.10	1.00	1.667
1.800	2.900	34.10	2.80	2.164
2.100	2.900	32.70	4.70	2.678
2.400	2.900	31.20	6.40	3.161
1.500	2.600	38.60	-2.10	.409
1.800	2.600	37.30	.20	1.355
2.100	2.600	35.40	2.80	2.084
2.400	2.600	33.30	5.10	2.711
2.100	2.300	39.30	.50	1.365
2.400	2.300	35.90	3.50	2.203
2.400	2.000	39.30	1.40	1.582
1.800	2.600	37.30	.20	1.355
2.100	2.600	35.40	2.80	2.084
2.400	2.600	33.30	5.10	2.711
2.700	2.600	31.20	6.90	3.260
3.000	2.600	29.50	8.20	3.708
3.300	2.600	28.10	9.30	4.114
3.600	2.600	27.00	10.10	4.443
3.900	2.600	26.10	10.80	4.739
4.200	2.600	25.30	11.40	5.013
4.500	2.600	24.70	12.00	5.259
4.800	2.600	24.10	12.50	5.495
2.100	2.300	39.30	.50	1.365
2.400	2.300	35.90	3.50	2.203
2.700	2.300	33.00	5.70	2.855
3.000	2.300	30.70	7.30	3.391
3.300	2.300	29.00	8.50	3.831
3.600	2.300	27.70	9.40	4.193
3.900	2.300	26.60	10.20	4.530
4.200	2.300	25.70	10.90	4.833
4.500	2.300	25.00	11.60	5.114
4.800	2.300	24.40	12.10	5.345
2.400	2.000	39.30	1.40	1.582
2.700	2.000	35.00	4.20	2.404
3.000	2.000	32.00	6.20	3.043
3.300	2.000	29.80	7.60	3.554
3.600	2.000	28.30	8.60	3.946
3.900	2.000	27.10	9.60	4.327
4.200	2.000	26.10	10.40	4.658
4.500	2.000	25.40	11.10	4.932
4.800	2.000	24.70	11.70	5.197
2.700	1.700	36.90	2.40	1.914
3.000	1.700	33.00	4.90	2.695
3.300	1.700	30.50	6.50	3.254
3.600	1.700	28.80	7.70	3.697
3.900	1.700	27.50	8.80	4.102
4.200	1.700	26.50	9.70	4.445
4.500	1.700	25.70	10.60	4.772
4.800	1.700	25.00	11.30	5.052
2.700	1.400	38.00	.80	1.489
3.000	1.400	33.50	3.50	2.361

3.300	1.400	30.90	5.30	2.964	
3.600	1.400	29.20	6.80	3.462	
3.900	1.400	27.90	8.00	3.880	
4.200	1.400	26.80	9.10	4.272	
4.500	1.400	26.00	10.10	4.614	
4.800	1.400	25.20	10.90	4.929	
2.700	1.100	37.60	-1.10	.923	
3.000	1.100	33.40	2.00	2.016	
3.300	1.100	31.00	4.00	2.668	
3.600	1.100	29.40	5.70	3.204	
3.900	1.100	28.10	7.20	3.684	
4.200	1.100	27.10	8.50	4.100	
4.500	1.100	26.20	9.60	4.475	
4.800	1.100	25.40	10.60	4.828	
2.700	.800	34.70	-2.60	-.200	
3.000	.800	32.30	.50	1.661	
3.300	.800	30.70	2.80	2.404	
3.600	.800	29.40	4.80	3.002	
3.900	.800	28.30	6.50	3.507	
4.200	.800	27.30	7.90	3.943	
4.500	.800	26.40	9.20	4.358	
4.800	.800	25.60	10.30	4.728	
2.700	.500	37.10	3.30	.464	*
3.000	.500	30.60	-.40	1.433	
3.300	.500	30.10	2.00	2.237	
3.600	.500	29.30	4.10	2.847	
3.900	.500	28.40	5.90	3.362	
4.200	.500	27.50	7.50	3.829	
4.500	.500	26.60	8.90	4.262	
4.800	.500	25.80	10.00	4.629	
2.700	.200	33.10	4.40	.538	*
3.000	.200	28.80	-.30	1.563	
3.300	.200	29.40	1.80	2.233	
3.600	.200	29.10	3.80	2.793	
3.900	.200	28.40	5.60	3.294	
4.200	.200	27.60	7.30	3.772	
4.500	.200	26.70	8.70	4.204	
4.800	.200	25.90	9.90	4.590	
2.700	-.100	30.40	-3.00	1.340	
3.000	-.100	34.20	-1.10	1.375	
3.300	-.100	35.60	1.60	1.555	
3.600	-.100	35.60	4.50	1.789	
3.900	-.100	35.10	7.20	2.024	
4.200	-.100	34.30	9.60	2.254	
4.500	-.100	33.50	11.70	2.467	
4.800	-.100	32.60	13.50	2.671	
2.700	-.400	29.90	-1.50	1.530	
3.000	-.400	34.10	.00	1.481	
3.300	-.400	35.70	2.40	1.617	
3.600	-.400	35.90	5.20	1.828	
3.900	-.400	35.30	7.80	2.058	
4.200	-.400	34.50	10.20	2.286	
4.500	-.400	33.60	12.20	2.496	
4.800	-.400	32.70	13.90	2.693	

The next output file from SAFCON is one containing the coordinates of the new contoured shear zone around the cavity. This file will be used as input for the next iteration in the same manner that the output from the previous run is input to this iteration. This input file for this run will not be listed. Because this file is input for the next iteration, the file number is incremented by 1 and is called RUNFF33.F1. This file is listed on the following page. (The actual output is listed as two columns of X and Y coordinates each, but for convenience, it is put onto one page here.)

-2.250	.000	-1.497	2.730
-2.250	-.250	-1.799	2.489
-2.250	-.500	-2.112	2.180
-2.250	-.750	-2.365	1.784
-2.250	-1.000	-2.606	1.457
-2.250	-1.250	-2.715	1.217
-2.250	-1.500	-2.811	.976
-2.250	-1.750	-2.871	.597
-2.250	-2.000	-2.811	.185
-2.000	-2.000	-2.679	-.004
-1.750	-2.000		
-1.500	-2.000		
-1.250	-2.000		
-1.000	-2.000		
-.750	-2.000		
-.500	-2.000		
-.250	-2.000		
.000	-2.000		
.250	-2.000		
.500	-2.000		
.750	-2.000		
1.000	-2.000		
1.250	-2.000		
1.500	-2.000		
1.750	-2.000		
2.000	-2.000		
2.250	-2.000		
2.250	-1.750		
2.250	-1.500		
2.250	-1.250		
2.250	-1.000		
2.250	-.750		
2.250	-.500		
2.250	-.250		
2.250	.000		
2.679	-.004		
2.811	.185		
2.871	.597		
2.811	.976		
2.715	1.217		
2.606	1.457		
2.365	1.784		
2.112	2.180		
1.799	2.489		
1.497	2.730		
1.244	2.833		
.931	2.988		
.581	3.108		
.244	3.125		
-.244	3.125		
-.581	3.108		
-.931	2.988		
-1.244	2.833		

The final file that is produced by SAFCON is the input file for the next run of the boundary element program. The filename is now RUNFF33.DAT and will look identical to the first file listed, only with a new set of boundary element points defining the new opening. P5005 will then produce RUNFF33.OUT and the process goes on.

Two other input files are used by SAFCON; PROP.PRM and PLOT.PRM. These contains constant rock properties and PLOT88 plotting parameters prespectively. These have been listed in Appendix E, page 144.